Technology Collaboration Programme
by iea

International Energy Agency
Photovoltaic Power Systems Programme

Task 17: PV and Transport

PVPS

PV-Powered Electric Vehicle Charging Stations

Requirements, barriers, solutions and social acceptance

2025

Report IEA-PVPS T17-04:2025

What is IEA PVPS TCP?

The International Energy Agency (IEA), founded in 1974, is an autonomous body within the framework of the Organization for Economic Cooperation and Development (OECD). The Technology Collaboration Programme (TCP) was created with a belief that the future of energy security and sustainability starts with global collaboration. The programme is made up of 6.000 experts across government, academia, and industry dedicated to advancing common research and the application of specific energy technologies.

The IEA Photovoltaic Power Systems Programme (IEA PVPS) is one of the TCP's within the IEA and was established in 1993. The mission of the programme is to "enhance the international collaborative efforts which facilitate the role of photovoltaic solar energy as a cornerstone in the transition to sustainable energy systems." In order to achieve this, the Programme's participants have undertaken a variety of joint research projects in PV power systems applications. The overall programme is headed by an Executive Committee, comprised of one delegate from each country or organisation member, which designates distinct 'Tasks,' that may be research projects or activity areas.

The 30 IEA PVPS members Australia, Austria, Belgium, Canada, China, Denmark, Enercity SA, European Union, Finland, France, Germany, India, Israel, Italy, Japan, Korea, Malaysia, Morocco, the Netherlands, Norway, Portugal, Solar Energy Research Institute of Singapore (SERIS), SolarPower Europe, South Africa, Spain, Sweden, Switzerland, Thailand, Turkey, United States.

Visit us at: www.iea-pvps.org

What is IEA PVPS Task 17?

The objective of Task 17 of the IEA Photovoltaic Power Systems Programme is to deploy PV in the transport, which will contribute to reducing CO_2 emissions of the transport and enhancing PV market expansions. The results contribute to clarifying the potential of utilization of PV in transport and to proposal on how to proceed toward realising the concepts.

Task 17's scope includes PV-powered vehicles such as PLDVs (passenger light duty vehicles), LCVs (light commercial vehicles), HDVs (heavy duty vehicles) and other vehicles, as well as PV applications for electric systems and infrastructures, such as charging infrastructure with PV, battery and other power management systems.

Authors

- **Main Content:** M. Sechilariu (France), A. Alchami (France), S. Cheikh-Mohamad (France), B. Robisson (France), M.C Brito (Portugal)
- **Editor:** Manuela Sechilariu (Task17 Subtask 2 Leader), A. Alchami (France)

COVER PICTURE

Living Lab and Experimental Platform - PV-powered charging station, Innovation Center of Université de Technologie de Compiègne, France

INTERNATIONAL ENERGY AGENCY

PHOTOVOLTAIC POWER SYSTEMS PROGRAMME

PV-Powered Electric Vehicle Charging Stations

Requirements, barriers, solutions and social acceptance

IEA PVPS
Task 17
PV and Transport

Report IEA-PVPS T17-04:2025
January - 2025

TABLE OF CONTENTS

ACKNOWLEDGEMENTS

This paper has received valuable contributions from several IEA-PVPS Task 17 members and other international experts. Many thanks to all of them.

The French contribution is funded by the Agency for Ecological Transition (ADEME) under grant numbers 1905C0043 (PV2E-Mobility) and 2308D0002 (T-IPV).

LIST OF ABBREVIATIONS

3G	Third Generation
AC	Alternating Current
ADEME	Agence De l'Environnement et de la Maîtrise de l'Énergie
BEV(s)	Battery Electric Vehicle(s)
CEA	Commissariat à l'Énergie Atomique et aux Énergies Alternatives
CO_2	Carbon Dioxide
COP	Conference of the Parties
COVID	COrona VIrus Disease
CPLEX	C language simPLEX algorithm
CPO	Charging Point Operator
CT(s)	Charging Terminal(s)
DC	Direct Current
DOD	Depth of Discharge
DSO	Distribution System Operator
EV(s)	Electric Vehicle(s)
EVCI	Electric Vehicle Charging Infrastructure
GHG	Greenhouse Gas
HMI	Human Machine Interface
HSi	Human-System interface
I2B	Infrastructure-To-Building
I2H	Infrastructure-To-Home
I2V	Infrastructure-To-Vehicle
ID	IDentification
IEC	International standard for Electric vehicle Conductive charging systems
IIREV(s)	Intelligent Infrastructure(s) Recharging Electric Vehicles
ISO	International Organization for Standardization
KPI	Key Performance Indicators
LCA	Life Cycle Assessment
MILP	Mixed-Integer Linear Programming
MPPT	Maximum Power Point Tracking
NMC	Nickel Manganese Cobalt
NOCT	Nominal Operating Cell Temperature

NREL	National Renewable Energy Laboratory
OCPP	Open Charge Point Protocol
PGCS	Public grid-powered charging station
PHEV(s)	Plug-in Hybrid Electric Vehicle(s)
PV	PhotoVoltaic
PVCS	PV-powered Charging Station
QR code	Quick Response code
RC	Reinforced Concrete
RFID	Radio Frequency IDentification
RTE	Réseau de Transport d'Electricité
SCADA	System Control and Data Acquisition
SIGE	Système d'Information pour la Gestion optimisée de l'Energie
SOC	State of Charge
STC	Standard Test Conditions
V2B	Vehicle-to-Building
V2G	Vehicle-to-Grid
V2H	Vehicle-to-home
V2V	Vehicle-to-Vehicle

EXECUTIVE SUMMARY

As the shift to electric mobility gains momentum, deploying efficient and sustainable Electric Vehicle (EV) charging solutions becomes crucial. In this context, the first report published by IEA Task 17 Subtask 2 highlights the main requirements and feasibility conditions for maximizing the benefits of photovoltaic (PV) energy through PV-powered charging stations (PVCS).

This second report explores the technical, economic, environmental, and social dimensions of EV charging infrastructure, with particular emphasis on microgrid-based stations that integrate photovoltaic sources and the smart energy management of these stations using intelligent charging systems. Additionally, it examines the socio-technical challenges related to user acceptance and the social acceptability of EV charging infrastructure, reflecting on how these factors influence the successful implementation of electromobility solutions.

This executive summary addresses five key topics. First, it outlines what was studied and the main findings. Then, it presents the key recommendations.

A. EV charging control and power management with demand response

The contribution of EVs in reducing greenhouse gas emissions depends on the energy mix of the public grid. However, the public grid may become vulnerable as the number of EVs increases drastically, as predicted in many global scenarios. Considering several factors—such as the number of passenger EVs, charging power values, EV consumption, and average daily urban or peri-urban trips of 20–60 km—a study investigates the power grid issues related to EV charging. The results show that while the grid can accommodate the total energy required for EV charging, the total power demand may pose a challenge. Although this study is based on data from the French electricity grid, the conclusions are broadly applicable.

B. Human-System Interface for PVCS

Human-System Interface (HSi) is essential for the local control of a PVCS. It enhances user interaction and system management. A well-designed HSi provides users with real-time data on charging status, energy production, and consumption, enabling them to make informed decisions about their charging habits. It also facilitates the monitoring and control of the charging process, allowing users to adjust settings based on their needs or preferences. Furthermore, the HSi plays a crucial role in troubleshooting and maintenance by providing alerts for system malfunctions or performance issues. By improving the overall user experience, the HSi encourages greater adoption of PV charging technology and supports the transition to renewable energy sources.

C. Smart Charging and real-time management for EVs

Smart charging and real-time management for EVs represent a transformative approach to energy utilization in the transportation sector, especially when integrated with PV systems. By leveraging advanced technologies and communication networks, smart charging systems optimize the charging process based on grid conditions, energy prices, and user preferences. This dynamic management allows vehicles to charge during off-peak hours when energy demand is low, reducing costs for users and minimizing strain on the grid. When combined with PV integration, these systems can harness solar energy to power EV charging, further enhancing sustainability.

Real-time data analytics enables efficient energy distribution, ensuring that charging stations adapt to fluctuating demand and effectively utilize renewable energy sources. A real-time energy management system using MILP optimization, implemented in France, demonstrated the feasibility of controlling EV charging while reducing energy costs. Another study conducted in France showed that synchronizing the power consumption of 24 charging points with solar energy production is feasible, increasing the self-production ratio while meeting user needs. A study in Portugal highlighted the potential of solar parking lots to enhance electric mobility while addressing challenges in aligning peak solar production with demand. With careful management and consideration of electricity pricing, these systems can achieve favourable economic returns within a reasonable payback period.

Although these findings are based on case studies in France and Portugal, they provide insights that lead to generalizable conclusions.

D. *Technical and economic feasibility analysis of PVCS*

The PVCS has been analyzed from technical, economic, and environmental perspectives. A three-step methodology leading to a quantitative evaluation of the PV benefits for the PVCS was designed. A tool has been proposed to adjust the investment cost of the PVCS based on four parameters: the type of PV panels, the number of PV panels, the number of terminals, and the capacity of the stationary storage. This decision-support tool can be used to optimally size the PVCS and, through simulation, determine the operating modes that maximize the use of PV energy for EV charging.

E. *Societal impact and social acceptability of PVCS*

The social acceptability of PVCS should be studied alongside the technical analysis, with the aim of improving the project and increasing public awareness. The purpose is to assess the acceptability of PVCS and their new associated services, such as smart charging and bidirectional energy transfer, through a field study. The study was conducted on a city scale and involved a large number of stakeholders. Consequently, it seeks to analyze the concept's limitations from the public's perspective and highlight the evolution of people's mindsets over the years.

Key recommendations

- Public grid impact
  - Considering the possibility that 10% of EVs may simultaneously use rapid charging (50 kW), the network must allocate at least 19% of its total installed power to meet the charging needs of 5 million EVs. Smart charging is essential and must go beyond the usual practice of reducing power at charging terminals.
  - The widespread use of PV sources for daytime charging can reduce dependence on the electricity grid. Through local energy production, PVCS enables EV charging, the return of excess energy to the grid, and the implementation of vehicle-to-grid (V2G) applications.
- Optimized Energy Use
  - Smart charging adjusts charging power and timing based on PV energy availability, grid conditions, and user preferences, ensuring the efficient use of PV energy and preventing grid overload.
  - Human-System Interfaces (HSI) for PVCS are essential for enabling the characterization of services and facilitating the retrieval of various types of

information. This includes the frequency of charging sessions, EV load patterns, management of EV charging sessions, PV energy consumption, sustainability reports of charging sessions via email, valley and peak power consumption from the utility grid, and time-of-use tariff proposals for EV drivers. HSI is crucial for communicating with users to meet their requests and inform them about the energy distribution during charging, whether from the grid, PV, or stationary storage.

  - Real-time control, based on an energy management optimization algorithm, maximizes PV energy benefits and minimizes total energy costs while meeting user demand through HSi.
  - Based on users' forecasted departure times, real-time control can fully recharge the EV's battery while maximizing the use of PV energy during the process. Depending on the departure time, most EVs are charged with more than 80% PV energy.
  - Using real parking occupancy data collected over a full year, smart charging at a PV-powered parking lot near a suburban train station on the outskirts of Lisbon, Portugal, resulted in a significant reduction (over 35%) in electricity imports from the grid.

- Global Cost and Carbon Impact Assessment
  - Based on the LCA, a specific calculation methodology is necessary to assess the overall cost and carbon impact of PVCS.
  - For a 30-year life cycle for PVCS:
    - The global cost includes approximately 40% investment costs and 49% maintenance costs.
    - Compared to traditional charging stations powered by grid electricity, the PVCS carbon impact is between 1,5 and 10 times smaller, depending on the energy mix implemented in the electricity grid.
  - Case Study: PVCS located in the north of France, covering 5 parking spots, equipped with a 22kWh stationary battery storage capacity, and recycled using pyrometallurgy. The installation consists of 28 kWp peak power across 70 panels installed on a surface of 124 m^2.
    - The global cost requires an initial investment of almost 65 k€, and may present a total cost of 150 k€ after 30 years.
    - The carbon impact assessment results show 40,7 gCO2eq/kWh, while a public grid-powered charging station shows an average of 275 gCO2eq/kWh for the European Union and 368 gCO2eq/kWh for the USA.
- Social acceptance
  - Based on a survey conducted in France on the social acceptance of PVCS and new services (particularly V2G), the study reveals that PVCS is socially acceptable to a large majority. However, some aspects, such as location, business model, and design, require careful consideration. Notably, over 83% of the 864 respondents agree with the V2G service. The main obstacles to the use of PVCS are often related to the efficiency of the PV panels, the recycling process, and pollution during the production phase.

1 REQUIREMENTS, BARRIERS AND SOLUTIONS FOR PV-POWERED CHARGING INFRASTRUCTURE FOR EV CHARGING

PVCS are becoming a sustainable solution for charging EVs. However, their integration requires comprehensive studies on specific requirements, barriers, and solutions. The technical requirements include the selection of an appropriate PV system, storage systems, and a control system. Meanwhile, barriers involve factors such as high initial investment costs, complex integration processes, and the need for standardized regulations. Innovative solutions like smart charging algorithms, grid integration techniques, and communication algorithms can help overcome these challenges. By adopting these measures, the widespread adoption of EVs will be facilitated, accelerating the transition to a low-carbon transportation system.

The first section explores the influence of the increasing number of EVs on the French electricity system. Through various scenarios, the analysis reveals the grid's capacity to manage the overall energy needed for EV charging, with potential challenges in total power demand. Additionally, it underscores that controlling EV charging can efficiently limit grid power demands, fostering the use of local and green energy sources.

The second section discusses the design of an interface for a PVCS that offers real-time monitoring and control of the charging process. The interface integrates information about the PV system, battery storage, and charging status to provide users with relevant and up-to-date data on the charging process. It also highlights the importance of effective human-system interfaces for promoting sustainable energy use and reducing greenhouse gas emissions.

The third section presents a cost optimization model for real-time power management of PVCS. The study considers various factors such as the availability of solar power, EV charging demand, and grid connection constraints to optimize the power allocation in real-time. The proposed model was tested using simulation and real-time experimentation, with results showing that it can effectively manage the power supply for EV charging while maximizing the utilization of solar energy and minimizing the charging cost.

The fourth section discusses the development of a supervision system to control EV charging at the CEA Cadarache research centre. The supervision system controls EV charging in real-time with two objectives: fully charging the EV batteries and synchronizing the power consumption of 24 charging points with the power production of a solar photovoltaic plant. The system aims to reduce the impact of EV charging on the power grid. Experimental results show that it is technically feasible to increase the self-production ratio by up to 60 percentage points while satisfying EV users.

The fifth section, examines the integration of solar energy and electric mobility in solar parking lots, focusing on park-ride locations near public transport connections. Its results highlight the relative mismatch between peak solar power and peak demand, as well as excess solar generation during weekends, challenging the economic returns for the investment. It also shows that smart charging or battery storage increases self-consumption rates but, at current prices, lead to lower returns than simpler energy management.

The final section proposes a methodology to assess the global cost and carbon impact of a PVCS. The results indicate that PVCS can significantly reduce both carbon emissions and implementation costs. However, the success of the implementation depends on various factors, including the use of newer technologies and recycled materials, which can lower the carbon footprint of the station below that of the French energy mix that is almost the most decarbonized in the world.

1.1 Public grid and distribution system operator point of view: EV charging control and power management with demand response

This section[1] studies the potential impact on the electricity grid following the integration of EVs. Additionally, it examines various strategies to mitigate the high-power demand caused by EVs.

1.1.1 Introduction

Based on the global growth in the number of electric vehicles (EVs) and the recent future scenarios released recently by the International Energy Agency [1], it appears that EVs, especially passenger cars, are becoming the norm for transportation. In 2020, the number of EVs reached 10 million, and considering the various policies and targets recently announced by governments and the private sector, the projection for 2030 is between 140 million and 245 million, depending on the sustainable development scenario. However, while there is currently a significant number of charging stations—primarily slow charging (private or public) and fast charging (public)—new trends and developments are required for EV charging stations, as well as changes in end-user behaviour.

The expected massive penetration of EVs raises questions about the charging process, the energy and power available from the public grid, and potential solutions in the event of grid vulnerabilities, considering the same power and energy capacity of the grid. The charging of EVs is generally done by drawing electrical power through a point of common coupling with the public grid. While the energy capacity of the grid may not seem problematic, the simultaneous charging of multiple EVs can cause local grid congestion, leading to severe issues, especially during peak hours. However, EVs are considered a flexible load, unlike uncontrollable loads. As a result, EV charging can be controlled and shifted to off-peak times to prevent peak loads by implementing a smart charging framework [2].

Different charging frameworks of EVs exist:

- Uncontrolled charging occurs when the EV begins charging immediately until its battery is fully charged or the EV user unplugs his vehicle. This approach is also referred to as uncoordinated or immediate charging, where the EV charges at maximum power without any restrictions. As a result, there is no interaction between the EV users and the electrical grid. This is considered the worst-case scenario because it charges the EV at maximum power to achieve full charge in the shortest time, placing strain on the grid and contributing to peak load issues [3] - [6].
- Delayed charging occurs when the park time (the duration an EV is parked at a station) is longer than the actual charging time required, therefore, the EV charging can be delayed, considering time-of-use pricing, and carried out during low-cost, off-peak energy periods [3] , [4]. However, the park time must be known by the charging terminal in advance.
- Average charging is considered when the EV is charged at constant power depending on the parking time during which the EV is able to meet the requested state of charge—

[1] This section is based on the following publication: M. Sechilariu, S. Cheikh-Mohamad and F. Locment, “Electric Vehicle Charging and Power Grid Issues Scenarios versus PV-powered charging stations”, in Colloque InterUT Systèmes sûrs et durables, Feb 2023. https://hal.science/hal-04011877

either partial or full—without needing to charge at full power [4] - [6]. This charging operation requires data from the EV's user and abilities to run the terminal with the calculated constant power, respecting the limited power of the charging terminal.

- Smart charging: EV users provide the charging station management with information regarding their parking time and the requested charge that must be supplied before leaving the station. Therefore, energy is used to supply the EVs while the public grid may control and shape the EV charging profiles, minimizing the charging costs. In addition, smart charging may be combined with renewable energy production, whether local or remote [3].

This generic classification implies, however other comments. can also be considered a smart charging framework, as it changes the charging start time, charging end time, and charging power, while most importantly delivering the requested energy to the EV. Additionally, average charging can be considered an uncoordinated charging framework, as it starts charging immediately when the EV is plugged in, but with limited power [6]. The delayed charging profile is similar to the uncontrolled charging profile but the peak load is shifted to overnight/dawn (around 05:00 AM to 09:00 AM). In contrast, in average charging, the profile is flattened instead of having a peak [4]. Uncoordinated charging of EVs may increase peak load, imposing a heavy burden on the public grid and leading to greater losses. Therefore, through smart or coordinated charging, EVs can become an asset for the grid by helping to increase the penetration of renewable energy, balance the energy system, and improve overall efficiency while satisfying EV user demands [7]. Coordinated charging is classified into two types, time-coordinated charging and power-coordinated charging as in [8]. In time-coordinated charging, the number of EVs that can charge is controlled to ensure the total load demand within the available power for EV charging. In contrast, in power-coordinated charging, the power allocated for EV charging is controlled to ensure that the total load demand stays within the available power.

The most important parameters in EV modeling are the charging/discharging rate, initial state of charge (SOC), battery capacity, charge-depleting distance, and user behaviour, which is difficult to predict in advance. Additionally, the arrival time at the charging station, departure time, and driving distance of the EV are variables that depend on user habits. However, these can be assumed to follow probability distribution functions [5], [9]. For this purpose, probability distribution functions are generated to determine the arrival time at the charging station, the departure time, and the driving distance of the EV. Then, the energy needed to fully charge the EV is calculated, and the total charging time of the EV is determined as the energy needed to fully charge the EV over the charging rate [5], [9], [10].

Following the literature review, scheduling the charging process of EVs is compulsory and the demand response highlights the off-peak hours as the best choice. Nevertheless, reconciling the incentive to switch from an internal combustion vehicle to an EV with the constraints imposed on users regarding hourly charging options will be difficult [11]. On the other hand, the literature does not reveal studies on the impacts on the public grid based on scenarios calculated or estimated from a power perspective. Therefore, it is less pertinent to analyse whether the proposed smart charging will meet users' requirements and the needs of the public grid without a significant enhancement of the grid's infrastructure.

To overcome this issue, an alternative may be the full utilization of renewable energies, thereby avoiding reliance on the public grid's spinning reserve, which is primarily composed of fossil fuel-based power plants [12].

Therefore, the electromobility requires EVs charging infrastructures based on renewable energy sources. In urban and peri-urban districts, photovoltaic (PV) panels are the most commonly used renewable energy sources. However, the intermittent nature of PV energy production makes the direct use of the PV power less efficient. Thus, for local production and consumption, a microgrid, based on PV sources, storage devices, loads, real-time power management, optimization subsystem, data collection system, and interfaces communication system become a solution for EVs charging.

This paper first introduces several scenarios regarding the impacts on the French public grid. Following that, it presents a PV-powered EV charging station, including stationary storage and public grid connection as backup power sources. Through three case studies, the conditions under which the PV energy production can alleviate the burden on the public grid—especially during peak hours—while satisfying end-user demand are investigated.

The main highlights presented in this study are the vulnerability of the public grid vulnerability under various scenarios based on the number of EVs, charging power values, EV consumption, and average daily urban and peri-urban trip of 20 to 60 km, along with data from the French public grid; and the conditions under which PV energy production involved in EV charging may mitigate issues faced by the public grid.

The article is organized as follows, Section 1.1.2 describes the impacts on the public grid when passenger EVs number drastically increases while Section 1.1.3 concludes the paper and provides perspectives.

1.1.2 Public grid impacts considering electromobility

The development of electric mobility, according to all forecasts, will be particularly sustained by 2035, everywhere in the world. In France, EVs have known sustained growth in the first half of 2020, with nearly 70 000 units sold in France, i.e., twice as many as over the same period in 2019, despite the health crisis. This strong growth is accompanied by a densification of the network of charging stations across the French territory. In December 2021 there were nearly 32 000 charging stations open to the public, directly or indirectly connected to the public grid and it is expected 100 000 charging stations in France by the end of 2022. Mechanically, this increase in the number of EVs and charging stations will induce an increase in power demand due to new charging needs. The electrical system must therefore adapt.

1.1.2.1 French transmission and distribution system operators' considerations

Regarding the French public grid, in [13] the French electricity public grid operator claim that the integration of the EVs into the French electricity system does not present particular difficulties for the public grid, both at the local level and at the national level, from an energy point of view. In addition, it is highlighted that the possibility of controlling EVs charging will facilitate a better integration of EVs in the medium term and also make it possible to promote local and / or green energy supply for extra-economic reasons, in particular by synchronizing the charging of EVs with the production of renewable energy.

From a power point of view, depending on their needs, in [13] it is well-considered that the end-users can choose a technical charging controlling solution by the activation on command or programming of the recharge / discharge and by smart communicating metering control functions leading to the adjustment of its charging power according to that of the home / building electric network. Thus, the users of the distribution network are the main beneficiaries of the control of EVs charging. In fact, the more the charging is controlled, the integration of the EVs into the power grid will be better. The benefit, for the electricity system and the community, goes to all public grid users. Furthermore, the assessment of the charging control gain against existing time-of-use offers is based on the difference between the cost of controlled charging and 'natural' charging. The control is optimized to minimize the cost of charging, as a function of the different price signals, which are the different elements of the invoice for charging. For a residential EV charging, by shifting charging during the off-peak period, when the home consumption is very low, the charging control can avoid increasing the contract subscription fee. For a fleet of a limited number of utilities charging, if the site does not have enough available power, the management of the charging may be operated by shifting it over time and over the different vehicles.

However, in [13] the studies are limited at up to 11 kW charging power. Moreover, the power analysis is not deeply investigated as well as how to reduce the cost of upgrading electrical networks without constraints for the users such as that of differentiated tariffs.

The French public grid operator estimates that in 2035 there could be up to 15,6 million EVs circulating in France [13]. Each of them would travel 14 000 kilometres per year with an average consumption of 15 kWh / 100 km. According to these assumptions, around 40 TWh of electricity would be needed to supply French EVs in 2035. This amount of energy represents approximately 7,5 to 8% of the 537,7 TWh of electricity produced each year in France (data from 2019), which it is not huge. However, these statistics remain limited to the energy consumption. However, regarding the power demand, for slow and fast charging terminals considering also the case of simultaneous connecting of some EVs, an analysis under several scenarios is necessary to identify the future issues that a public grid can have during the massive increase of EVs. The purpose of this section is to enlighten the reader on the public grid impacts considering the EVs massive growth.

Knowing that an EV consumes often between 10 and 20 kWh of electricity every 100 km, therefore, millions of EVs traveling thousands of kilometres each year could end up consuming a large part of the electricity produced in France each year. Thus, to assess how much energy and power will be required in the coming years to charge EVs, it is necessary to design a robust model based on the number of EVs in circulation in the future, number of kilometres traveled each day in a year by these EVs, and the amount of the power demanded by these vehicles to charge depending mainly on the traveled distance. Nevertheless, the charging power may be very different depending on EV model, traveled distance, user needs and behaviour, etc.

1.1.2.2 Impact of EVs energy and power demand on a public grid

To design a reliable model of power demand for EV charging, data obtained through learning methods (such as deep learning coupled with artificial intelligence) or measured data are necessary. However, to our knowledge, these models have not yet been developed or published. Therefore, regarding the power demand for EV charging—whether for slow, fast, or ultra-fast charging—considering the case of simultaneous connections of multiple EVs and the associated charging power distribution coefficients, an analysis based on several key assumptions is necessary to identify the future issues that a public grid may face during the massive increase in EV adoption.

For a public grid, the suggested analysis—considering both the demanded energy and the demanded power—may be conducted based on several assumptions:

- the total number of EVs in circulation, N_{EVs};
- the daily distance in kilometres, D;
- the available power of the charging terminals,$P_{CHARG_{TERM}}$;
- the simultaneous connection of some EVs.

Based on a daily urban/peri-urban trip and an average consumption of kWh per 100 km, the total energy demand of EVs is calculated in kWh following (1.1-1):

$$E_{EVs_{DEM_{TOT}}}[kWh] = \frac{(C \times D \times N_{DAYS} \times N_{EVs})}{100} \qquad (1.1\text{-}1)$$

where $E_{EVs_{DEM_{TOT}}}$ is the total EVs energy demand in kWh, C is the average consumption in kWh / 100 km, N_{DAYS} is the considered number of days, and N_{EVs} is the number of EVs.

Regarding the power analysis, the theoretical total power demand of EVs is calculated in kW following (1.1-2):

$$P_{EVs_{DEM_{TOT}}}[kW] = P_{CHARG_{TERM}} \times N_{EVs} \qquad (1.1\text{-}2)$$

where $P_{EVs_{DEM_{TOT}}}$ is the theoretical total EVs power demand in kW.

Assuming that a number of EVs charge simultaneously, the simultaneous demanded power is calculated in kW according to (1.1-3) or (1.1-4):

$$P_{EVs_{SIM}}[kW] = \gamma \times P_{EVs_{DEM_{TOT}}} \qquad (1.1\text{-}3)$$

Where γ is the simultaneity coefficient during the peak hours in percentage and the $P_{EVs_{SIM}}$ is the simultaneous demanded power in kW.

Knowing that the charging power may vary significantly depending on the EV model, traveled distance, user needs and behaviour, and other factors, several charging powers may be considered. To simplify, this study only considers simultaneity under a charging power distribution for slow, fast, and ultra-fast charging. In this case, the simultaneously demanded power is calculated in kW according to (1.1-4) :

$$P_{EVs_{SIM}}[kW] = \gamma \times \left[\left(\sigma_S \times P_{CHARG_{TERM_S}}\right) + \left(\sigma_f \times P_{CHARG_{TERM_F}}\right) + \left(\sigma_{uf} \times P_{CHARG_{TERM_{UF}}}\right)\right] \qquad (1.1\text{-}4)$$

where σ_S, σ_f, and σ_{uf} are the number of EVs charging in slow, fast, and ultra-fast charging respectively and the $P_{CHARG_{TERM_S}}$, $P_{CHARG_{TERM_F}}$, and $P_{CHARG_{TERM_{UF}}}$ are the terminal charging power for slow, fast and ultra-fast charging respectively in kW.

Knowing that the energy consumption for an EV is often between 10 kWh/100 km and 20 kWh/100 km, an average consumption of 15 kWh/100 km may be considered reasonable. Therefore, based on a daily urban/peri-urban trip with a consumption of $C = 15\ kWh/100\ km$, the total energy and power demand of EVs is calculated for domestic, slow, fast, and ultra-fast charging terminals.

Considerations regarding the French public grid are also required: the grid is characterized by a total yearly energy production of 537,7 TWh (E_G) and a total installed capacity of 135,328 GW (P_G) (data from 2019, before COVID-19 crisis).

Regarding the increase in the numbers of EVs, three different stocks of EVs are considered in the following.

1.1.2.3 Impact of EVs on French power grid for $\gamma = 10\%$

Table 1.1-1 summarizes the impacts on energy of three scenarios regarding the EVs stocks, considering a distance of 60 km. Based on these assumptions, EVs charging induces a minor impact on the total energy produced.

Table 1.1-1 Impact of EVs on energy

EVs data		Energy	
N_{EVs}	D	$E_{EVs\,DEM\,TOT}$ (GWh/year)	$E_{EVs\,DEM\,TOT}/E_G$ (%)
1 Million	60	3 285	0,61
5 Million	60	16 425	3,05
15 Million	60	49 275	9,16

Table 1.1-2 and Table 1.1-3 summarize the impacts on power with 10% of possible simultaneous charging of EVs.

Table 1.1-2 Impact of EVs on French power grid for domestic and slow charging terminals.

N_{EVs}	$P_{CHARG\,TERM} = 2{,}3\ kW$ Domestic terminal			$P_{CHARG\,TERM} = 7\ kW$ Slow charging terminal		
	$P_{EVs\,DEM\,TOT}$ GW	$P_{EVs\,SIM}$ GW	$P_{EVs\,SIM}/P_G$ %	$P_{EVs\,DEM\,TOT}$ GW	$P_{EVs\,SIM}$ GW	$P_{EVs\,SIM}/P_G$ %
1 Million	2,3	0,23	0,17	7	0,7	0,52
5 Million	11,5	1,15	0,85	35	3,5	2,59
15 Million	34,5	3,45	2,55	105	10,5	7,76

Table 1.1-3 Impact of EVs on French power grid for fast and ultra-fast charging terminals.

N_{EVs}	$P_{CHARG\,TERM} = 22\ kW$ Fast charging terminal			$P_{CHARG\,TERM} = 50\ kW$ Ultra-fast charging terminal		
	$P_{EVs\,DEM\,TOT}$ GW	$P_{EVs\,SIM}$ GW	$P_{EVs\,SIM}/P_G$ %	$P_{EVs\,DEM\,TOT}$ GW	$P_{EVs\,SIM}$ GW	$P_{EVs\,SIM}/P_G$ %
1 Million	22	2,2	1,63	50	5	3,69
5 Million	110	1,1	8,13	250	25	18,47
15 Million	330	3,3	24,39	750	75	55,42

One notes that for the most critical case of 15 million EVs in circulation charged by a slow charging terminal with a required power of 7 kW, the impact of EV charging on energy demand and total installed power is minor; however, demand response management must be involved. Conversely, for 15 million EVs charged by a fast charging terminal with a required power of 22 kW, EV charging induces a major impact on the public grid (nearly 25% of the total installed power), and a significant impact (more than 55% of the total installed power) occurs for EVs charged by an ultra-fast charging terminal with a required power of 50 kW. Even with strong implementation, demand response management will not be sufficient to maintain a correct supply for the French territory.

Considering only fast-charging terminals with power up to 50 kW and only 10% of possible simultaneous charging during peak hours, the installed power is significantly impacted when connecting millions of EVs.

1.1.2.4 Impact of EVs on French power grid for $\gamma = 10\%$ and distributed charging power

This scenario becomes more realistic considering that, by 2035, most of users will have integrated the control of EV charging by shifting their charging to off-peak periods, avoiding exceeding the subscribed power, and managing EV charging operations by shifting them over time and across different vehicles. Among the projected 15,6 million of EVs in 2035, it is assumed that 30% will always be under charging control, while the other 70% may charge depending on users' needs at public charging stations. Thus, the scenario focuses on these $N_{EVs} = 10{,}9\, million$ of EVs, with 10% charging simultaneous at slow, fast, and ultra-fast power during the peak hours (meaning that a global γ of 10% is considered). To differentiate the various charging operations, the following distribution of the number of EVs charging at slow, fast, and ultra-fast rates is taken into account: $\sigma_S = 3{,}27\, million$ (30% of NEVs), $\sigma_f = 5{,}45\, million$ (50% of NEVs), and $\sigma_{uf} = 2{,}18\, million$ (20% of NEVs). This distribution of charging power during peak hours is an arbitrary choice, but it makes sense given the assumptions made at the beginning of this third scenario.

The $P_{EVs_{SIM}}$ in kW is calculated following (1.1-4) and the result is given in (1.1-5)

$$P_{EVs_{SIM}} = 25{,}18\, kW \tag{1.1-5}$$

According to (1.1-5), it is noted that even under an optimistic scenario and without considering the already existing ultra-fast charging terminal between 100 kW and 400 kW, there is always a significant impact on the public grid, with more than 18,5% of the total installed power. Therefore, although the electricity grid operator considers that the overconsumption of electricity generated by EVs should be absorbed without difficulty by the current infrastructure, this study shows that the growth of EVs must be approached with careful consideration of power demand and peak demand across different charging types. Additionally, robust EV charge control and power management solutions are required.

Furthermore, it is essential to ensure that users can charge their EVs throughout the territory and not only at their homes. Traditional tariff control systems, based on peak and off-peak hours, combined with smart metering signals, could be strengthened to encourage EVs to charge automatically during periods of low power demand.

On the other hand, local PV energy production combined with efficient energy management, can reduce the impacts of EVs on the electrical system by decreasing the power demanded from the grid [13], consequently increasing the proportion of PV energy used for charging EVs. Therefore, a charging control system based on a microgrid is necessary to prevent the saturation of the power grid.

1.1.3 Conclusions

The public grid impact study shows that the energy consumption of EVs is not an issue for a well-developed power grid, while the power demand of EVs—especially during peak hours—represents the major impact. Even under the scenario calculated with the most optimistic conditions and without considering the already existing ultra-fast charging terminals (greater than 100 kW), a significant impact remains, with more than 18,5% of the total installed power. Despite the electricity grid operator's optimistic opinion regarding the current infrastructure, this study indicates that the growth of EVs necessitates charging control and peak power demand management with as few user constraints as possible. However, in all scenarios, user behaviour is identified as a key parameter in this issue.

REFERENCES

[1] IEA Global EV Outlook 2021. Available online: https://www.iea.org/reports/global-ev-outlook-2021 (accessed on 23 April 2021).

[2] Nour, M., Chaves-Ávila, J. P., Magdy, G., Sánchez-Miralles, Á., Review of Positive and Negative Impacts of Electric Vehicles Charging on Electric Power Systems, Energies, vol. 13, no. 18, Art. no. 18, Jan. 2020, doi:10.3390/en13184675.

[3] Chen, C., Duan, S., Microgrid economic operation considering plug-in hybrid electric vehicles integration, Journal of Modern Power Systems and Clean Energy, vol. 3, no. 2, pp. 221–231, Jun. 2015, doi: 10.1007/s40565-015-0116-0.

[4] Zhang, L., Brown, T., Samuelsen, G. S., Fuel reduction and electricity consumption impact of different charging scenarios for plug-in hybrid electric vehicles, Journal of Power Sources, vol. 196, no. 15, pp. 6559–6566, 2011, doi: https://doi.org/10.1016/j.jpowsour.2011.03.003 .

[5] Li, H., Gong, X., Chen, W., Zeng, X., Optimal Scheduling of Electric Vehicles and Isolated Microgrid based on Differential Search Algorithm, WCICA 2018 13th World Congress on Intelligent Control and Automation, Jul. 2018, pp. 1115–1119. doi: 10.1109/WCICA.2018.8630690.

[6] Clairand, J.-M., Rodríguez-García, J., Álvarez-Bel, C., Smart Charging for Electric Vehicle Aggregators Considering Users' Preferences, IEEE Access, vol. 6, pp. 54624–54635, 2018, doi: 10.1109/ACCESS.2018.2872725.

[7] Rawat, T., Niazi, K. R., Comparison of EV smart charging strategies from multiple stakeholders' perception, The Journal of Engineering, vol. 2017, no. 13, pp. 1356–1361, 2017, doi: 10.1049/joe.2017.0553.

[8] Kumar, K. N., Sivaneasan, B., So, P. L., Impact of Priority Criteria on Electric Vehicle Charge Scheduling, IEEE Transactions on Transportation Electrification, vol. 1, no. 3, pp. 200–210, Oct. 2015, doi: 10.1109/TTE.2015.2465293.

[9] Akram, U., Khalid, M., Shafiq, S., An Improved Optimal Sizing Methodology for Future Autonomous Residential Smart Power Systems, IEEE Access, vol. 6, pp. 5986–6000, 2018, doi: 10.1109/ACCESS.2018.2792451.

[10] Huang, T., Wang, J., Research on charging and discharging control strategy of electric vehicles and its economic benefit in microgrid, in 2016 IEEE International Conference on Power and Renewable Energy (ICPRE), Oct. 2016, pp. 518–522. doi: 10.1109/ICPRE.2016.7871130.

[11] Sechilariu, M., Molines, N., Richard, G., Martell-Flores, H., Locment, F., Baert, J., Electromobility Framework Study: Infrastructure and Urban Planning for EV Charging Station Empowered by PV-based Microgrid, IET Electr. Syst. Transp., Vol. 9, pp 176–185, 2019.

[12] Ghotge, R., Snow, Y., Farahani, S., Lukszo, Z., Wijk, A.V., Optimized Scheduling of EV Charging in Solar Parking Lots for Local Peak Reduction under EV Demand Uncertainty, Energies, Vol. 13, pp 1275, 2020.

[13] RTE / Avere-France Issues in the development of electromobility for the electricity system, May 2019. Available online: https://www.rte-france.com/actualites/developpement-du-vehicule-electrique-et-systeme-electrique-une-faisabilite-sereine-et and https://www.rte-france.com/en (accessed on 20 April 2021).

[14] Cheikh-Mohamad, S.; Sechilariu, M.; Locment, F.; Krim, Y. PV-Powered Electric Vehicle Charging Stations: Preliminary Requirements and Feasibility Conditions. Appl. Sci. 2021, 11, 1770. https://doi.org/10.3390/app11041770

1.2 Human-System Interfaces for PV-Powered Electric Vehicles Charging Station

In this section[2]©, a human-system interface (HSi) for PV-powered EV charging stations is presented. The proposed environment is designed to analyze the energy system in three main segments: EVs' charging behaviour, drive decarbonization, and grid optimization. The HSi can work in 'simulation mode' and 'real-time mode'. In both cases, it calculates, collects, and transmits data from a MATLAB-Simulink model of a grid-connected DC microgrid. The tool displays useful information about the microgrid's status, the charging behaviour of EV users and the adoption of green energy in each charging session.

1.2.1 Introduction

The electric vehicle (EV) market is steadily expanding worldwide. To further propel this technology, development and research efforts are focused on enhancing the charging infrastructure for EVs. Additionally, the focus also lies on increasing the interest of new EV users by ensuring that the charging infrastructure offers them a level of comfort comparable to that of internal combustion engine vehicles [1][2]. To further encourage EV adoption, the literature presents technical, social, and economic studies [3]. The challenges related to the sustainability of the power grid are also analyzed in [4]. Due to the growth of the EV market and the higher current rates needed in the charging process, the power demand from the utility grid is expected to soar in the coming decades [5][6]. In order to cope with this issue, studies focus on how to power EVs with renewable energy as stated in [7][8]. Likewise, the implementation of smart charging strategies is analyzed to minimize the energy cost and optimize charging time [9][10]. Moreover, in the last decade, new services enabling the provision of energy to the grid, home, or building— known as vehicle-to-grid (V2G), vehicle-to-home (V2H), and vehicle-to-building (V2B), have been introduced [11].

Recent studies [12][13] have presented the microgrids as a feasible alternative in the development of the EVs charging network. Founded on renewable energy sources, microgrids offer advantages to utilities, customers, and society at large. They enhance power quality, providing economic benefits to users. Another positive aspect is the improvement of electric reliability, ensuring a continuous power flow during grid outages. Lastly, microgrids promote clean energy and reduce CO_2 emissions [14]. However, their implementation relies on prior knowledge of technical-economic aspects, environmental information (location, climate, standards, regulations, local energy price, etc.) and coverage. Several software tools and new approaches are employed to address these factors. The aim is to support engineers in proposing optimal designs and ensuring the correct behaviour of the microgrid while in operation [15][16]. In these studies, the tools widely used are HOMER® Microgrid Software by the company HOMER Energy, and EnergyPLAN, developed by the Sustainable Energy

---

[2] This section is based on the following publication: C.E. Montaño-Salcedo, M. Sechilariu and F. Locment, "Human-System Interfaces for PV-Powered Electric Vehicles Charging Station," 2021 IEEE 30th International Symposium on Industrial Electronics (ISIE), 2021, pp. 1-6, https://doi.org/10.1109/ISIE45552.2021.9576251

Planning Research group at Aalborg University (in cooperation with the company PlanEnergi). Both tools primarily focus on analysing and evaluating the economic and technical impact of various energy technologies, considering their cost, availability, and electric load. However, these tools do not include environmental and social analyses, which could lead to project failures. Regarding monitoring technologies, microgrid requires supervisory control and data acquisition systems [17][18] to monitor and control measurements, thereby ensuring the proper performance of this type of energy system.

In the following, a user-friendly graphical interface for a PV-Powered EVs charging station is presented. The graphical environment is based on MATLAB® App designer, as it is interactive and ensures ease of use. It helps to the HSi's operator to study smart charging techniques, propose efficient and optimal green energy management schemes, and evaluate the capacity of the energy system considering different EV charging behaviour patterns. Furthermore, it allows for the assessment of the potential to connect EVs with an urban energy system and the utility grid via V2B and/or V2G services. From the EV driver's side, the tool may support the design of EV user-welfare strategies based on monetary benefits, cost savings in EV charging, and the environmental repercussions of charging. The remainder of this paper is organized as follows: Firstly, a PV-Powered EVs charging station is presented in Section 1.2.2. The interface design and the algorithms implemented are described in Sections 1.2.3 and 1.2.4. The testing results and simulation results are given in Sections 1.2.5 and 1.2.6. Finally, conclusions and perspectives are drawn.

1.2.2 Theoretical framework

The PV-powered EVs charging station is based on an intelligent infrastructure for recharging EVs (IIREVs) as presented in [3]. It is an innovative and environmentally friendly urban energy system based on a grid-connected DC microgrid. The IIREVs mainly comprises a renewable source (PV arrays), storage devices (lithium-ion batteries and supercapacitors), a connection to the public grid, loads (a heterogeneous fleet of EVs and buildings), and charging terminals (CTs). The entire system is presented in Figure 1.2-1, where I2B, I2H, and I2V denote infrastructure-to-building, infrastructure-to-home, and infrastructure-to-vehicle respectively.

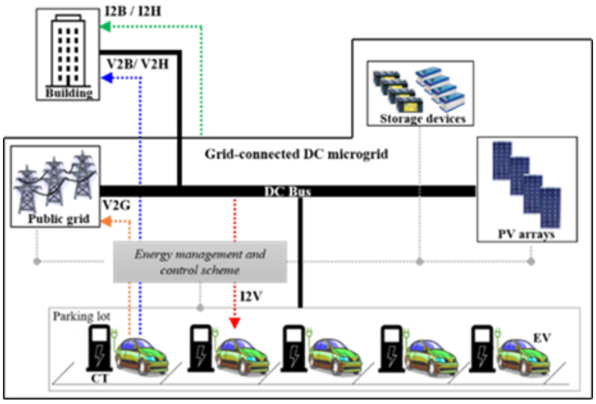

Figure 1.2-1 Example of IIREVs

The storage devices are used to complement the intermittency of the PV power, supply energy to end users and, if available, inject power to the public grid. The public grid supports the energy system when the solar irradiance is low, making the PV power insufficient to charge the EVs. Furthermore, when the PV power and the storage power are higher than required from EVs or building, the excess power can be sold to the public grid. The energy management and control scheme subsystems are essential for maintaining the power supply-demand balance and ensuring generation and energy consumption at minimal cost. In addition to a detailed description of each component of the system and the interactions among them, control and energy management algorithms are presented in [14].

The IIREVs interacts with different energy sources in the system, such as the storage system, the public grid, the PV, as well as with EVs users, and a nearby building. The urban energy system is able to manage optimized power flows in accordance with the requirements of EVs users, building/home owners, and the public power grid, considering the services shown in Figure 1.2-1:

- V2G service: An EV discharges its battery into the public grid;
- V2B/V2H service: An EV discharges its battery into a building or home;
- I2B/I2H service: IIREVs provides electrical supply to a building or home;
- I2V service: IIREVs provides electrical supply to EVs.

The V2G service helps to flatten consumption peaks at the power grid level, whereas V2B/V2H services level out consumption peaks at the building or home level and ensure a continuous supply during electrical outages. The I2B/I2H implies that any excess energy generated by IIREVs, which is not utilized by the EVs, is directly directed to supply the building.

1.2.3 HSi for PV-powered EVs charging stations

1.2.3.1 Graphical User Interface description

This section introduces the HSi for PV-powered charging stations. The HSi facilitates the adjustment, definition, and customization of IIREVs' operational criteria while monitoring their control performance. From the perspective of an HSi operator, the interface functions as an analysis tool, enabling the study of the implications of technical constraints within a microgrid. This includes other entities involved in the charging station, such as EVs and the utility grid, which affect the design and planning of the energy system. Additionally, it plays a crucial role in ensuring reliability and efficiency in this specific application.

The primary objective of this tool is to delineate the services offered by IIREVs, as mentioned in Section 1.2.2. To achieve this, the interface utilizes various operational parameters from IIREVs while considering restrictions imposed by the public grid. Similarly, it considers EV user preferences, such as the desired charging mode and the state of charge ($SOC_{request}$).

Furthermore, the HSi incorporates additional features that enable the examination of various energy segments within IIREVs, as outlined in Table 1.2-1.

Table 1.2-1 HSi features for IIREVs' energy segment

IIREVs' Energy Segment	Key Performance Indicators (KPI)
EV Charging Behaviour	• The frequency and distribution of charging sessions over time. • Identification of patterns and EV load in the parking lot. • Verification and monitoring of charging sessions at the parking lot.
Decarbonization Efforts	• Identification of EVs that are currently using or not renewable source/storage energy. • Generation of a sustainability report via email once a charging process is completed. • Generation of educational messages to the EV user about the economic and environmental impact before they being a charging session.
Grid Optimization	• Determine the valley and peak power consumption from the utility grid. • Propose a time-of-use (TOU) tariff to the EV user based on electricity price forecasting. • Suggest that the EV user participate in a demand response program through the V2G service.

1.2.3.2 Layout design

Figure 1.2-2 shows the interface windows of the developed graphical environment. It comprises three principal tabs:

- the Charging Station tab,
- the IIREVs parameters tab and
- the Dashboard tab.

The initial tab establishes user preferences for the EVs situated in the parking lot. The IIREVs parameters tab provides control and monitoring capabilities for the parameters of each energy source within the microgrid, including their load status. The subsequent tab is specifically designed to showcase, track, and analyze essential data and metrics. The remaining tabs are used to dynamically display results obtained from PV, storage device, and each CT.

In simulation mode, the interface offers the HSi user the ability to choose between three different charging modes (slow, average, fast) and set the $(SOC_{request})$ each CT. The panel EV data emulates the information provided by the EV, such as the initial SOC $(SOC_{arrival})$ and the type of EV from various manufactures. To make the simulation as realistic as possible, a switch button was included to mimic the locking connector located in the CT's power cable. When the unlock/lock switch is set to the lock position, the power cable is secured to the inlet connector of the EV. In this condition, the simulator detects an EV at the parking lot.

Then, a status button facilitates the initiation of the charging process within the CT. Similarly, the interface allows the definition of two services (I2V and V2G) and sets the power limitation for the IIREVs.

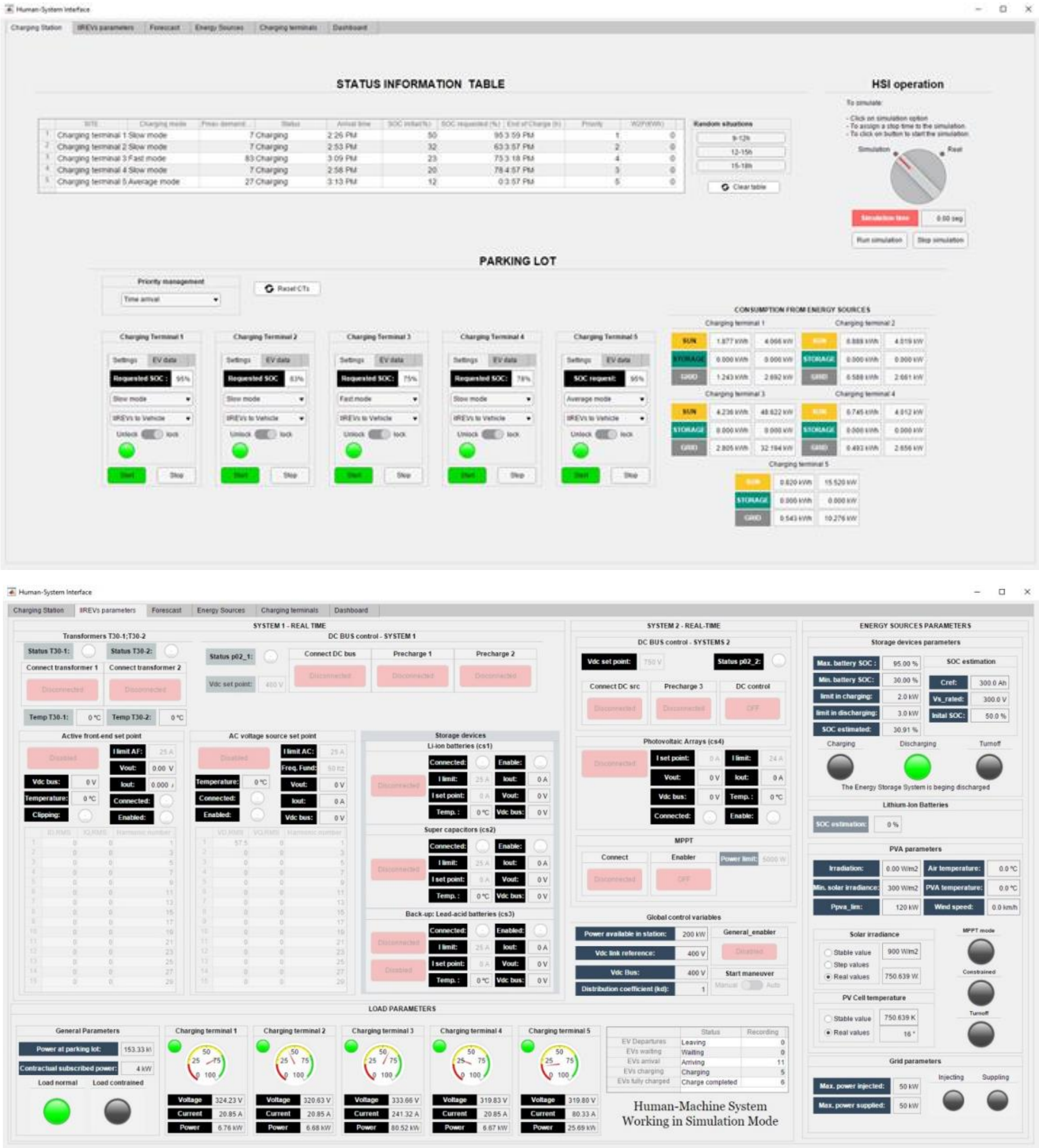

Figure 1.2-2 Main tabs of the HSi

The status information table displays the status of the CTs. To study the implications of 'user-welfare' and 'supplier-welfare' on the charging station, a priority management component was added to the HSi. This feature allows a priority to be assigned to each CT based on its number and arrival time. Additionally, it considers the maximum price that an EV user is willing to pay for the service, referred to as their 'willingness-to-pay'.

The IIREVs parameters tab covers the global parameters related to the PV, the public grid, the storage, loads, and the DC bus voltage of the IIREVs. The PV panel allows to set the peak power provided by the PV panel manufacturer under industrial standard test conditions $P_{PV_{STC}}$

and the minimum of solar irradiance. The latter represents the lowest level for the PV power and the power output to be greater than zero. To obtain an effective, accurate, and reliable simulation, real data on solar irradiance and PV cell temperature can be enabled from the interface. From the grid and the storage parameters panels, the HSi operator can customize the maximum power supply or inject into the public grid, along with and other storage parameters. The power consumption of EVs is displayed on the load parameter panel, which also includes a module to record the number of EVs in the IIREVs and their status (e.g., EV arrivals, waiting for charge, charging, or leaving the station).

In ‘real-time mode’, the interface can manage and control parameters of a real IIREVs, such as inverters enabler and the adjustments of various setpoints. Additionally, all measurement data can be accessed through the interface. A summary on this tool is shown in Table 1.2-2.

Table 1.2-2 Summary of the HSi modules in the tool

Tab interface	HSi module
Charging Station tab	• Status Information Table: Displays the status information of each charging session. • Parking lot: Emulates EV arrivals and user preferences. • Priority management: Manages prioritization strategies at the charging station. • Random behaviour: Simulates random EV behaviour over the course of a day. • Energy sources: Specifies the type of energy source per unit of energy.
IIREVs parameters tab	• Simulation and real-time parameters: the management and monitoring of parameters related to the energy system, energy sources, and loads.
Forecast tab	• Daily grid load forecasting. • Electricity price forecasting from France’s utility grid. • Solar irradiance forecasting. • Cloud opacity forecasting.
Energy sources and charging terminal tabs	• These tabs dynamically display incoming data from each energy source and each CT.
Dashboard tab	• A basic dashboard that shows the HSi operator, the total energy distribution of IIREVs, as well as each charging session.

1.2.4 HSi’s Management Strategy

Figure 1.2-3 illustrates the EV management strategy implemented for each CT within the HSi. An EV arrival is identified when three conditions are met on the interface: the $SOC_{arrival} > 0$, the unlock/lock indicator is set to ‘1’, and a type of EV is specified. In standby mode, an EV may initially enter a waiting state if the power available at the station $P_{EVs_{lim}}$ is insufficient for any of the available charging modes. Alternatively, the EV user has the option to abort the charge and leave the station (EV disconnect state). If the user agrees to the initial power system restriction or if the $P_{EVs_{lim}}$ is adequate for the chosen charging mode, the $SOC_{request}$ can be indicated by the EV user. This action serves as a transition to the priority assignment state, where the priority management strategy is activated, assigning a priority to the EV.

The charging mode preference initiates the available power test state. In this state, the HSi executes an algorithm that compares the power available in the IIREVs with the power demanded by the selected charging mode P_{EVs_D}.

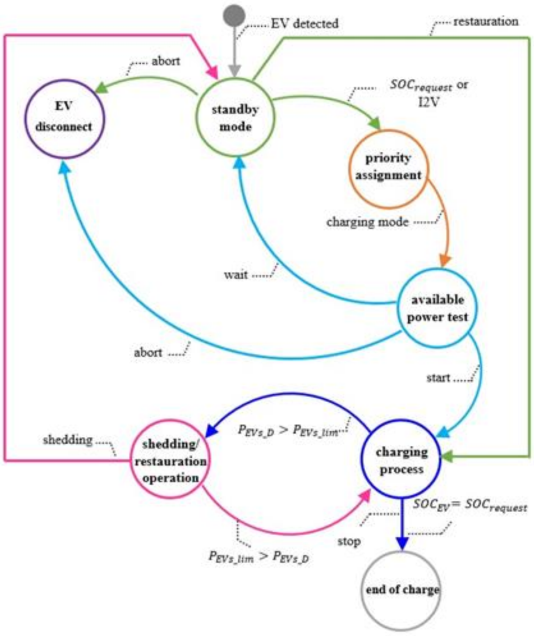

Figure 1.2-3 I2V's service state diagram implemented on the HSi

The strategy is explained in more detail in [19]. Table 1.2-3 describes the conditions, options and events involved in this state. If the condition, $P_{EVs_{demand}} < P_{EVs_{lim}}$, comes into effect, the EV can be charged. Conversely if $P_{EVs_{demand}} > P_{EVs_{lim}}$ is fulfilled, the user must choose between waiting or aborting the charge. If the user decides to wait, and the $P_{EVs_{lim}} > P_{EVs_{demand}}$ occurs, the EV starts the charging process. By comparing the $P_{EVs_{lim}}$ with the total power demanded by EVs at the station (P_{EVs_D}), the shedding and restoration operation is carried out. When the user desires to stop charging, or when $SOC_{request}$ is reached, the charging process is finalized.

Table 1.2-3 Conditions and transitions for the available power test state

Condition	Option	Transition	States	
			Previous	New
$P_{EVs_{demand}} < P_{EVs_{lim}}$	The EV can be charged	start	available power test	charging process
$P_{EVs_{demand}} > P_{EVs_{lim}}$	The EV shall wait to charge or abort the charge.	wait /abort	available power test	standby mode/ EV disconnect.
$P_{EVs_{demand}} < P_{EVs_{lim}}$	The EV can be charged	restauration	standby mode	charging process

1.2.5 Functional Testing

An essential process carried out before a real-time implementation of the HSi is the testing phase. The purpose of this phase is to validate that the interface design complies with the initial requirements proposed in accordance with the needs of the operator and the user. Likewise, it serves to ensure that all features are functioning properly. The HSi testing conducted in this study is based on a black-box testing technique [20]. This technique evaluates and validates the functional characteristics of the tool by simulating its actual use while disregarding the code structure. The testing encompasses the performance of each component on the interfaces, such as buttons control, menus, dialog boxes, lamps status, input/output fields, and so on. In this study, the Seeheim Model is used to test the basic functional aspect of the HSi [21].

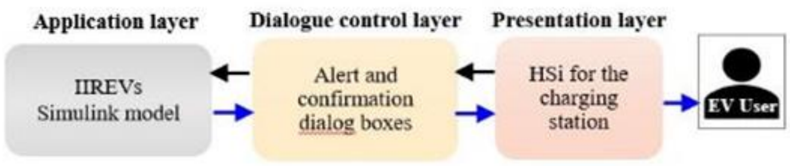

Figure 1.2-4 The Seeheim Model adapted for testing the HSi

In Figure 1.2-4, the black arrow indicates the actions taken from one layer to another while the blue arrow refers to feedback received from a layer. The presentation layer is responsible for the physical appearance of the HSi, including the screen presentation, display components and their remaining interaction functions. The dialogue control layer manages the interaction with the users, whereas the application model layer integrates the user interface with a real application. In this work, a MATLAB® -Simulink model of the IIREVs is used to emulate this latter layer. To test the functional characteristics of the HSi, several test scenarios are proposed. EVs (EV User) arrive at the charging station at different interval, varying in their initial SOC and desired SOC. It is assumed that all EVs have the same type of battery and the intention to charge it. The testing procedure for a charging process on the interface is shown in Figure 1.2-5.

When the unlock/lock switch is set to the lock position, the power cable is secured to the EV's inlet connector. The charging station detects an occupied EV charging slot (stage 1). Once all EV data and user preferences are provided, the process can be initialized by pressing the start button HSi (stage 2). The charging station complies with demanded power requirements (stage 3), and charging can be initiated by pressing the start button (stage 4). The SOC requested, charging mode, lock /unlock switch and state of the start button serve as action inputs to stimulate the presentation layer. The power demanded by EV users is the action input for the dialogue control layer. If the charging station does not have available power, the new power demand must be chosen by the EV user; this power serves as the action input to the application model layer. The action input and feedback outputs of the test procedure are shown in Figure 1.2-5.

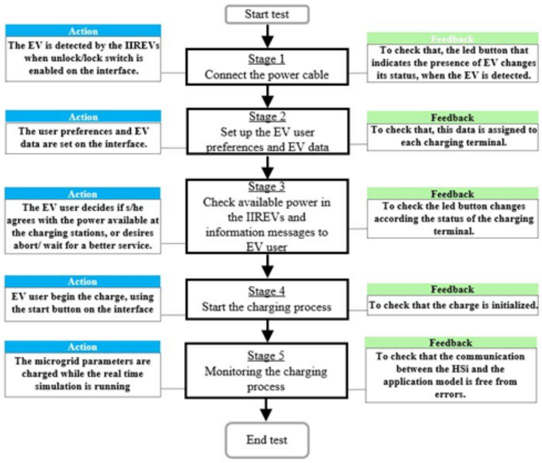

Figure 1.2-5 Test procedure for evaluating the HSi

1.2.6 Simulation results

While the HSi has been successfully tested in real-time, this paper specifically aims to verify, through simulation, the performance of the HSi, considering two KPIs.

- The frequency of charging sessions and
- The identification of EVs that are currently using renewable source or storage energy.

Figure 1.2-6 illustrates the simulation scenario where EVs arrive at each charging terminal within the IIREVs between 09:00 AM and 06:00 PM on April 27, 2021. To replicate the environmental conditions on that day, the HSi communicates with a cloud-based service known as Solarcast®, which offers tailored, site-specific predictions of solar irradiance, cloud opacity, and air temperature. This real-time data and technical parameters set up in [18] is defined on the HSi and used while the simulation is running in the background.

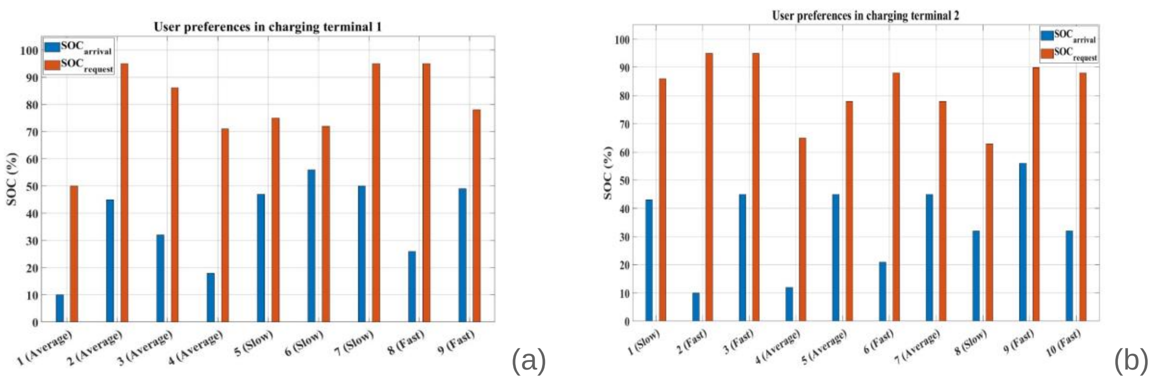

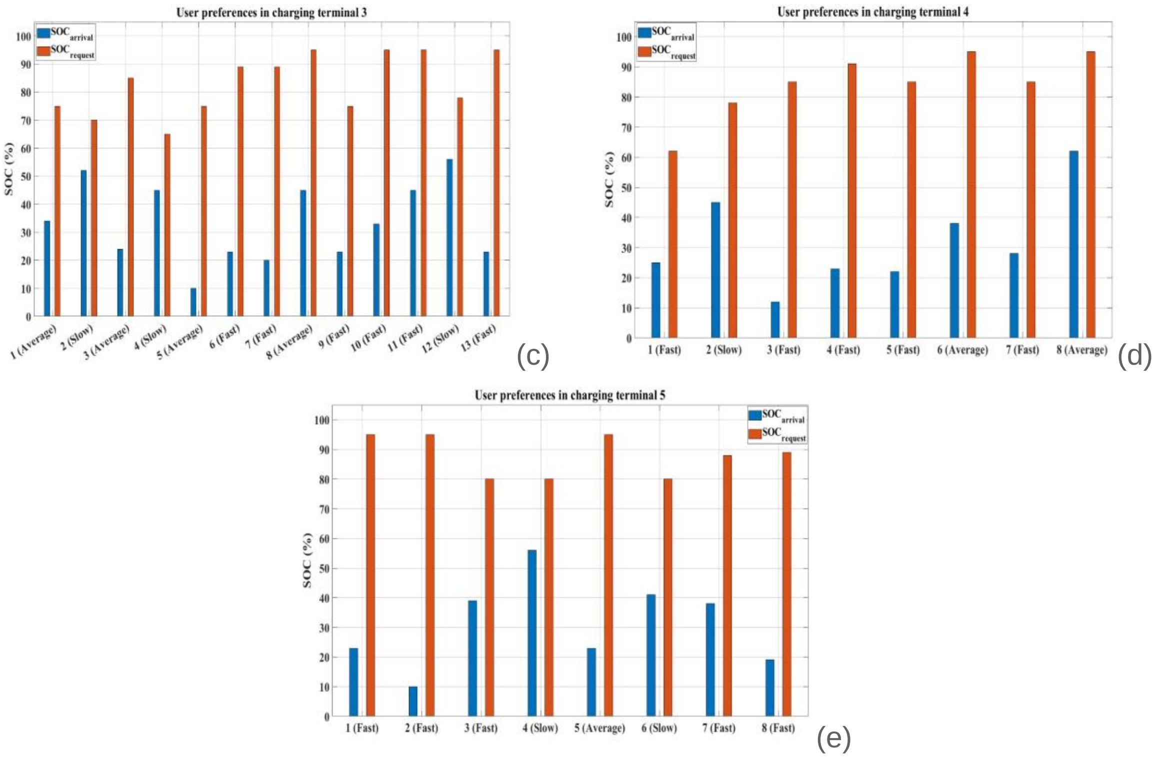

Figure 1.2-6 Charging sessions and user preferences in the IIREVs:

a) Charging terminal 1; b) Charging terminal 2; c) Charging terminal 3; d) Charging terminal 4; e) Charging terminal 5

Upon each arrival at IIREVs, the EV user chooses three preferences: the $SOC_{request}$, the charging mode (Fast mode = 83 kW, Average mode = 27 kW, Slow mode = 7 kW) and all cases in which they wish to utilize the I2V service. The EV user preferences in each charging session and CTs are depicted in Figure 1.2-6. In CT4 and CT5, eight charging sessions were initialized and completed. In the case of CT1, CT2, and CT3, 9,10,13 charging sessions were reached, respectively. In total, 48 EVs arrived at the charging station and most of them chose the fast or average charging mode. The preceding scenario seeks to emulate the hypothetical situation in which EVs require fast charging to continue any commercial activity. Figure 1.2-7 shows the energy consumption distribution at the charging station. The storage capacity is initially set to 50%, while the over-charge/over-discharge protections are set to 30% and 90% respectively. While the storage capacity does not exceed these limits, the EVs charging processes are supported solely by the PV and storage.

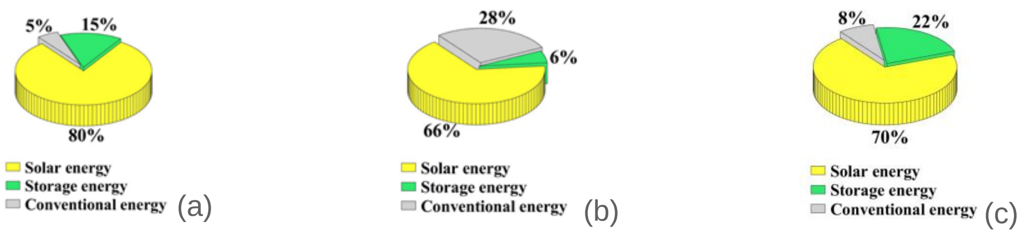

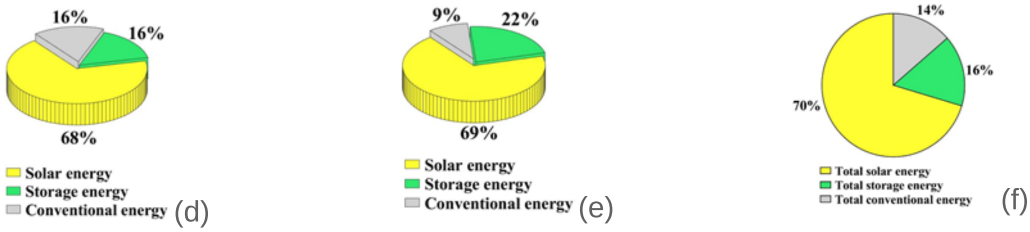

Figure 1.2-7 Energy consumption distribution at IIREVs:

a) Charging terminal 1; b) Charging terminal 2; c) Charging terminal 3; d) Charging terminal 4; e) Charging terminal 5; f) At charging station

On the contrary, the charging process for EVs is solely supported by the PV and the public grid. In this particular scenario, the overall adoption of green energy by EV users was 86%, offset by the contribution of grid energy, which accounted for 14%.

The HSi is designed to evaluate the utilization of conventional and renewable energy for two key stakeholders in the energy ecosystem: the IIREVs operator and the EV user. This approach may pave the way for creating a well-designed business model that facilitates the economic and sustainable development of PV-powered EV charging stations. It also promotes the integration and engagement of EV users in utilizing renewable energy, ultimately contributing to the increased adoption of EVs in the years to come.

1.2.7 Conclusion

This paper introduces an HSi designed for a PV-powered EV charging station. From the perspective of a system operator, the HSi enables the characterization of I2V and V2G services. Additionally, it facilitates the retrieval of various information, including the frequency of charging sessions, EV load patterns, management of EV charging sessions, renewable energy consumption by EVs, a sustainability report of the charging sessions via email, and valley and peak power consumption from the utility grid, as well as a time-of-use tariff proposal for EV drivers.

Furthermore, the graphical environment provides valuable insights into daily grid load, electricity prices, solar irradiance, and cloud opacity forecasting. Future work will focus on experimental tests to validate how the interface collects data from real IIREVs and enables an HSi operator to have supervisory control and efficient energy management.

REFERENCES

[1] T. Chen et al., "A Review on Electric Vehicle Charging Infrastructure Development in the UK," Journal of Modern Power Systems and Clean Energy, vol. 8, no. 2, pp. 193-205, 2020.

[2] H. S. Das, M. M. Rahman, S. Li, and C. W. Tan, "Electric vehicles standards, charging infrastructure, and impact on grid integration: A technological review," Renewable and Sustainable Energy Reviews, vol. 120, p. 109618, 2020/03/01/ 2020.

[3] M. Sechilariu, N. Molines, G. Richard, H. Martell-Flores, F. Locment, and J. Baert, "Electromobility framework study: infrastructure and urban planning for EV charging station empowered by PV-based microgrid," IET Electrical Systems in Transportation, vol. 9, no. 4, pp. 176-185, 2019.

[4] M. Muratori, "Impact of uncoordinated plug-in electric vehicle charging on residential power demand," Nature Energy, vol. 3, no. 3, pp. 193-201, 2018.

[5] P. Gao, H.-W. Kaas, D. Mohr, and D. Wee, "Disruptive trends that will transform the auto industry," McKinsey & Company, vol. 1, no. January, pp. 1-9, 2016.

[6] P. Gao, H.-W. Kaas, D. Mohr, and D. Wee, "Automotive revolution–perspective towards 2030 How the convergence of disruptive technology-driven trends could transform the auto industry," Advanced Industries, McKinsey & Company, 2016.

[7] C. Schuss, T. Fabritius, B. Eichberger, and T. Rahkonen, "Impacts on the Output Power of Photovoltaics on Top of Electric and Hybrid Electric Vehicles," IEEE Transactions on Instrumentation and Measurement, vol. 69, no. 5, pp. 2449-2458, 2020.

[8] K. Araki, L. Ji, G. Kelly, and M. Yamaguchi, "To do list for research and development and international standardization to achieve the goal of running a majority of electric vehicles on solar energy," ed: Multidisciplinary Digital Publishing Institute, 2018.

[9] M. Nour, S. M. Said, A. Ali, and C. Farkas, "Smart charging of electric vehicles according to electricity price," in 2019 International Conference on Innovative Trends in Computer Engineering (ITCE), 2019, pp. 432-437: IEEE.

[10] L. Gong, W. Cao, K. Liu, J. J. S. C. Zhao, and Society, "Optimal charging strategy for electric vehicles in residential charging station under dynamic spike pricing policy," vol. 63, p. 102474, 2020.

[11] L. Dickerman and J. Harrison, "A New Car, a New Grid," IEEE Power and Energy Magazine, vol. 8, no. 2, pp. 55-61, 2010.

[12] M. Dicorato, G. Forte, M. Trovato, C. B. Muñoz, and G. Coppola, "An Integrated DC Microgrid Solution for Electric Vehicle Fleet Management," IEEE Transactions on Industry Applications, vol. 55, no. 6, pp. 7347-7355, 2019.

[13] M. S. Rahman, M. J. Hossain, J. Lu, F. H. M. Rafi, and S. Mishra, "A Vehicle-to-Microgrid Framework With Optimization-Incorporated Distributed EV Coordination for a Commercial Neighborhood," IEEE Transactions on Industrial Informatics, vol. 16, no. 3, pp. 1788-1798, 2020.

[14] M. Sechilariu and F. Locment, Urban DC microgrid: intelligent control and power flow optimization. Butterworth-Heinemann, 2016.

[15] H. O. Guelleh, I. M. Mujtaba, and R. Patel, "Computational Tools used in Hybrid Renewable Energy Systems Optimization-An overview," in Computer Aided Chemical Engineering, vol. 48, S. Pierucci, F. Manenti, G. L. Bozzano, and D. Manca, Eds.: Elsevier, 2020, pp. 1477-1482.

[16] A. Kumar, A. R. Singh, Y. Deng, X. He, P. Kumar, and R. C. Bansal, "A Novel Methodological Framework for the Design of Sustainable Rural Microgrid for Developing Nations," IEEE Access, vol. 6, pp. 24925-24951, 2018.

[17] G. Artale et al., "Real-Time Power Flow Monitoring and Control System for Microgrids Integration in Islanded Scenarios," IEEE Transactions on Industry Applications, vol. 55, no. 6, pp. 7186-7197, 2019.

[18] F. Hassan and J. Geza, "Sample Case Studies for Real-Time Operation," in Microgrid Planning and Design: A Concise Guide: IEEE, 2019, pp. 121-131.

[19] D. Wang, F. Locment, and M. Sechilariu, "Modelling, Simulation, and Management Strategy of an Electric Vehicle Charging Station Based on a DC Microgrid," Applied Sciences, vol. 10, no. 6, p. 2053, 2020.

[20] M. Khan, F. J. I. J. o. A. C. S. Khan, and Applications, "A Comparative Study of White Box, Black Box and Grey Box Testing Techniques," vol. 3, pp. 12-15, 2012.

[21] S. W. L. Yip and D. J. Robson, "Graphical user interfaces validation: a problem analysis and a strategy to solution," in Proceedings of the Twenty-Fourth Annual Hawaii International Conference on System Sciences, 1991, vol. ii, pp. 91-100 vol.2.

1.3 Real-Time Power Management Including an Optimization Problem for PV-Powered Electric Vehicle Charging Stations

This section presents real-time power management, including an optimization problem formulated as MILP, for a microgrid-based intelligent infrastructure for recharging EVs (IIREVs). The DC microgrid includes photovoltaic sources, stationary storage, a power grid connection, and EV batteries as the load. The objective of the optimization problem is to minimize the total energy cost. Simulation and experimental results under different meteorological conditions demonstrate the feasibility of the proposed control and its superiority over the storage-priority strategy.[3]

1.3.1 Introduction

CO_2 emissions are a major contributor to global warming. The transport sector accounts for 25% of global energy consumption and, as a result, contributes significantly to these emissions [1][2]. Renewable energy sources have the potential to reduce greenhouse gases, including CO_2, by decreasing reliance on fossil fuel-powered electrical plants. In this context, the energy transition promotes the expansion of renewable energy, but it also introduces new challenges for grid operators regarding reliability and quality [3]. Microgrids, in particular, can help balance local energy production and consumption, offering benefits to end-users by reducing electricity costs, such as lower transmission and distribution expenses, and minimizing energy loss during transmission. Microgrids typically incorporate renewable energy sources, such as photovoltaics (PV) and wind power, as well as storage devices and loads, and they can be connected to the larger grid [4]. Electric vehicles (EVs) have garnered global attention due to their advantages: zero tailpipe emissions, quiet operation, high energy efficiency, and simple mechanical structure [5][6]. The EV market continues to grow [1][7][8]. However, the increasing demand for EV charging, which adds more loads to the grid, poses significant challenges for grid operators [9][10]. As a result, effectively managing EV charging will become a critical priority.

1.3.1.1 Literature review

Recent studies have aimed to design microgrids for EV charging. The authors of [11] proposed a mixed-integer linear programming (MILP) model for an EV charging station integrated into a DC microgrid to determine optimal operation planning, focusing on optimizing daily operational costs based on forecasts of PV production and EV operation. A hybrid optimization problem for energy storage management was proposed in [12], aiming to minimize EV charging costs in a PV-integrated charging station using time-of-use wholesale electricity pricing. In [13], the authors presented meta-heuristic methods such as binary particle swarm optimization and binary grey wolf optimization, studying an optimal charging coordination strategy for randomly arriving plug-in EVs. A MILP optimization model was proposed in [14] to minimize microgrid operation costs by aggregating an EV charging station for an islanded microgrid, and in [15],

---

[3] This section is based on the following publication: S. Cheikh-Mohamad, M. Sechilariu, and F. Locment, "Real-Time Power Management Including an Optimization Problem for PV-Powered Electric Vehicle Charging Stations," Applied Sciences, vol. 12, no. 9, p. 4323, Apr. 2022, http://dx.doi.org/10.3390/app12094323

to minimize energy generation costs and load shedding, considering various constraints in a microgrid integrating battery EV charging stations.

A heuristic operation problem was proposed in [2] for a commercial building microgrid that integrates EVs and a PV system, with a strategy focused on acquiring real-time data rather than forecasting EV charging demand or PV production. In [16], a genetic algorithm optimization was studied to solve a multi-criteria optimization problem, aiming to minimize EV charging costs, maximize the use of PV and storage devices, and reduce storage device degradation. MILP optimization was also proposed in [17] to address a day-ahead optimization problem for the optimal scheduling and operation of a prosumer owning renewable energy sources and a plugged-in EV. A feed-forward artificial neural network was used for weather prediction in the energy management system. Linear programming and quadratic programming optimization problems were addressed in [18] to minimize the total operating costs of building a microgrid integrating a heterogeneous fleet of EVs.

A multi-objective scheduling optimization problem based on genetic algorithms was presented in [19] for microgrids including EVs, aimed at reducing grid loss and charging costs, considering various constraints on microgrid sources and EV charging characteristics. In [20], the authors presented an optimal model for an energy management strategy in a real microgrid integrating a PV system with storage devices, smart buildings, and a plug-in EV, minimizing total energy consumption costs by reducing the power supplied from the grid. A robust optimization was described in [21] and compared with stochastic optimization to minimize the economic and environmental costs of a microgrid integrating PV and EVs. They developed a mathematical model to account for the uncertainty of EV charging behaviour and PV power production.

Model predictive control was depicted in [22], utilizing a smart charging strategy that considers future EV charging demand, aiming to reduce peak energy demand at an EV parking lot with PV sources. A multi-objective evolutionary particle swarm optimization problem was presented in [23] to minimize costs and grid overloading for high energy demands in EV scheduling based on a day-ahead scenario. In [24], a novel convex quadratic objective function was proposed to minimize power losses in a microgrid through a two-stage optimization method, exploring different penetration levels of plug-in hybrid EVs and their behaviour.

The authors of [25] proposed a stochastic planning model as a convex programming problem to optimize component sizes by minimizing total costs at an EV charging station, considering uncertainties in PV production, EV charging demand, and various constraints. In [26], an improved optimal sizing methodology for a typical residential microgrid integrating renewable energy sources and EVs was proposed to lower greenhouse gas emissions and costs. An annealing mutation particle swarm optimization was studied in [27] for optimal microgrid dispatching to minimize environmental protection costs and operation and maintenance costs in a multi-objective economic dispatch model. In [28], a multi-agent particle swarm optimization model was presented for a grid-connected PV, energy storage system, and EV charging station to size the PV and energy storage systems and set the charging/discharging pattern for the storage system.

A machine learning-based approach was proposed in [29] for energy management in a microgrid with a reconfigurable structure based on remote switching of ties and sectionalizing. The authors also introduced a modified optimization problem based on the dragonfly algorithm due to the complexity of the problem. The optimal configuration of PV-powered EV charging stations was studied in [30], evaluating the technical and economic impacts under different solar irradiation profiles in Vietnam using the HOMER Grid program. In [31], a genetic algorithm-based optimization model was proposed to optimize the scheduling and usage of energy sources in an intelligent hybrid energy system, including EVs and a micro-combined heat and power system.

In [32], a bi-level robust optimization was proposed to optimize the design of an EV charging station with distributed energy resources. In [33], an optimization model for a battery-swapping station was introduced to minimize EV charging costs by optimizing the charging schedule for swapped EV batteries. An optimal charging profile was proposed in [34] to minimize EV battery degradation and extend battery lifetime.

A robust optimal power management system was presented in [35] for a standalone hybrid AC/DC microgrid. The MILP optimization problem aimed to supervise power flow in the hybrid microgrid, satisfying load demand while maximizing the usage of renewable sources (PV and wind), minimizing diesel generation, extending battery life, and limiting converter usage between AC and DC microgrids. An energy management system for a grid-connected microgrid was addressed in [36] using a MILP model to minimize total energy costs over 24 hours, factoring in load demand, grid tariffs, and renewable energy production. A long short-term memory network was proposed for power prediction of renewable energy sources and load demand, with real-time implementation enabled by a receding horizon strategy to minimize prediction errors and optimize the first-hour forecast, updated every hour.

Finally, in [37], a modular modeling method was described for an energy management system for urban multi-energy sources, including cooling, heating, and renewable sources, allowing for complex system topologies. They conducted various case studies under different climate conditions and electrical loads, comparing their results with a rule-based algorithm to demonstrate annual cost reductions. In [38], the technical, economic, and environmental aspects of renewable energy in a microgrid were investigated, where an equilibrium optimization problem minimized operational costs for a system including PV, wind turbines, and a biomass generator. The simulation results confirmed the proposed algorithm's effectiveness in reducing costs and emissions. Similarly, in [39], an equilibrium optimization problem was presented for optimal PV-storage system integration in a radial distribution network, addressing multi-objective functions to minimize investment, operational, and environmental costs. The method was compared with other techniques to validate its effectiveness.

Lastly, in [40], the authors proposed an equilibrium algorithm to optimally find the parameters for lithium-ion batteries, formulated as a nonlinear optimization problem. The proposed method was compared with recent techniques, proving its accuracy and closeness to experimental results. An artificial hummingbird optimization technique was presented in [41] to find unknown parameters of lithium-ion batteries used in EVs. The experimental tests demonstrated that the proposed technique achieved the highest precision compared to other methods.

1.3.1.2 Research gaps

In the previously cited references, the optimization was performed using the EV charging prediction profile for the entire day as part of day-ahead planning. This prediction is based on contextual assumptions, such as the schedule according to the occupancy of a car park or the average EV autonomy, which have not yet been validated in real-world scenarios. In this work, the objective is to perform real-time control under optimization to minimize energy costs and maximize PV energy utilization for each EV within an intelligent infrastructure for recharging electric vehicles (IIREVs), considering the intermittent and random arrival of EVs and incorporating EV user interaction.

In this approach, the optimization is performed more realistically at the random arrival of each EV. Therefore, when a new EV arrives at the station, the state of charge (soc_s) of the stationary storage and the current state of charge of EVs (sov_{EV_v}) already charging are updated for appropriate optimization.

1.3.1.3 Contributions

The main contributions of this work are:

- Proposing EV power profiles based on the EV users' interactions with the human-machine interface (HMI);
- Introducing a new method for real-time power management, including energy cost and PV energy optimization for the IIREVs, considering the intermittent and random arrival of EVs, where optimization is performed at each EV's arrival;
- Analysing the energy distribution by source category for EV charging and the entire station energy system;
- Validating the proposed control through simulations and real-time experimental tests under different meteorological conditions and random EV power profiles.

This article is organized as follows: Section 1.3.2 presents the control system for the IIREVs, followed by a detailed explanation of the MILP optimization problem, including constraints and the objective function. Section 1.3.3 presents simulation results and analyses for different case studies. Section 1.3.4 discusses the results obtained from real-time experimental tests. Finally, the conclusions and future work are presented in Section 1.3.5.

1.3.2 Supervisory and Control System Based on Real-Time Power Management

Figure 1.3-1 shows the DC microgrid, referred to as IIREVs, which includes PV sources, stationary storage, a power grid connection, and EVs as DC loads. The PV sources operate in two modes: maximum power point tracking (MPPT), where maximum power is drawn using a perturb-and-observe algorithm, and PV power limitation, where the PV power is restricted in case of excess production [42], as the surplus can no longer be fully injected into the storage or the grid.

The stationary storage acts as a backup source, serving as an energy reservoir when PV power is insufficient to charge the EVs. In cases of insufficient PV power, the grid ensures system security by supplying power to the EVs if the stationary storage has reached its lower limit (empty or at minimum discharge power). Conversely, the DC microgrid can sell power to the grid by injecting excess PV power when production is surplus, and the stationary storage has reached its upper limit (full or at maximum charging power) [43].

As for EV charging, two modes are available: full charging, as requested by the users, and EV shedding, which occurs when it is not possible to fully supply the EVs with power.

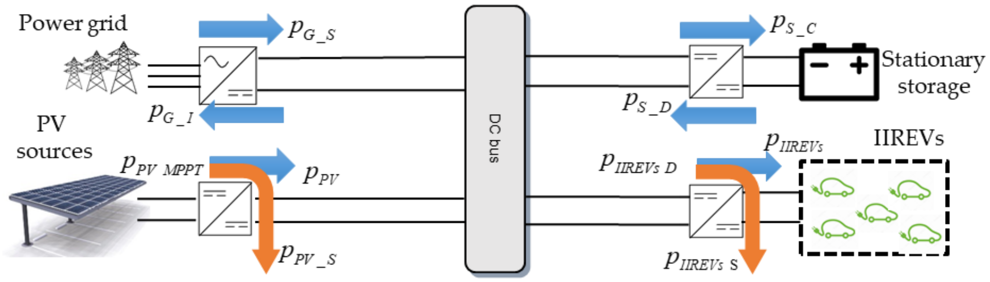

Figure 1.3-1 Power flow for the intelligent infrastructure for recharging EVs

The power flow for IIREVs is shown in Figure 1.3-1, where $p_{PV_{MPPT}}$ is the PV MPPT power, p_{PV} is the PV power, p_{PV_S} is the PV shed power, p_{G_I} is the grid injection power, p_{G_S} is the grid supply power, p_{S_C} is the stationary storage charging power, p_{S_D} is the stationary storage discharging power, p_{IIREVs_D} is the IIREVs' total demand power, p_{IIREVs} is the IIREVs' total power, and p_{IIREVs_S} is the IIREVs' shed power.

The components of the IIREVs are connected to a common DC bus via their dedicated converters. PV sources are linked to the DC bus through a DC/DC converter to extract maximum power using MPPT. The stationary storage is connected through a reversible DC/DC converter. The EV batteries, as DC loads, are also connected via DC/DC converters. The grid is linked through a three-phase bidirectional AC/DC converter. It is essential to ensure a constant power supply and mitigate any power imbalance between production and EV demand.

The supervisory control system for the IIREVs is shown in Figure 1.3-2. The supervisory control system consists of four layers: prediction, energy cost optimization, operation, and HMI. The design and implementation of the IIREVs' control are based on the interaction between EV users and the DC microgrid. The energy cost optimization and operation layers form the control block, which is responsible for maintaining power balance.

The prediction layer is based on weather forecasts. The energy cost optimization is based on the production prediction and consumption profile. They are calculated based on data from the prediction layer and the interaction with the HMI. From the prediction layer, messages from the smart grid about energy system limits, grid power limits, and dynamic energy pricing are communicated. From the interaction with the HMI, the EV users choose their charging mode (M_v), desired state of charge of their EV at departure ($SOC_{EV_{des_v}}$) in real-time, and get the state of charge of their EV at arrival ($SOC_{EV_{arr_v}}$).

MILP optimization is used for the technical-economic dispatching of the microgrid sources and load. This supervisory control has the advantage of interacting with the EV users to perform the optimization; however, if the choices of the EV users are not feasible, they have to change them in order to perform the optimization [44].

The main challenge lies in handling the discrete events from the HMI. The optimization results communicate the predictive control settings to the operation layer and update the smart grid about the power references for the stationary storage and the power grid. The operation layer contains the algorithm that maintains power balance while respecting the system's constraints and physical limits [4]. It also sets the PV power limitations and performs EV shedding if necessary.

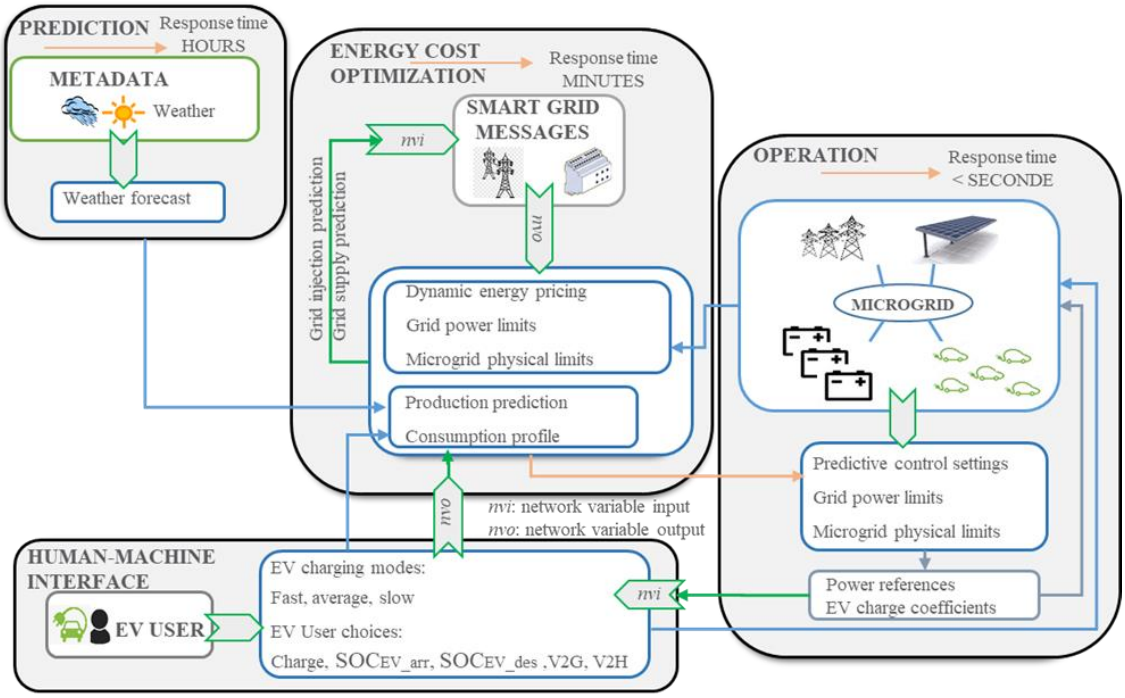

Figure 1.3-2 Supervisory control system for the IIREVs

1.3.2.1 Prediction layer

Météo France provides hourly predictions allowing the calculation of PV power prediction, which is based on solar irradiation (g) and ambient temperature (T_{amb}) forecast data [45]. The PV power prediction $p_{PV_{MPPT_{pred}}}$ is calculated in MPPT mode for each time instant t_i [46] as given in following equations:

$$p_{PV_{MPPT_{pred}}} = P_{PV_{STC}} \times \frac{g(t_i)}{1000} \times [1 + \gamma \times (T_{PV}(t_i) - 25)] \times N_{PV} \tag{1.3-1}$$

$$with\ t_i = \{t_0, t_0 + \Delta t, t_0 + 2\Delta t, \ldots, t_f\},$$

$$T_{PV}(t_i) = T_{amb}(t_i) + g(t_i) \times \frac{NOCT - T_{air-test}}{G_{test}} \tag{1.3-2}$$

where $P_{PV_{STC}}$ is the PV power under standard test conditions (STC), γ is the power temperature coefficient ($-0{,}29\%/°C$), T_{PV} is the PV cell temperature, N_{PV} is the number of PV panels, $t_0, t_0 + \Delta t,$ and t_f are the initial time instant, time interval between two samples, and time instant at the end of time operation, respectively, $NOCT$ is the nominal operating cell temperature ($41°C$), $T_{air-test}$ is the fixed air temperature ($20°C$), and G_{test} is the fixed solar irradiation ($800\ W/m^2$).

1.3.2.2 Human-Machine Interface

As for the EVs, it is possible to charge them in three modes: slow, average, and fast. All EVs can handle up to fast mode, and they are considered to have the same energy capacity. The HMI allows the EV users to set their $SOC_{EV_{arr_v}}$, M_v and $SOC_{EV_{des_v}}$, and, therefore, the estimated charging time, $t_{est_{ch_v}}$, which is the required time to reach $SOC_{EV_{des_v}}$, is calculated as given in :

$$t_{est_{ch_v}} = \frac{SOC_{EV_{des_v}} - SOC_{EV_{arr_v}}}{P_{EV_{max_v}}} \times E \qquad (1.3\text{-}3)$$

where E is the EV's battery capacity, and $P_{EV_{max_v}}$ is the maximum charging power based on the charging mode set by the EV user. The HMI for the IIREVs is shown in Figure 1.3-3 and is well explained in detail in [47].

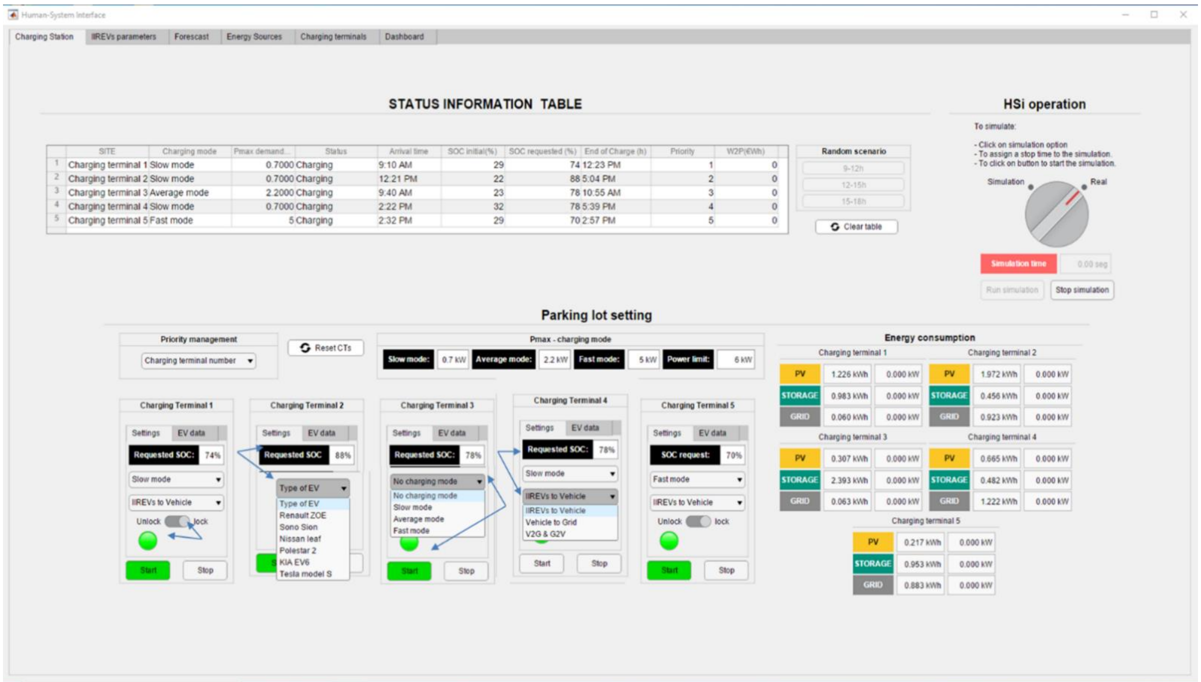

Figure 1.3-3 Human-machine interface for the IIREVs

1.3.2.3 Energy cost optimization

The energy cost optimization layer interacts with the prediction layer and the HMI to execute the optimization. The objective of the optimization is to achieve the lowest energy cost and maximize PV power for each EV. The power sharing between the stationary storage and the grid is represented by the power distribution coefficient, which is calculated from this layer using the power references obtained during optimization. The benefits of optimization encompass several aspects: reducing grid peak power consumption, minimizing energy costs, determining whether stationary storage or the grid provides the better contribution, and avoiding EV and PV shedding. Communication with the smart grid informs the system about grid power limits for injection and supply, as set by a contract with the grid operators, as well as real-time energy pricing. Additionally, the physical limits of the stationary storage must be known. The objective is to minimize the total energy cost while adhering to various constraints [45].

The constraints and objective function are presented in the following subsections.

1.3.2.3.1 PV Sources

The two operation modes for the PV are MPPT and limited power. The PV power that must be shed is noted as p_{PV_S} . Therefore, p_{PV} is calculated [45] as given by:

$$p_{PV}(t_i) = p_{PV_{MPPT}}(t_i) - p_{PV_S}(t_i) \tag{1.3-4}$$

where $p_{PV_S} = 0$ is in MPPT mode; it should not be negative in power limitation mode.

Thus, constraints are added as follows:

$$p_{PV}(t_i) \geq 0 \tag{1.3-5}$$

$$0 \leq p_{PV_S}(t_i) \leq p_{PV_{MPPT}}(t_i) \tag{1.3-6}$$

1.3.2.3.2 Stationary Storage

The stationary storage, represented by lithium-ion batteries, must be protected from overcharging and over-discharging; thus the maximum storage power $P_{S_{max}}$ and the maximum and minimum state of charge of the storage $SOC_{S_{max}}$ and $SOC_{S_{min}}$ must be respected to extend the storage lifetime [45][48] as given by (1.3-7) and (1.3-8) . The simplified state of the charge of the storage soc_S evolution [43] is given by (1.3-9) for simplicity, where self-discharge and temperature are not considered:

$$-P_{S_{max}} \leq p_S(t_i) \leq P_{S_{max}} \tag{1.3-7}$$

$$SOC_{S_{min}} \leq soc_S(t_i) \leq SOC_{S_{max}} \tag{1.3-8}$$

$$soc_S(t_i) = SOC_{S_0} + \frac{1}{3600 \times E_{bat}} \int_0^t p_S(t_i)\, dt \tag{1.3-9}$$

where SOC_{S_0} is the initial soc_S , and E_{bat} is the storage energy capacity (kWh) and the storage power $p_S(t_i) = p_{S_C}(t_i) - p_{S_D}(t_i)$. The PV power should not be limited if $SOC_{S_{max}}$ is not reached; this constraint is given by:

$$p_{PV_S} = 0 \; if \; SOC_S(t_i) < SOC_{S_{max}} \tag{1.3-10}$$

1.3.2.3.3 Grid Connection

The smart grid transmits messages to IIREVs to respect the maximum grid supply $P_{G_{S_{max}}}$ and injection $P_{G_{I_{max}}}$ limits set by the grid [45], as in (1.3-11) , where :$p_G(t_i) = p_{G_I}(t_i) - p_{G_S}(t_i)$

$$-P_{G_{S_{max}}} \leq p_G(t_i) \leq P_{G_{I_{max}}} \tag{1.3-11}$$

1.3.2.3.4 Electric Vehicles

EV batteries, seen as the entire microgrid's load, can be shed, $p_{IIREV_{S_S}}$, when $p_{IIREV_{S_D}}$ cannot be fully supplied due to deficient in power, e.g., the storage and grid have reached their limits [45]. Hence, p_{IIREV_S} is given by equation (1.3-12), and knowing that $p_{IIREV_{S_S}}$, should not be negative, thus, constraints equations (1.3-13) and (1.3-14) are added as follows:

$$p_{IIREVs}(t_i) = p_{IIREVs_D}(t_i) - p_{IIREVs_S}(t_i) \quad (1.3\text{-}12)$$

$$p_{IIREVs}(t_i) \geq 0 \quad (1.3\text{-}13)$$

$$0 \leq p_{IIREVs_S}(t_i) \leq p_{IIREVs_D}(t_i) \quad (1.3\text{-}14)$$

No PV shedding power is required when PV power can be fully used, and no EV shedding power is imposed when EVs can be fully charged. Thus, the constraints of equations (1.3-15) and (1.3-16) must be respected.

$$if\ p_{PV_{MPPT}}(t_i) \geq p_{IIREVs_D}(t_i)\ then \begin{cases} p_{IIREVs_S}(t_i) = 0 \\ p_G(t_i) \geq 0 \\ p_S(t_i) \geq 0 \end{cases} \quad (1.3\text{-}15)$$

$$if\ p_{PV_{MPPT}}(t_i) \leq p_{IIREVs_D}(t_i)\ then \begin{cases} p_{IIREVs_S}(t_i) = 0 \\ p_G(t_i) \leq 0 \\ p_S(t_i) \leq 0 \end{cases} \quad (1.3\text{-}16)$$

The EV users can select their charging mode and other choices that are expressed in the IIREVs' interface. The following EV constraints given in (1.3-17) – (1.3-31) represent the EV users' interaction:

a) *EV charging mode*

$$if\ M_v = 1\ then\ 0 \leq p_{EV_v}(t_i) \leq P_{EV_{fast_{max}}}\ \forall\ t_i \in [t_{arr_v}; t_{dep_v}] \quad (1.3\text{-}17)$$

$$with\ v = \{1,2, \dots N_v\}$$

$$if\ M_v = 2\ then\ 0 \leq p_{EV_v}(t_i) \leq P_{EV_{aver_{max}}}\ \forall\ t_i \in [t_{arr_v}; t_{dep_v}] \quad (1.3\text{-}18)$$

$$if\ M_v = 3\ then\ 0 \leq p_{EV_v}(t_i) \leq P_{EV_{slow_{max}}}\ \forall\ t_i \in [t_{arr_v}; t_{dep_v}] \quad (1.3\text{-}19)$$

$$p_{EV_v}(t_i) = 0\ \forall\ t_i \notin [t_{arr_v}; t_{dep_v}] \quad (1.3\text{-}20)$$

where v is the index of the EV, p_{EV_v} is the EV charging power of v vehicle, t_{arr_v} and t_{dep_v} are the arrival and departure time of v vehicle, respectively, and N_v is the total number of EVs.

b) *Total EV charging power*

$$p_{IIREVs_D} = \sum_v^{N_v} p_{EV_v}(t_i)\ \forall\ t_i \in [t_{arr_v}; t_{dep_v}] \quad (1.3\text{-}21)$$

c) *EV state of charge:*

$$SOC_{EV_{min}} \leq soc_{EV_v}(t_i) \leq SOC_{EV_{max}}\ \forall\ t_i \in [t_{arr_v}; t_{dep_v}] \quad (1.3\text{-}22)$$

$$soc_{EV_v}(t_i) = 0\ \forall\ t_i \notin [t_{arr_v}; t_{dep_v}] \quad (1.3\text{-}23)$$

$$soc_{EV_v}(t_i) = SOC_{EV_{arr_v}}(t_i)\ \forall\ t_i = t_{arr_v} \quad (1.3\text{-}24)$$

$$SOC_{EV_{arr_v}}(t_i) \geq SOC_{EV_{min}}\ \forall\ t_i = t_{arr_v} \quad (1.3\text{-}25)$$

$$soc_{EV_v}(t_i) \geq SOC_{EV_{arr_v}}(t_i)\ \forall\ t_i \in [t_{arr_v}; t_{dep_v}] \quad (1.3\text{-}26)$$

$$SOC_{EV_{dep_v}}(t_i) \geq SOC_{EV_{des_v}}(t_i)\ \forall\ t_i = t_{dep_v} \quad (1.3\text{-}27)$$

$$soc_{EV_v}(t_{i+1}) = SOC_{EV_{arr_v}}(t_i) + \frac{p_{EV_v}(t_i) \times \Delta t_i}{E}\ \forall\ t_i \in [t_{arr_v}; t_{dep_v}] \quad (1.3\text{-}28)$$

$$soc_{EV_v}(t_i) = SOC_{EV_{dep_v}}(t_i)\ \forall\ t_i = t_{dep_v} \tag{1.3-29}$$

where soc_{EV_v} is the state of charge of v vehicle, $SOC_{EV_{min}}$, $SOC_{EV_{max}}$, and $SOC_{EV_{dep_v}}$ are the minimum, maximum, and departure state of charge of v vehicle, respectively;

d) Acceptance criteria

The estimated charging time of the EV set by the user is t_{ch_v}, given by (1.3-30).

$$t_{ch_v} = t_{dep_v} - t_{arr_v} \tag{1.3-30}$$

$$\frac{SOC_{EV_{des_v}} - SOC_{EV_{arr_v}}(t_i)}{P_{EV_v}} \times E \ \leq t_{ch_v}\ \forall\ t_i \in \left[t_{arr_v}; t_{dep_v}\right] \tag{1.3-31}$$

If the constraints defined by (1.3-30) and (1.3-31) are not qualified, then the EV user must change their choices, e.g., estimated charging time and/or desired soc of EV at the departure time and charging mode. It is worth mentioning that $t_{est\,ch_v}$ is the minimum charging time imposed by the IIREVs, which is calculated based on the choices of the EV user. t_{ch_v} is the time of the EV spent at the IIREVs, which is set by its user. Therefore, t_{ch_v} should be equal to or greater than $t_{est\,ch_v}$ .The dynamic soc evolution of v vehicle, SOC_{EV_v}, is given by (1.3-28).

1.3.2.3.5 Power balancing

All power signs are assigned positives, and the physical law of power balancing [45] can be given by (1.3-32):

$$p_{PV}(t_i) + p_{S_D}(t_i) + p_{G_S}(t_i) = p_{IIREVs}(t_i) + p_{S_C}(t_i) + p_{G_I}(t_i) \tag{1.3-32}$$

As previously noted, k_D is the coefficient representing the sharing power between the stationary storage and the grid, given by (1.3-33):

$$k_D(t_i) = \frac{p_{S_C}(t_i) + p_{S_D}(t_i)}{p_{S_C}(t_i) + p_{S_D}(t_i) + p_{G_I}(t_i) + p_{G_S}(t_i)} \tag{1.3-33}$$

1.3.2.3.6 Objective function

The total energy cost, C_{total}, considers the cost of the supplied power from the grid, the profit of injected power into the grid, the cost of the storage degradation when operating, the penalty cost if the EV at departure has not reached its desired SOC, and the cost of the PV shedding power, which represents the PV power that has not taken advantage of it. Therefore, the objective function is to minimize C_{total} , given by equations (1.3-34) – (1.3-38) :

$$C_{total} = C_G + C_S + C_{PVS} + C_{EV_{penalty}} \tag{1.3-34}$$

$$C_G = \sum_{t_i=t_0}^{t_F} [c_G(t_i) \times \Delta t \times (-p_{G_I}(t_i) + p_{G_S}(t_i))] \tag{1.3-35}$$

$$c_G(t_i) = \begin{cases} c_{G_{NH}}\ for\ t\ \in normal\ hours \\ c_{G_{PH}}\ for\ t\ \in peak\ hours \end{cases}$$

$$C_S = \sum_{t_i=t_0}^{t_F} [c_S(t_i) \times \Delta t \times (p_{S_C}(t_i) + p_{S_D}(t_i))] \tag{1.3-36}$$

$$C_{PVS} = \sum_{t_i=t_0}^{t_F} [c_{PVS}(t_i) \times \Delta t \times p_{PVS}(t_i)] \tag{1.3-37}$$

$$C_{EV_{penalty}} = \sum_{v}^{N_v}[c_{EV_{penalty}} \times (SOC_{EV_{des_v}} - SOC_{EV_{dep_v}}) \times E] \tag{1.3-38}$$

where C_G , C_S , C_{PVS} , and $C_{EV_{penalty}}$ are the grid, storage, PV shedding energy costs, and EV penalty cost, respectively, and c_G , c_S , c_{PVS} , and $c_{EV_{penalty}}$ are the grid, storage, PV shedding energy tariffs, and EV penalty tariff, respectively. Lastly, the final optimization problem is given by:

$$min\ (C_{total} = C_G + C_S + C_{PVS} + C_{EV_{penalty}}) \tag{1.3-39}$$

with respect to all the aforementioned equations.

The decision variables in this optimization problem are p_{EV_v} , p_{IIREVs_S} , p_G, p_{PV_S}, p_S , soc_S , and soc_{EV_v} , in which they are continuous variables.

1.3.2.4 Operation layer

The energy optimization layer finds the optimal power flow of the sources and the EVs based on $p_{PV_{MPPT_{pred}}}$ and k_D. The coefficient is calculated based on the optimized power flow obtained by CPLEX [49]. This coefficient controls the operational layer for the IIREVs in real-time operation. The advantage of k_D is balancing the power flows, coupling the energy management easily while respecting all constraints [45].

The operational layer must consider optimized power flow in real operating conditions, $p_{PV_{MPPT}}$ and p_{IIREVs_D} . In addition, the operation management must ensure robustness and withstand uncertainties in the forecast data. Then, this layer calculates the power references and performs PV shedding or EV shedding when necessary. The actual operating conditions lead to a reference power p_{ref} to stabilize the DC bus voltage, defined by (1.3-40) and (1.3-41).

$$p_{ref}(t_i) = p_{PV_{MPPT}}(t_i) - p_{IIREVs_D}(t_i) - C_p(V_{ref} - v_{DC_{bus}}) \tag{1.3-40}$$

$$p_{ref}(t_i) = p_{G_{ref}}(t_i) + p_{S_{ref}}(t_i) \tag{1.3-41}$$

where C_p , V_{ref} and $v_{DC_{bus}}$ are the proportional controller gain, reference voltage, and the actual voltage of the DC bus, respectively. The stationary storage power reference can be calculated as in (1.3-42):

$$p_{S_{ref}}(t_i) = k_D(t_i) \times p_{ref}(t_i) \tag{1.3-42}$$

where k_D is defined in the interval [0;1].

The grid power reference $p_{G_{ref}}$ is calculated taking into account the stationary storage physical limit, which means $p_{S_{ref}} = 0$ if the storage reaches its maximum $SOC_{S_{max}}$ or minimum $SOC_{S_{min}}$ limits or its maximum power $P_{S_{max}}$, and the grid power reference becomes. Figure 1.3-4 shows the control algorithm of the power balancing strategy for the IIREVs.

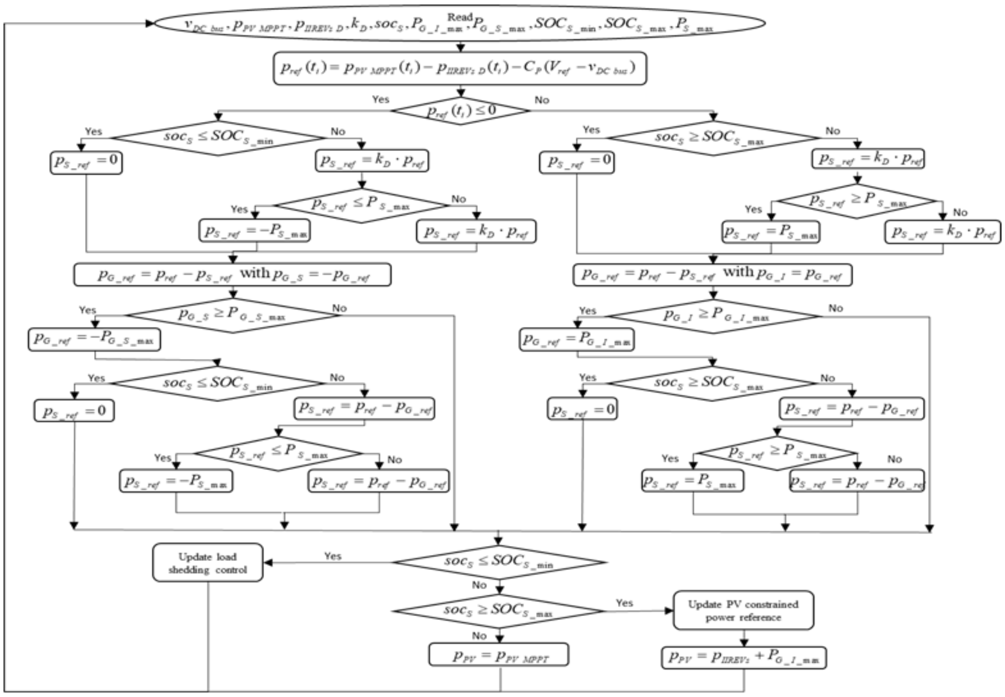

Figure 1.3-4 Control algorithm for IIREVs.

To prove the feasibility of the optimization problem, it is compared with a storage priority algorithm simulation without optimization 'Sim w/o opt', where k_D is one in this operation mode. Moreover, these operation modes are compared with an ideal case, 'Opt for real conditions', which is based on real PV MPPT and IIREV powers.

1.3.3 Simulation Results and Analyses

A Simulink model is developed to simulate the IIREVs with a step time of 0,01 s, which contains five chargers with three charging modes in real-time operation and balances the power of DC bus. $SOC_{EV_{arr_v}}$, $SOC_{EV_{dep_v}}$, t_{arr_v} and M_v are randomly generated. $SOC_{EV_{arr_v}}$ and $SOC_{EV_{dep_v}}$ are generated in the interval (20%, 50%) and (70%, 100%), respectively. Regarding the EV batteries, lithium-ion batteries were considered, and their capacities are assumed to be capable of handling up to fast charge. Sunpower SPR X21-345 with 21% efficiency under STC is considered as PV panels, and the system loss was estimated at 14%.

Table 1.3-1 provides the parameters used for optimization and power balancing control, and Table 1.3-2 provides the options assumed by the EV users, randomly generated in MATLAB, where five EVs are expected to come for charging. The grid peak hours are arbitrarily assumed to be 12:00 PM – 01:00 PM and 03:00 PM – 04:00 PM. The energy tariffs are chosen arbitrarily in a way to prioritize the sources used for the EV charging as given by:

$$c_S \leq c_G \leq c_{PVS} \leq c_{EV_{peanlty}} \qquad (1.3\text{-}43)$$

Table 1.3-1 Optimization and simulation parameter values

$SOC_{S_{min}}$	20%	$P_{EV_{fast_{max}}}$	50 kW	$P_{S_{max}}$	34,5 kW	$c_{G_{NH}}$	0,1 €/kWh
$SOC_{S_{max}}$	80%	$P_{EV_{aver_{max}}}$	22 kW	$p_{PV_{MPPT}}$	28,98 kWp	$c_{G_{PH}}$	0,7 €/kWh
$SOC_{EV_{min}}$	20%	$P_{EV_{slow_{max}}}$	7 kW	N_{PV}	84 PV	c_S	0,01 €/kWh
$SOC_{EV_{max}}$	100%	$P_{G_{I_{max}}}$	50 kW	V_{ref}	400 V	c_{PVS}	1,2 €/kWh
SOC_{S_0}	50%	$P_{G_{S_{max}}}$	50 kW	E_{bat}	90 kWh	$c_{EV_{penalty}}$	2,5 €/kWh
				E	50 kWh		

Table 1.3-2 Assumed options by the EV users

EVs	$SOC_{EV_{arr}}$	$SOC_{EV_{des}}$	t_{arr}	$t_{es_{ch}}$	M
EV1	29%	74%	09:10 AM	03h 13 min	Slow
EV2	23%	78%	09:40 AM	01h 15 min	Average
EV3	22%	88%	12:20 PM	04h 43 min	Slow
EV4	32%	78%	02:20 PM	03h 18 min	Slow
EV5	29%	70%	02:30 PM	25 min	Fast

At each event, like EV arrival, the optimization is executed. Then, the corresponding k_D is calculated as in equation (1.3-33) from the optimized power flow for the corresponding EV arrival event. The obtained k_D is then inserted into the Simulink model, which runs in real-time conditions. At each EV arrival, the desired parameters, soc_S and soc_{EV_v} currently in charge, are actualized and inserted; then, the supervisory control of the IIREVs executes the optimization, and the EV starts charging.

The following subsections present different case studies to prove the feasibility of the optimization problem formulated as MILP under different meteorological conditions.

1.3.3.1 Case 1—High Irradiation Profile without Fluctuations

The case of 29 June 2019, in Compiegne, France, is considered. Figure 1.3-5 shows $p_{PV_{MPPT_{pred}}}$ and $p_{PV_{MPPT}}$.

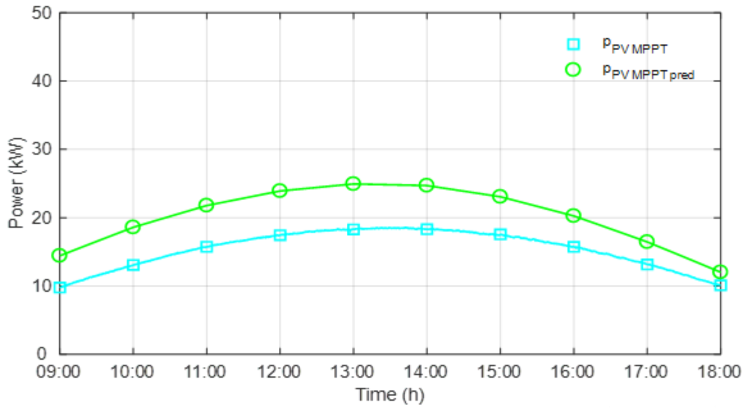

Figure 1.3-5 PV MPPT real and predicted powers—case 1

In this case, the PV power production is considered significant since the weather is sunny and clear, so the irradiation is high, and there are no fluctuations. The IIREVs demand power is based on the data given in Table 1.3-2. Figure 1.3-6 shows the power flow and storage state of charge for 'Sim w/o opt' and simulation with optimization 'Sim with opt' for case 1, which is based on introducing the k_D, which is calculated in the optimization layer, into the real-time operation algorithm in Simulink.

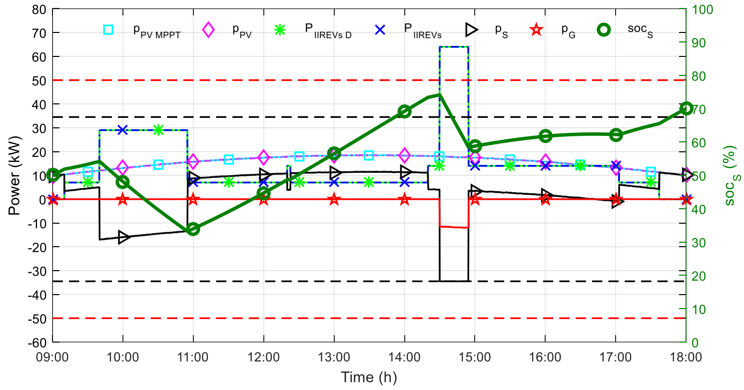

(a)

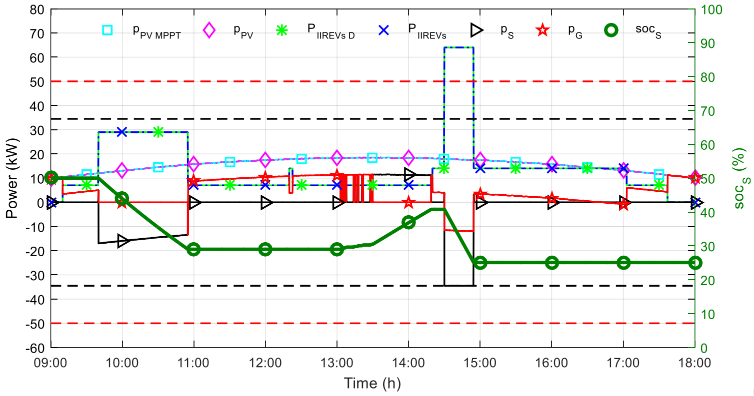

(b)

Figure 1.3-6 Power flow and storage state of charge in (a) 'Sim w/o opt' and (b) 'Sim with opt'—case 1

In Figure 1.3-6 (a), the storage has priority over the grid either to be discharged or to be charged. However, when EV5 arrives, the IIREVs demand power greater than the PV and storage powers that they can supply, where the black dotted lines represent the maximum storage power and the red dotted lines represent the maximum grid power that can be reached. Therefore, the grid supplies power to charge the EVs. On the other hand, in Figure 1.3-6 (b), the power flow of the storage and the grid is based on the coefficient k_D . Since between 12:00 PM and 01:00 PM is considered a peak period, by selling energy to the grid operator, it is possible to make profits and, thus, reduce the total cost of energy. However, after 01:00 PM, the storage can be recharged to be able to charge the future EVs with sufficient storage energy. Therefore, when EV5 arrives, the PV, storage and grid can together supply the EVs.

Figure 1.3-7 shows the EV energy distribution for ‘Sim w/o opt’ and ‘Sim with opt’. The calculation of EV energy distribution is detailed in [50].

(a) (b)

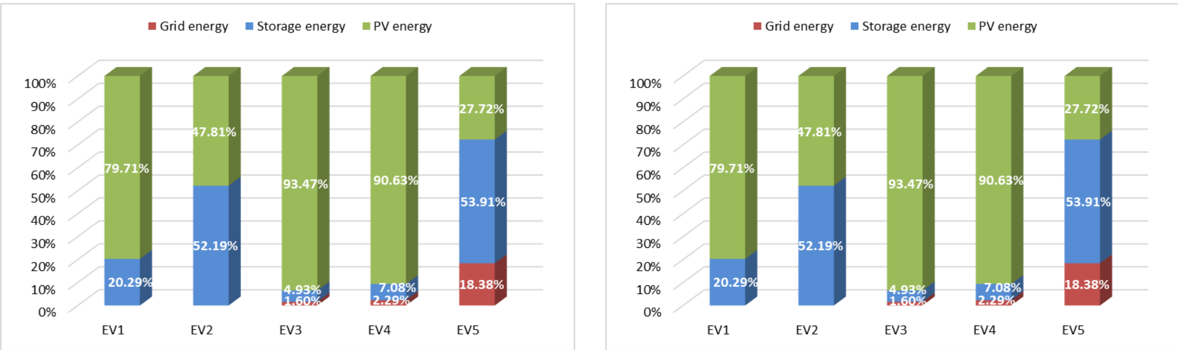

Figure 1.3-7 EV energy distribution in (a) ‘Sim w/o opt’ and (b) ‘Sim with opt’—case 1

EV1, EV3, and EV4 depend mainly on PV energy since they charge in slow mode. EV2 depends on PV and storage with a slightly equal percentage. EV5 depends on the PV, storage and grid energy. The percentage of grid energy is significantly greater than the other EVs, since it is charging in fast mode.

Figure 1.3-8 (a) shows the energy system distribution for ‘Sim w/o opt’, ‘Sim with opt’ and ‘Opt for real conditions’. There is no grid injection in the ‘Sim w/o opt’, while for the ‘Sim with opt’ and ‘Opt for real conditions’, there is grid injection, which indicates that selling energy to the grid and the charging energy of the storage was sufficient to get the best energy distribution for the EVs.

The percentage of accuracy is the ratio of the total cost over the total cost of the ‘Opt for real conditions’. The closer the percentage to 100%, the more accurate it is. If the percentage is greater than 100%, the total cost is greater than ‘Opt for real conditions’, while if the percentage is below 0%, the total cost is the opposite case of ‘Opt for real conditions’. Figure 1.3-8 (b) shows the energy system cost, where the energy costs in ‘Sim with opt’ are closer to the ideal case ‘Opt for real conditions’, resulting in profits with 99,95% accuracy. Conversely, it is the opposite situation in ‘Sim w/o opt’ with −11,96% accuracy. Thus, this proves the superiority of the optimization algorithm over the storage priority algorithm. The negative sign implies that the IIREV operators make a profit in particular by selling energy to the grid.

(a) (b)

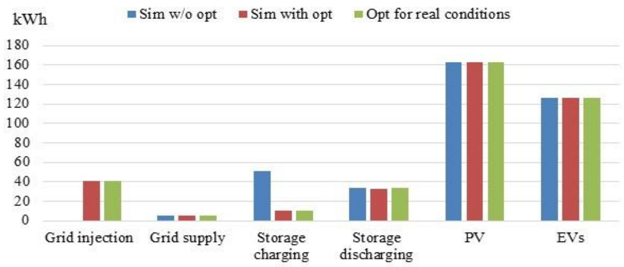

Case Operation	Grid Cost (c€)	Storage Cost (c€)	Total Cost (c€)	% of Accuracy
Sim w/o opt	48,22	84,47	132,69	−11,96%
Sim with opt	−1152,69	43,69	−1109,01	99,95%
Opt for real conditions	−1152,97	43,44	−1109,53	-

Figure 1.3-8 Energy system distribution and (b) energy system cost—case 1

1.3.3.2 Case 2—Low Irradiation Profile without Fluctuations

The case of October 5th, 2018, in Compiegne, France, is considered. Figure 1.3-9 shows $p_{PV_{MPPT_{pred}}}$ and $p_{PV_{MPPT}}$.

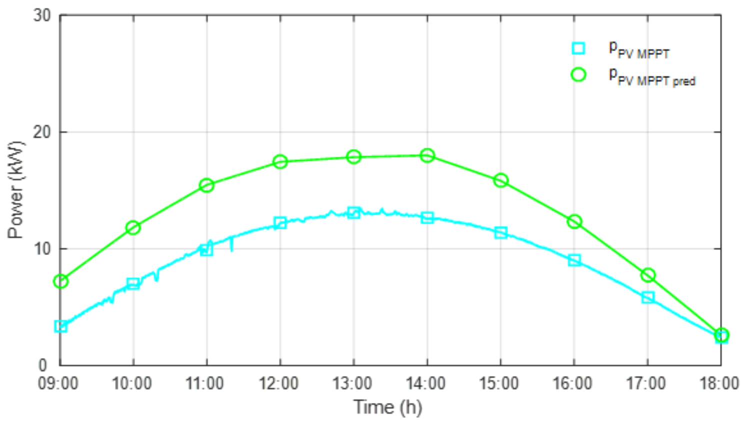

Figure 1.3-9 PV MPPT real and predicted powers—case 2

In this case, the weather is clear, so there are no fluctuations; however, the PV power production is not very high. The IIREV demand power is based on the data in Table 1.3-2. Figure 1.3-10 shows the power flow and storage state of charge for 'Sim w/o opt' and simulation with optimization 'Sim with opt' for case 2.

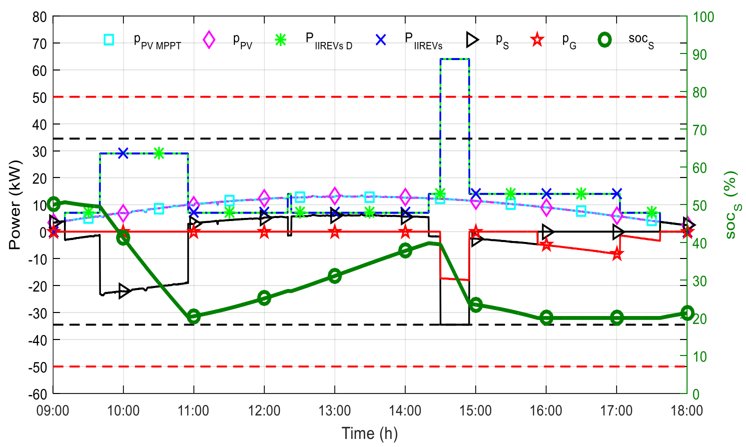

(a)

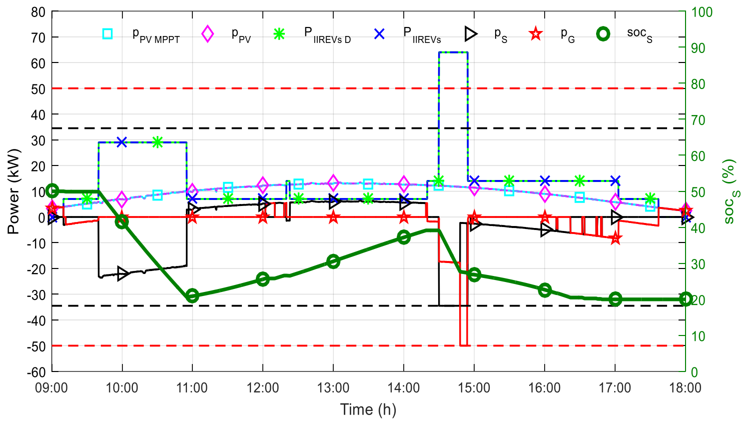

(b)

Figure 1.3-10 Power flow and storage state of charge in (a) 'Sim w/o opt' and (b) 'Sim with opt'—case 2

In Figure 1.3-10 (a), the storage always has priority over the grid. However, when EV5 arrives, the grid supplies power with the PV and the storage to charge the EVs, where the black dotted lines represent the maximum storage power and the red dotted lines rep-resent the maximum grid power that can be reached. On the other hand, in Figure 1.3-10 (b), the power flow of the storage and the grid is based on the coefficient k_D . Since the PV production is not high, the storage reached its lower limit at the departure of EV2. Therefore, the storage is required to be recharged to be able to charge the future EVs with sufficient storage energy. Therefore, when EV5 arrives, the PV, storage and grid can together supply the EVs. However, between 12:00 PM and 01:00 PM is considered a peak period, so by selling a little energy to the grid operator, it is possible to make small profits. Additionally, between 03:00 PM and 04:00 PM is a peak period, so in 'Sim with opt', the power flow is better distributed since the storage is kept to supply power instead of grid power, while in 'Sim w/o opt', the storage reached its lower limit before 04:00 PM, and the grid continued to supply power to the EVs.

Figure 1.3-11 shows the EV energy distribution for 'Sim w/o opt' and 'Sim with opt'.

(a) (b)

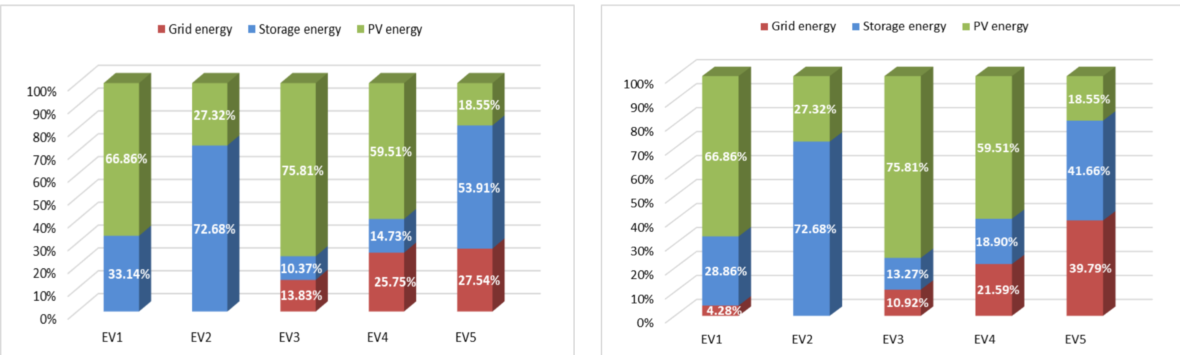

Figure 1.3-11 EV energy distribution in (a) 'Sim w/o opt' and (b) 'Sim with opt'—case 2

EV1, EV3, and EV4 depend mainly on PV energy since they charge in slow mode. EV2 depends on PV and storage. Figure 1.3-11 shows that EV5, which is in fast mode, is charged from the grid with a high percentage. This will increase the charging price for the EV user. In Figure 1.3-11 (b), EV5 is charged from the grid with a higher percentage than in 'Sim w/o opt', while EV3 and EV4 have been charged from the storage with a higher percentage than in 'Sim w/o opt', based on giving a better energy cost as shown.

Figure 1.3-12(a) shows the energy system distribution for 'Sim w/o opt' and 'Sim with opt'. There is no grid injection in the 'Sim w/o opt', while for the 'Sim with opt', there is a little bit of grid injection, which refers to selling energy to the grid and having ap-proximately the same storage charging energy. Figure 1.3-12 (b) shows the energy system cost, where the energy costs in 'Sim with opt' are closer to the ideal case 'Opt for real conditions' with 99,37% accuracy and lower cost than in 'Sim w/o opt' with 164,04% accuracy (overpriced). In this case, the PV production is not high; however, selling a little bit of energy to the grid during the peak time could reduce the total cost of the system. Thus, it proves the superiority of the optimization algorithm over the storage priority algorithm.

(a)

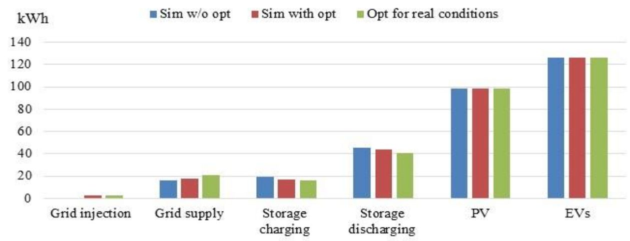

(b)

Case Operation	Grid Cost (c€)	Storage Cost (c€)	Total Cost (c€)	% of Accuracy
Sim w/o opt	196.59	64.75	261.34	164.04%
Sim with opt	97.82	60.49	158.31	99.37%
Opt for real conditions	102.36	56.94	159.31	-

Figure 1.3-12 (a) Energy system distribution and (b) energy system cost—case 2

1.3.3.3 Case 3—High Irradiation Profile with High Fluctuations

The case of 12 May 2019, in Compiegne, France, is considered. Figure 1.3-13 shows $p_{PV_{MPPT_{pred}}}$ and $p_{PV_{MPPT}}$.

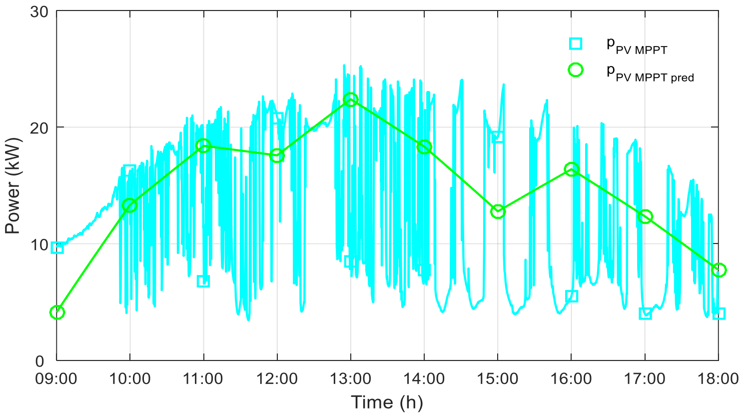

Figure 1.3-13 PV MPPT real and predicted powers and IIREV demand power—case 3

In this case, the irradiations are high, and the weather is cloudy, so there are high fluctuations. The IIREVs demand power is based on the data Table 1.3-2. Figure 1.3-14 shows the power flow and storage state of charge for 'Sim w/o opt' and simulation with optimization 'Sim with opt' for case 3.

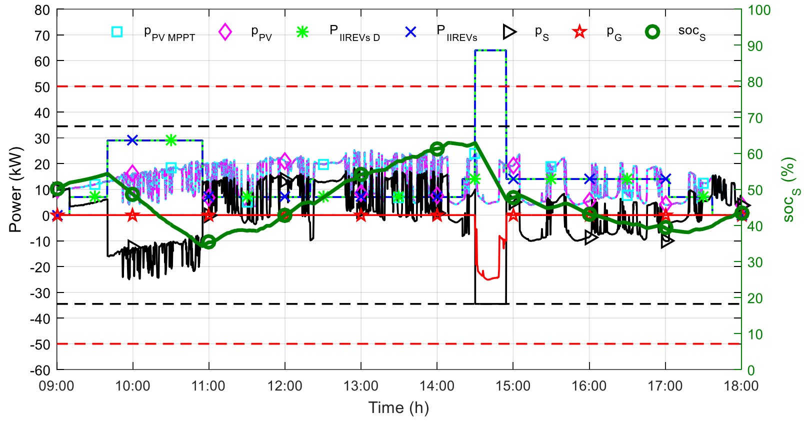

(a)

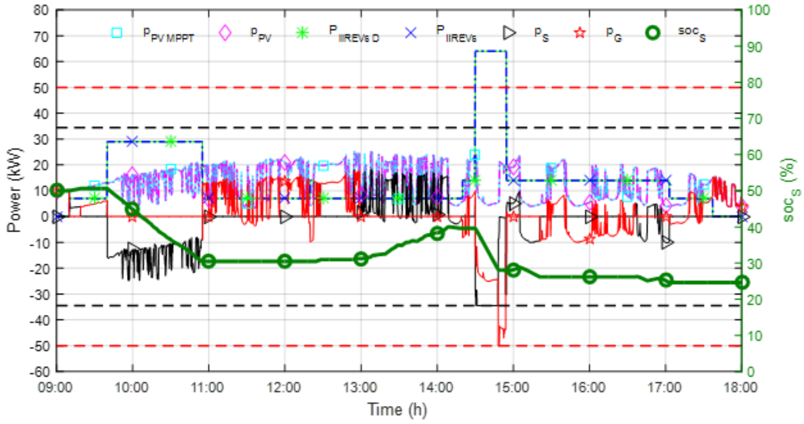

(b)

Figure 1.3-14 Power flow and storage state of charge in (a) 'Sim w/o opt' and (b) 'Sim with opt'—case 3

In Figure 1.3-14 (a), the storage always has priority over the grid, either to be discharged or to be charged. However, when EV5 arrives, the IIREV demand power is greater than the PV and storage power that can be supplied, where the black dotted lines represent the maximum storage power and the red dotted lines represent the maximum grid power that can be reached. Therefore, the grid supplies power to charge the EVs. On the other hand, in Figure 1.3-14 (b), the power flow of the storage and the grid is based on the coefficient k_D . Since between 12:00 PM and 01:00 PM is considered a peak period, by selling energy to the grid operator, it is possible to make profits. However, after 01:00 PM, the storage can be recharged to be able to charge the future EVs with sufficient storage energy.

Figure 1.3-15 shows the EV energy distribution for 'Sim w/o opt' and 'Sim with opt'.

(a) (b)

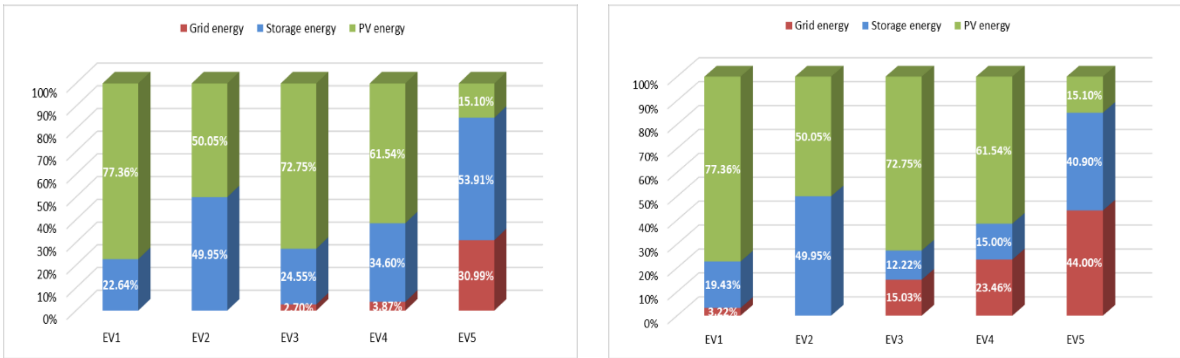

Figure 1.3-15 EV energy distribution in (a) ‘Sim w/o opt’ and (b) ‘Sim with opt’—case 3

EV1, EV3, and EV4 depend mainly on PV energy since they charge in slow mode. EV2 depends on PV and storage with a slightly equal percentage. Figure 1.3-15 shows that EV5, which is in fast mode, is charged from the grid with a high percentage. This will increase the charging price for the EV user. In Figure 1.3-15 (b), EV3, EV4, and EV5 are charged from the grid with a higher percentage than in ‘Sim w/o opt’; due to the high fluctuations, the power distribution was not as suitable. However, the energy cost obtained from optimization stays better than in ‘Sim w/o opt’ and returns profits due to selling energy to the grid.

Figure 1.3-16 (a) shows the energy system distribution for ‘Sim w/o opt’ and ‘Sim with opt’. There is no grid injection in the ‘Sim w/o opt’, while for the ‘Sim with opt’, there is grid injection, which is referred to selling energy to the grid and maintaining a little storage charging energy. Figure 1.3-16 (b) shows the energy system cost; due to the high fluctuations in the real PV profile, the prediction profile was not so accurate. However, the energy costs in ‘Sim with opt’ are closer to the ideal case ‘Opt for real conditions’ with 75,45% accuracy and return profits, while it is the opposite situation in ‘Sim w/o opt’ with −26,46% accuracy. Thus, it proves the superiority of the optimization algorithm over the storage priority algorithm.

(a) (b)

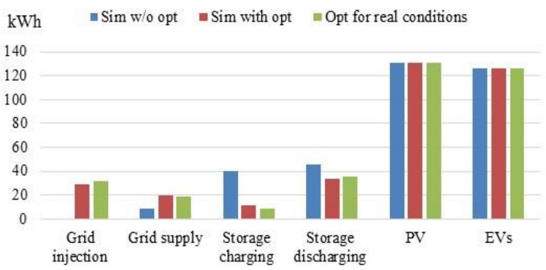

Case Operation	Grid Cost (c€)	Storage Cost (c€)	Total Cost (c€)	% Accuracy
Sim w/o opt	81,32	85,96	167,29	−26,46%
Sim with opt	−522,01	45,1	−476.92	75,45%
Opt for real conditions	−676.51	44,4	−632,12	-

Figure 1.3-16 (a) Energy system distribution and (b) energy system cost—case 3

1.3.3.4 Discussion

In case 1, the PV production is high without fluctuations. In ‘Sim with opt’, selling energy to the grid is preferred to make profits. Moreover, charging the storage a little bit could be interesting to get the same EVs energy distribution in ‘Sim with opt’ as in ‘Sim w/o opt’.

In case 2, the PV production is low without fluctuations. The energy distribution especially for EV5 is better in ‘Sim w/o opt’ since it is charged with a lower percentage of grid energy than in ‘Sim with opt’. This could be explained by the fact that in ‘Sim w/o opt’, the storage is always used until it reaches its limits, while in ‘Sim with opt’, the power flow is based on the coefficient k_D to minimize the total cost. Therefore, the total cost in ‘Sim with opt’ is lower than ‘Sim w/o opt’. Moreover, charging the storage is necessary after the departure of EV2, since the storage has reached its limit.

In case 3, the PV production is high with high fluctuations. In ‘Sim with opt’, selling energy to the grid is preferred to make profits. Moreover, charging the storage a little bit could be interesting to get a closer EV energy distribution in ‘Sim with opt’ as in ‘Sim w/o opt’. Since there are high fluctuations, the power distribution is not that accurate; however, the total cost for ‘Sim w/o opt’ brings profits to the IIREVs operator, and it is better than ‘Sim w/o opt’.

To summarize the three cases studied, ‘Sim with opt’ performs better than ‘Sim w/o opt’ in minimizing the total cost of the IIREVs with high accuracy in case 1 and case 2, where they are without fluctuations. For the EV energy distribution, in ‘Sim with opt’, the results are satisfying in case 1 as they are approximately identical, while in case 2, the coefficient k_D gives better energy distribution for the system to have a lower cost than ‘Sim w/o opt’ instead of giving a better energy distribution for EVs. Therefore, the EV user charging in fast mode should be willing to pay a high price. In case 3, due to high fluctuations, the optimization is not very accurate, as the PV prediction is hourly coming from Météo France. However, the total cost in ‘Sim with opt’ is still better than ‘Sim with opt’ due to selling energy to the grid and making profits, yet the EV energy distribution is not as well distributed in ‘Sim with opt’ as in ‘Sim with opt’.

In optimization, it is always preferred to sell energy to the grid to make profits. However, the goal, besides minimizing the total cost, is to have better EV energy distribution by reducing the grid energy consumed by the EVs. Therefore, it is important to recharge the storage. For the three cases taken in this study, after the departure of EV2, soc_S decreases, and in case 2, it has reached the lower limit. It is expected for three more EVs to come for recharging at the IIREVs, and it is supposed that at least one EV could charge in fast mode. The average energy demand for each EV is 25 kWh, and so it is 75 kWh for the three EVs to come. Based on the data from Table 1.3-2, the capacity of the storage that can be used is 27 kWh (30% of 90 kWh). After the departure of EV2, if soc_S is 20%, then it is empty, and if it is 30%, then only 9 kWh with PV and grid energy could be used to charge 75 kWh. This will result in increasing the energy supplied by the grid to charge the coming EVs. Thus, after the departure of EV2, if PV power is higher than the IIREV demand power, the storage should be recharged. Hence, the interest is to minimize the total cost of the IIREVs and to have the best EV energy distribution.

1.3.4 Real-Time Experimental Tests

The real-time experimental tests were done in the testbed presented in Figure 1.3-17(a) that emulates the IIREVs, having a step time of 1/14 kHz. The chargers are emulated with two DC emulators having each 6 kW, designated by charging terminals equipped with multi-electrical outlets as shown in Figure 1.3-17 (b). It is considered that the DC emulator 1 is a charging terminal with two electrical outlets to emulate EV1 and EV2 and the DC emulator 2 is a charging terminal with three electrical outlets to emulate EV3, EV4, and EV5. The existing testbed allows the PV power profile to be emulated, which permits it to repeat the experimental test and compare it in two scenarios, with and without optimization.

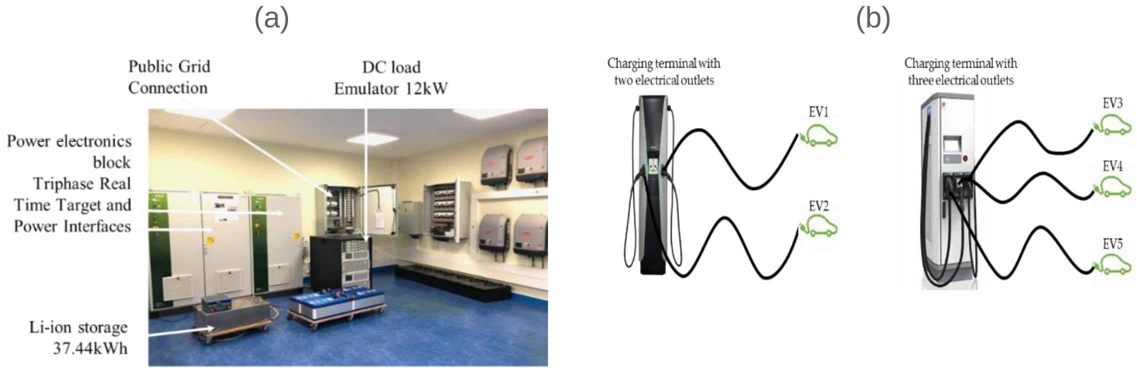

Figure 1.3-17 (a) Testbed for the IIREV experimental platform and (b) representative image of the multi-outlet charging terminals

Table 1.3-3 Real-time experiment parameter values

$SOC_{S_{min}}$	35%	$P_{EV_{fast_{max}}}$	5 kW	$P_{S_{max}}$	3,45 kW	$c_{G_{NH}}$	0,1 €/kWh
$SOC_{S_{max}}$	60%	$P_{EV_{aver_{max}}}$	2,2 kW	$p_{PV_{MPPT}}$	4,14 kWp	$c_{G_{PH}}$	0,7 €/kWh
$SOC_{EV_{min}}$	20%	$P_{EV_{slow_{max}}}$	0,7 kW	N_{PV}	12 PV	c_S	0,01 €/kWh
$SOC_{EV_{max}}$	100%	$P_{G_{I_{max}}}$	5 kW	V_{ref}	400 V	c_{PVS}	1,2 €/kWh
SOC_{S_0}	50%	$P_{G_{S_{max}}}$	5 kW	E_{bat}	37,44 kWh	$c_{EV_{penalty}}$	2,5 €/kWh
				E	5 kWh		

The parameter values used in Table 1.3-3 were chosen with a scale divided by ten, compared to the simulation, due to the physical limitations of the available sources and equipment. The existing stationary storage had an energy capacity of 37,44 kWh, which is considered high; therefore, the SOC limits were chosen to be between 60% and 35% in-stead of 80% and 20%.

In the real-time experiment, at each EV arrival, the optimization was executed when the EV user came to the charging station and input their preferences, which were communicated with the dSPACE. Then, Python read the data from dSPACE and created the files required to run the optimization in C++, solved by CPLEX. Then, Python calculated $k_D$and sent it in dSPACE to be read in a real-time experimental model. Figure 1.3-18 shows the flowchart of the optimization solving for the 'real-time exp'. The corresponding k_D was calculated as in (1.3-33) from the optimized power flow for the corresponding EV arrival event. The obtained k_D was then updated into the Simulink model.

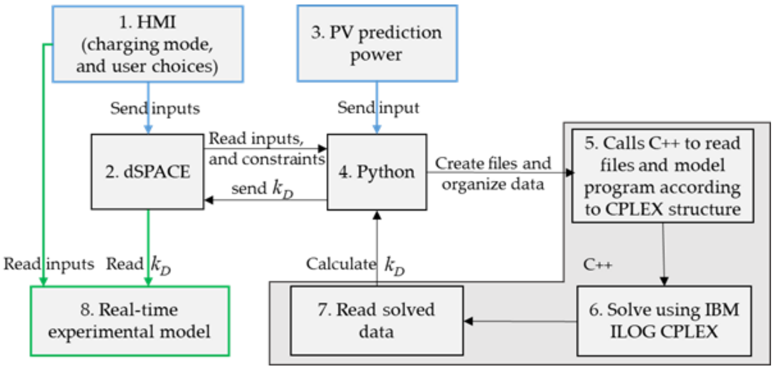

Figure 1.3-18 Flowchart of optimization solving

To be specific, at the start of the real-time experimental test, when no EVs were present, the optimization algorithm was executed for the first time using only the predicted PV power. When the first EV arrived at the station, the EV data were registered, and the user selected their desired SOC and charging mode. These data were communicated instantly by the real-time experimental model and transmitted via a fiber optic cable to ensure communication with analog input/output ports.

Next, dSPACE received the EV data as an analog input, which Python then read to create the necessary files, including the parameters and profiles for predicted PV power and EV power profiles acquired from the HMI. Python then called C++ to solve the optimization problem using the CPLEX solver. Once resolved, Python calculated k_D and sent it as an analog output to dSPACE, which in turn transmitted it to the real-time experimental model. When additional EVs arrived at the station, the same procedure was repeated with updated DC microgrid data (such as the SOC of the stationary storage and the SOC of the charging EVs). The following subsections present two case studies to prove the feasibility of the optimization problem in real-time experimental tests formulated as MILP under different meteorological conditions.

1.3.4.1 Experimental Test 1

The case of October 14th, 2021, in Compiegne, France, is considered. Figure 1.3-19 shows $p_{PV_{MPPT_{pred}}}$ and $p_{PV_{MPPT}}$, where the irradiations are intermediate with low fluctuations.

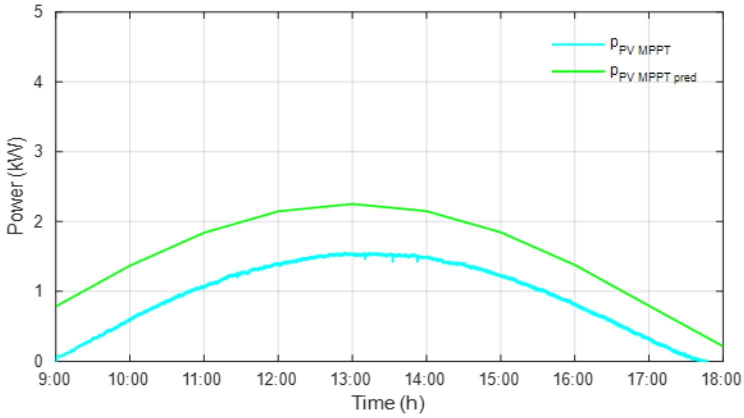

Figure 1.3-19 PV MPPT real and predicted powers and IIREV demand power—experimental test 1

In this case, the irradiations are intermediate, and the weather is a bit cloudy, so there are low fluctuations. The IIREV demand power is based on the data in Table 1.3-2. Figure 1.3-20 shows the power flow and storage state of charge for 'real-time exp' with opt and the DC bus voltage - experimental test 1a.

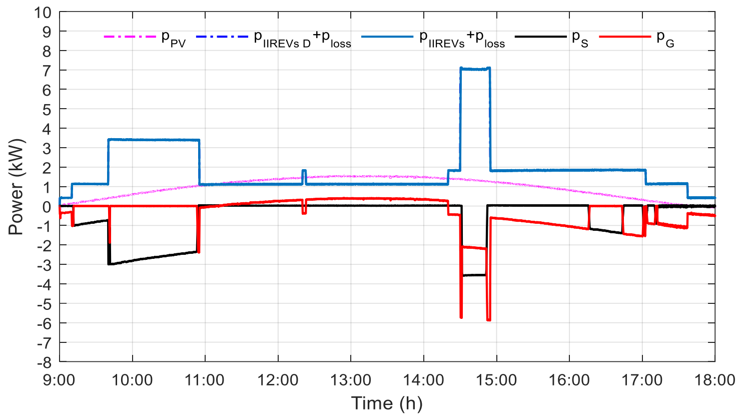

(a)

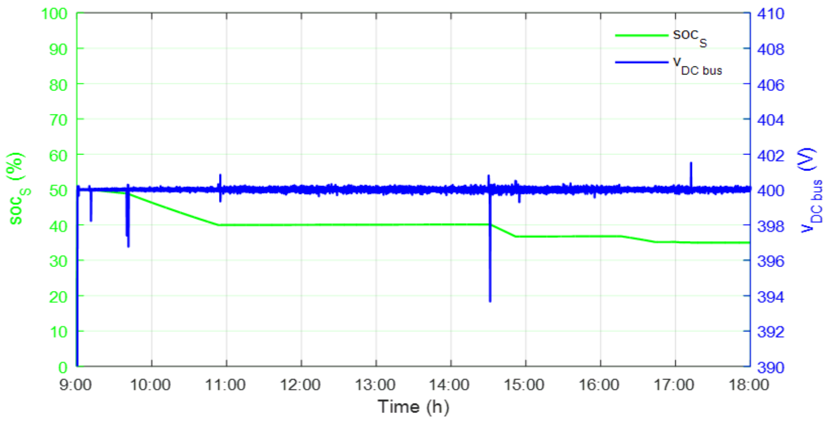

(b)

Figure 1.3-20 Power flow and storage state of charge for 'real-time exp' with opt (a) and (b) storage state of charge and DC bus voltage—experimental test 1a

In Figure 1.3-20 (a), the power flow of the storage and the grid is based on the coefficient k_D . From 09:00 AM until 09:10 AM and 03:00 PM until 04:00 PM, the grid is used, but this is not accurate since, in prediction, PV power is higher than the real PV power, and it is also higher than the IIREV demand power. However, when EV5 arrives, the IIREV demand power is greater than the PV and storage power that they can supply. Therefore, the grid supplies power to charge the EVs. Between 11:00 AM and 02:20 PM, by selling energy to the grid operator, it is possible to make profits, especially from 12:00 PM and 01:00 PM, as it is considered a peak period. Around 05:00 PM, when there is no PV power and the storage is empty, the grid supplies power, regardless of the   value. Figure 1.3-20 (b) shows the evolution of the storage SOC, where the storage discharge energy from 09:10 AM to 10:50 AM, 02:25 PM to 02:50 PM and around 04:20 PM to 04:50 PM. Figure 1.3-20 (b) also shows the stability of the DC bus voltage even with small fluctuations, which are due to the switching of DC converters, and spikes of a few voltages happen when each EV starts charging and when it finishes charging.

Figure 1.3-21 shows the power flow and storage state of charge for 'real-time exp' without optimization and the DC bus voltage - experimental test 1b.

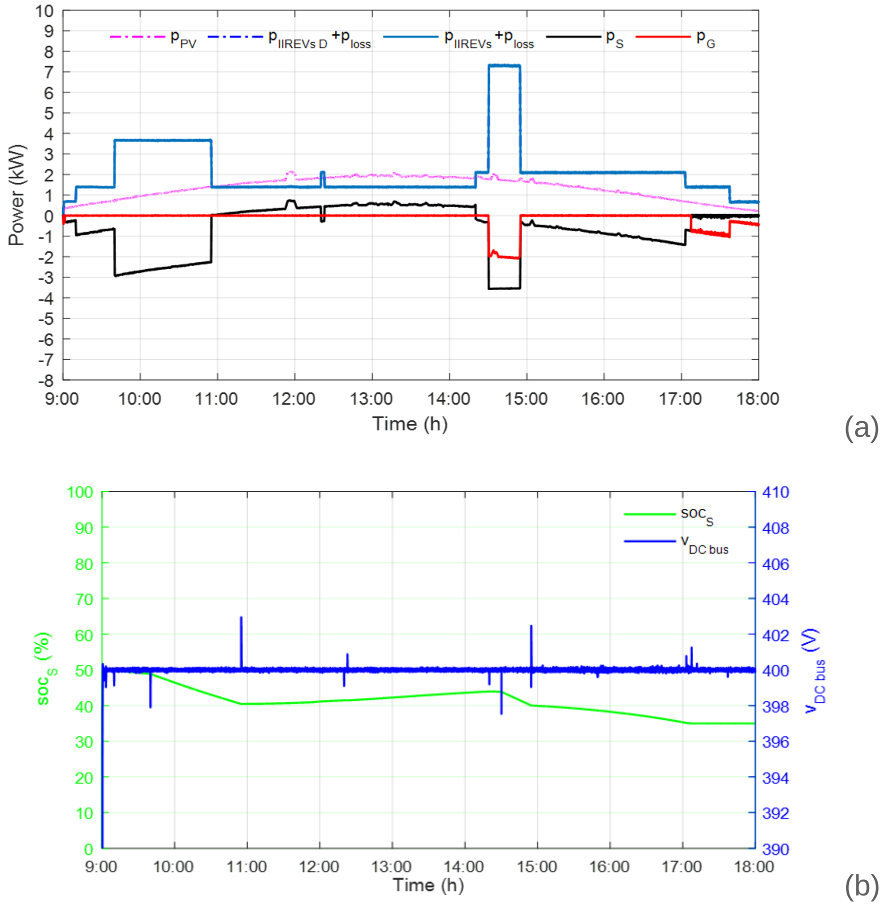

Figure 1.3-21 Power flow and storage state of charge for 'real-time exp' without optimization (a) and (b) storage state of charge and DC bus voltage—experimental test 1b

In Figure 1.3-21 (a), the storage is always prioritized to be either charged or discharged. However, when EV5 arrives, the IIREV demand power is greater than the PV and storage power that they can supply. Therefore, the grid supplies power to charge the EVs. The grid continues supplying power to the IIREVs as the storage is empty around 05:10 PM Figure 1.3-21 (b) shows the evolution of the storage SOC, where the storage is recharged from 10:50 AM to 02:25 PM after being discharged and then again discharges energy when EV5 arrives until it is empty. Figure 1.3-21 (b) also shows the stability of the DC bus voltage even with small fluctuations, which are due to the switching of DC converters, and the spikes of a few voltages happen when each EV starts charging and when it finishes charging.

Table 1.3-4 shows the energy system cost for 'real-time exp' with opt, where the energy costs are low due to selling energy to the grid and are far from the optimal energy cost for real conditions, which is 11,12 c€. For 'real-time exp' without optimization, the energy cost is lower than in optimization due to the storage discharging energy in the peak hour from 03:00 PM to 04:00 PM. As shown in Figure 1.3-19, the PV power prediction is overestimated and much higher than the real PV power. Therefore, in 'Opt for real conditions', where the optimization is performed without uncertainties, it gives the optimal energy cost without error. It avoids grid supply energy, whereas in 'real-time exp' with opt, it predicted falsely to inject around 12:30 PM and 03:00 PM to 04:00 PM, as shown in Figure 1.3-20 (a). Moreover, when EV5 arrives, the storage is discharged to the maximum power and then becomes empty around 05:00 PM.

However, in 'Opt for real conditions', the grid supplies its maximum power when EV5 arrives, and the storage is preserved to discharge at peak hours from 03:00 PM to 04:00 PM. This explains the difference in the grid cost and the total cost for both cases.

Table 1.3-4 Energy system cost - experimental test 1

Case Operation	Grid Cost (c€)	Storage Cost (c€)	Total Cost (c€)
Real-time exp w/o opt	13,90	8,52	22,73
Real-time exp with opt	59,18	5,68	64,86
Opt for real conditions	5,51	5,61	11,12

Figure 1.3-22 shows the EV energy distribution for 'real-time exp' with and without opt.

In Figure 1.3-22, EV1 and EV3 depend mainly on PV energy since they charge in slow mode. EV2 depends on storage more than PV. EV5 depends on PV, storage and grid energy. The percentage of grid energy is significantly greater than the other EVs since it is charging in fast mode. Figure 1.3-21 (a) shows a better EV energy distribution than in Figure 1.3-21 (b), especially for EV4, where it was charged by the storage in the peak period from 03:00 PM to 04:00 PM and the grid is less used for all EVs.

(a) (b)

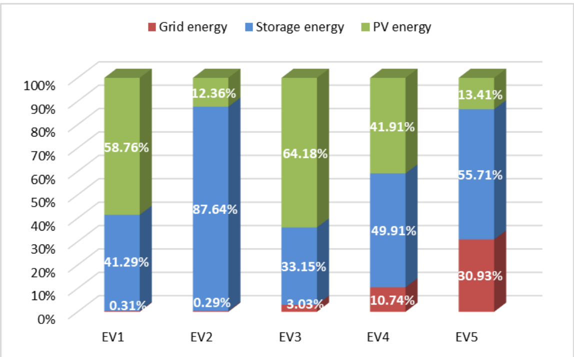

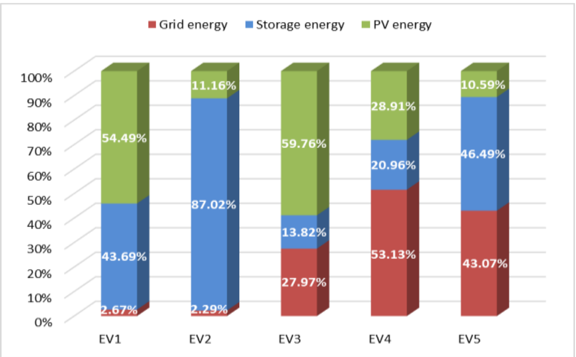

Figure 1.3-22 EV energy distribution for 'real-time exp' (a) without opt and (b) with opt—experimental test

1.3.4.2 Experimental Test 2

The case of October 27th, 2021, in Compiegne, France, is considered. Figure 1.3-23 shows $p_{PV_{MPPT_{pred}}}$ and $p_{PV_{MPPT}}$, where the irradiations are intermediate and the weather is a bit cloudy, so there are low fluctuations. The IIREV demand power is based on the data in Table 1.3-2.

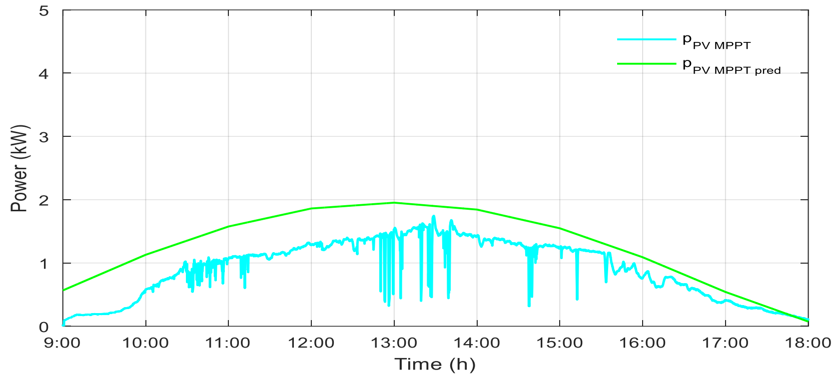

Figure 1.3-23 PV MPPT real and predicted powers and IIREV demand power—experimental test 2

Figure 1.3-24 shows the power flow and storage state of charge for 'real-time exp' without optimization and the DC bus voltage - experimental test 2.

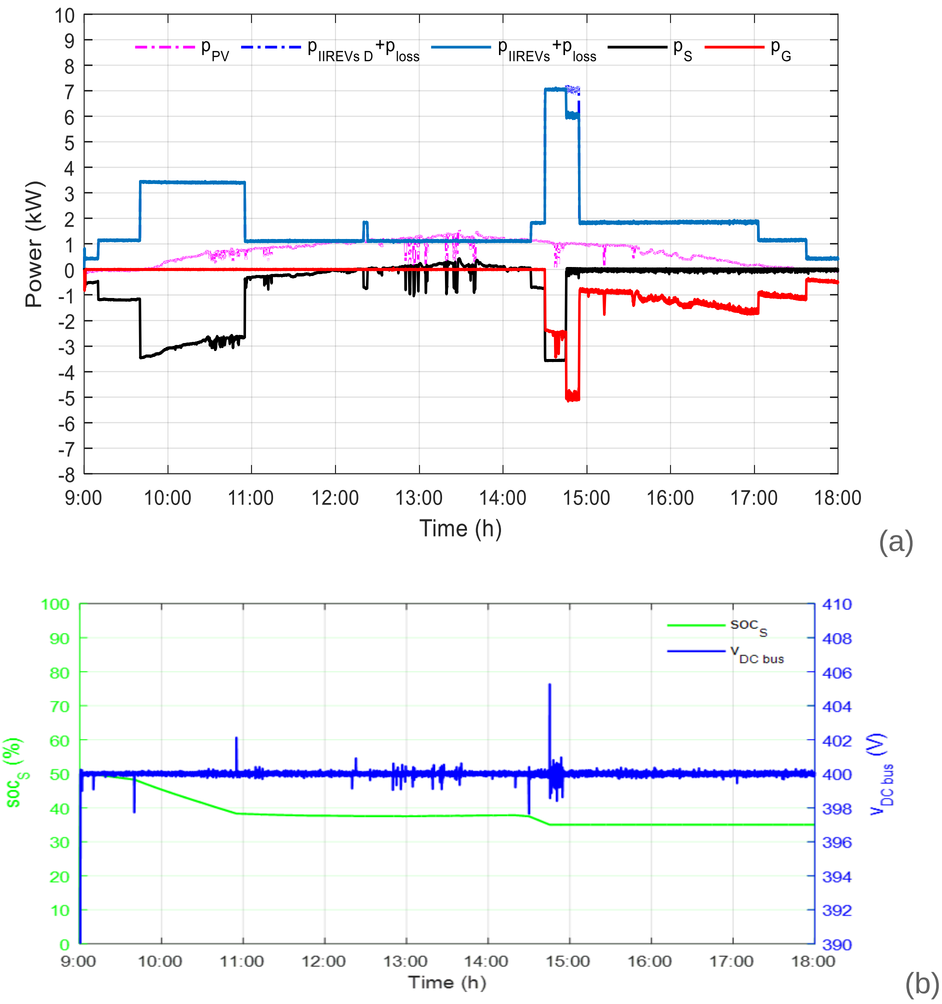

Figure 1.3-24 Power flow and storage state of charge for 'real-time exp' without optimization (a) and (b) storage state of charge and DC bus voltage—experimental test 2

In Figure 1.3-24 (a), the storage is always prioritized to be either charged or discharged. However, after EV5 arrives and around 02:45 PM, the storage is empty. The grid supplies power, but it is insufficient to fully charge the EVs, and therefore, EV shedding is applied from 02:45 PM until the departure of EV5 from the IIREVs at 02:55 PM. After EV5's departure, the grid continues supplying power to the IIREVs as the storage is empty. Figure 1.3-24 (b) shows the evolution of the storage SOC, where it is always discharging almost all the time until it is empty around 2:45 PM, and the stability of the DC bus voltage is present even with small fluctuations. Spikes of a few voltages happen when each EV starts charging and when it finishes charging.

Figure 1.3-25 shows the power flow and storage state of charge for 'real-time exp' with optimization and the DC bus voltage - experimental test 2b.

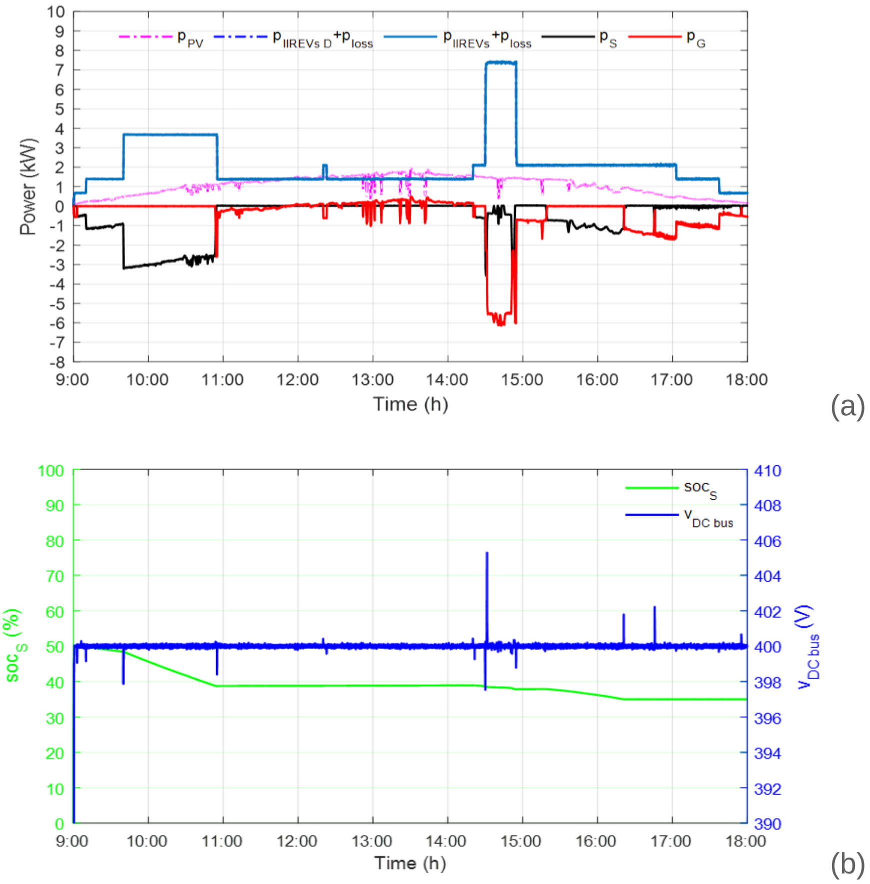

Figure 1.3-25 Power flow and storage state of charge for 'real-time exp' with optimization (a) and (b) the storage state of charge and DC bus voltage—experimental test 2b

In Figure 1.3-25 (a), the power flow of the storage and the grid is based on the coefficient k_D. From 12:00 PM until 02:20 PM, the PV injects little energy to the grid during the peak hour, yet some fluctuations still happen where the grid supplies power. However, when EV5 arrives, the IIREV demand power is greater than the PV and storage power that they can supply. Therefore, the grid supplies power to charge the EVs with maximum power, and the storage is preserved. From 03:15 PM to 04:15 PM, the storage discharges energy until it is empty to avoid the high cost of grid supply power, as it is considered a peak period. After 04:15 PM, the grid supplies power, regardless of the value. Figure 1.3-25 (b) shows the evolution of the storage SOC, where the storage discharges energy from 09:10 AM to 10:50 AM, 02:25 PM to 02:50 PM and around 03:15 PM to 04:15 PM. Figure 1.3-25 (b) also shows the stability of the DC bus voltage even with small fluctuations, which are due to the switching of DC converters, and the spikes of a few voltages happen when each EV starts charging and when it finishes charging.

Table 1.3-5 shows the energy system cost for ‘real-time exp’ without optimization, where the energy costs are higher than in optimization due to the cost of EV shedding. The real-time experiment with optimization is closer to the optimization for real conditions, as it avoids EV shedding and gives better energy costs of 60,91 c€. In ‘Opt for real conditions’, where the optimization is performed without uncertainties, it gives the optimal energy cost without error, which is 53,37 c€. It avoids EV shedding and grid supply energy, and when EV5 arrives, the storage is discharged to the maximum power, then becomes empty around 02:45 PM, provoking EV shedding. However, in ‘Opt for real conditions’, the grid supplies its maximum power when EV5 arrives, and the storage is preserved to discharge at peak hours from 03:00 PM to 04:00 PM. This explains the difference in the grid cost and the total cost for both cases.

Table 1.3-5 Energy system cost - experimental test 2

Case Operation	Grid Cost (c€)	Storage Cost (c€)	EV Shedding Cost (c€)	Total Cost (c€)
Real-time exp w/o opt	109,83	6,17	40,72	156,73
Real-time exp with opt	54,88	5,73	0	60,91
Opt for real conditions	47,75	5,61	0	53,37

Figure 1.3-26 shows the EV energy distribution for ‘real-time exp’ with and without optimization.

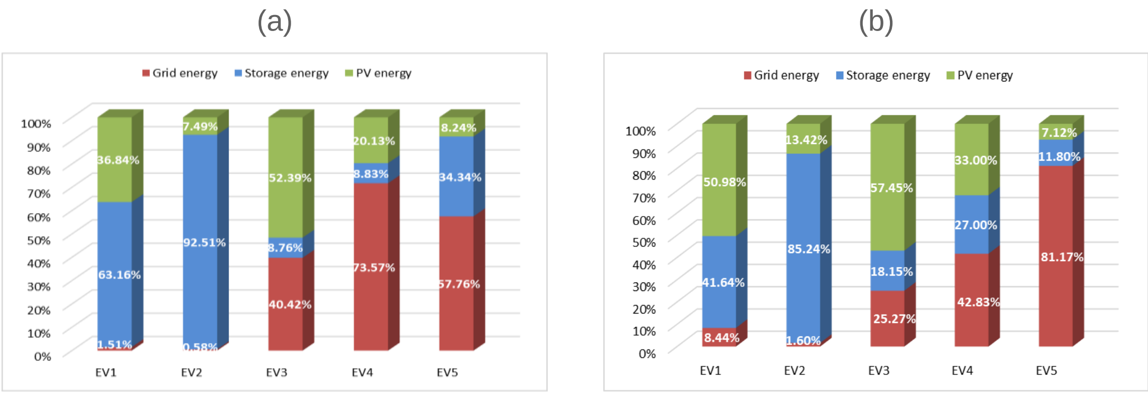

Figure 1.3-26 EV energy distribution for ‘real-time exp’ (a) without optimization and (b) with optimization—experimental test 2

In Figure 1.3-26, the share of PV energy is not significant even for EVs charging in slow mode. Thus, the share of storage energy is high for EV1 and EV2, while the share of grid energy is high for EV3, EV4, and EV5 as the storage is empty early, around 02:45 PM. Figure 1.3-26 (b) shows a better EV energy distribution than Figure 1.3-26 (a), where EV3 and EV4 were charged by the storage instead of the grid, whereas for EV5, the storage was preserved to discharge at the peak hour from 03:00 PM to 04:00 PM, and therefore EV5, charging in fast mode, was charged mainly by the grid.

1.3.4.3 Discussion

For ‘real-time exp’ with optimization, selling energy to the grid is preferred to make profits based on the coefficient k_D to minimize the total cost. Thus, with optimization gives better energy cost than without optimization. Furthermore, the EV energy distribution can be considered for ‘real-time exp’ with optimization to be better than without optimization.

To sum up, ‘with opt’ performs better than ‘w/o opt’ in minimizing the total cost of the IIREVs, and for the EV energy distribution, the results are satisfying with optimization, which is not the case without optimization, as the share of storage and grid energies are higher than the share of PV energy.

1.3.5 Conclusion

The simulation and real-time experimental results prove the superiority of the optimization problem formulated as MILP and solved by CPLEX over the storage priority algorithm. The results also show the feasibility of the proposed supervisory control of the IIREVs, which contains the HMI and the energy management with power balancing and interacts with the smart grid. The proposed supervisory control executes efficiently with respect to the constraints and fulfilling the EV user demands. Furthermore, the EVs that charge in slow mode depend mainly on PV energy, while for average or fast charging, they depend on the PV, storage and grid power sources. The EV energy distribution is considered good compared to the storage priority; only in the case with high fluctuations was the EV energy distribution better in storage priority. In addition, selling energy to the grid returns profits to the IIREV operator and makes optimization better than the storage priority algorithm.

The optimization takes into consideration the intermittent arrival and departure of EVs. Further works will concentrate on realizing optimization taking into consideration the intermittent arrival and departure of EVs with services such as vehicle-to-grid, vehicle-to-home, and infrastructure-to-home.

REFERENCES

[1] Sechilariu, M.; Locment, F.; Darene, N. Social Acceptance of Microgrids Dedicated to Electric Vehicle Charging Stations. In Proceedings of the 2018 7th International Conference on Renewable Energy Research and Applications (ICRERA), Paris, France, 10–17 October 2018; IEEE: Paris, France, 2018; pp. 1374–1379

[2] Liu, N.; Chen, Q.; Liu, J.; Lu, X.; Li, P.; Lei, J.; Zhang, J. A Heuristic Operation Strategy for Commercial Building Microgrids Containing EVs and PV System. IEEE Trans. Ind. Electron. 2015, 62, 2560–2570. https://doi.org/10.1109/TIE.2014.2364553

[3] Honarmand, M.; Zakariazadeh, A.; Jadid, S. Integrated Scheduling of Renewable Generation and Electric Vehicles Parking Lot in a Smart Microgrid. Energy Convers. Manag. 2014, 86, 745–755. https://doi.org/10.1016/j.enconman.2014.06.044.

[4] Sechilariu, M.; Molines, N.; Richard, G.; Martell-Flores, H.; Locment, F.; Baert, J. Electromobility Framework Study: Infrastructure and Urban Planning for EV Charging Station Empowered by PV-Based Microgrid. IET Electr. Syst. Transp. 2019, 9, 176–185. https://doi.org/10.1049/iet-est.2019.0032.

[5] Global EV Outlook 2020—Analysis. Available online: https://www.iea.org/reports/global-ev-outlook-2020 (accessed on 30 October 2020).

[6] Wang, Z.; Zhang, Y.; You, S.; Xiao, H.; Cheng, M. An Integrated Power Conversion System for Electric Traction and V2G Operation in Electric Vehicles With a Small Film Capacitor. IEEE Trans. Power Electron. 2020, 35, 5066–5077. https://doi.org/10.1109/TPEL.2019.2944276.

[7] Liu, C.; Chau, K.T.; Wu, D.; Gao, S. Opportunities and Challenges of Vehicle-to-Home, Vehicle-to-Vehicle, and Vehicle-to-Grid Technologies. Proc. IEEE 2013, 101, 2409–2427. https://doi.org/10.1109/JPROC.2013.2271951

[8] Jin, C.; Tang, J.; Ghosh, P. Optimizing Electric Vehicle Charging: A Customer's Perspective. IEEE Trans. Veh. Technol. 2013, 62, 2919–2927. https://doi.org/10.1109/TVT.2013.2251023.

[9] Xia, Y.; Hu, B.; Xie, K.; Tang, J.; Tai, H. An EV Charging Demand Model for the Distribution System Using Traffic Property. IEEE Access 2019, 7, 28089–28099. https://doi.org/10.1109/ACCESS.2019.2901857.

[10] Habib, S.; Khan, M.M.; Abbas, F.; Sang, L.; Shahid, M.U.; Tang, H. A Comprehensive Study of Implemented International Standards, Technical Challenges, Impacts and Prospects for Electric Vehicles. IEEE Access 2018, 6, 13866–13890. https://doi.org/10.1109/ACCESS.2018.2812303.

[11] Aluisio, B.; Bruno, S.; De Bellis, L.; Dicorato, M.; Forte, G.; Trovato, M. DC-Microgrid Operation Planning for an Electric Vehicle Supply Infrastructure. Appl. Sci. 2019, 9, 2687. https://doi.org/10.3390/app9132687.

[12] Chaudhari, K.; Ukil, A.; Kumar, K.N.; Manandhar, U.; Kollimalla, S.K. Hybrid Optimization for Economic Deployment of ESS in PV-Integrated EV Charging Stations. IEEE Trans. Ind. Inform. 2018, 14, 106–116. https://doi.org/10.1109/TII.2017.2713481.

[13] Suyono, H.; Rahman, M.T.; Mokhlis, H.; Othman, M.; Illias, H.A.; Mohamad, H. Optimal Scheduling of Plug-in Electric Vehicle Charging Including Time-of-Use Tariff to Minimize Cost and System Stress. Energies 2019, 12, 1500. https://doi.org/10.3390/en12081500.

[14] Deepak Mistry, R.; Eluyemi, F.T.; Masaud, T.M. Impact of Aggregated EVs Charging Station on the Optimal Scheduling of Battery Storage System in Islanded Microgrid. In Proceedings of the 2017 North American Power Symposium (NAPS), Morgantown, WV, USA, 17–19 September 2017; pp. 1–5.

[15] Davis, N.; Johnson, B.; McJunkin, T.; Scoffield, D.; White, S. Dispatch Control with PEV Charging and Renewables for Multiplayer Game Application. In Proceedings of the 2016 IEEE Conference on Technologies for Sustainability (SusTech), Phoenix, AZ, USA, 9–11 October 2016; pp. 156–161.

[16] Petrusic, A.; Janjic, A. Renewable Energy Tracking and Optimization in a Hybrid Electric Vehicle Charging Station. Appl. Sci. 2021, 11, 245. https://doi.org/10.3390/app11010245.

[17] Faraji, J.; Abazari, A.; Babaei, M.; Muyeen, S.M.; Benbouzid, M. Day-Ahead Optimization of Prosumer Considering Battery Depreciation and Weather Prediction for Renewable Energy Sources. Appl. Sci. 2020, 10, 2774. https://doi.org/10.3390/app10082774.

[18] Bucić, P.; Lešić, V.; Vašak, M. Distributed Optimal Batteries Charging Control for Heterogenous Electric Vehicles Fleet. In Proceedings of the 2018 26th Mediterranean Conference on Control and Automation (MED), Zadar, Croatia, 19–22 June 2018; pp. 837–842.

[19] Xu, T.; Sun, H.; Zhu, B.; Long, Y.; Wang, H.; Li, Z. Economic Optimization Control of Microgrid with Electric Vehicles. In Proceedings of the 2018 5th International Conference on Information Science and Control Engineering (ICISCE), Zhengzhou, China, 20–22 July 2018; pp. 733–736.

[20] Moya, F.D.; Torres-Moreno, J.L.; Álvarez, J.D. Optimal Model for Energy Management Strategy in Smart Building with Energy Storage Systems and Electric Vehicles. Energies 2020, 13, 3605. https://doi.org/10.3390/en13143605.

[21] Shi, R.; Zhang, P.; Zhang, J.; Niu, L.; Han, X. Multidispatch for Microgrid Including Renewable Energy and Electric Vehicles with Robust Optimization Algorithm. Energies 2020, 13, 2813. https://doi.org/10.3390/en13112813.

[22] Ghotge, R.; Snow, Y.; Farahani, S.; Lukszo, Z.; van Wijk, A. Optimized Scheduling of EV Charging in Solar Parking Lots for Local Peak Reduction under EV Demand Uncertainty. Energies 2020, 13, 1275. https://doi.org/10.3390/en13051275.

[23] Oliveira Farias, H.E.; Sepulveda Rangel, C.A.; Weber Stringini, L.; Neves Canha, L.; Pegoraro Bertineti, D.; da Silva Brignol, W.; Iensen Nadal, Z. Combined Framework with Heuristic Programming and Rule-Based Strategies for Scheduling and Real Time Operation in Electric Vehicle Charging Stations. Energies 2021, 14, 1370. https://doi.org/10.3390/en14051370.

[24] Nafisi, H.; Agah, S.M.M.; Askarian Abyaneh, H.; Abedi, M. Two-Stage Optimization Method for Energy Loss Minimization in Microgrid Based on Smart Power Management Scheme of PHEVs. IEEE Trans. Smart Grid 2016, 7, 1268–1276. https://doi.org/10.1109/TSG.2015.2480999.

[25] Yan, D.; Ma, C. Stochastic Planning of Electric Vehicle Charging Station Integrated with Photovoltaic and Battery Systems. Transm. Distrib. IET Gener. 2020, 14, 4217–4224. https://doi.org/10.1049/iet-gtd.2019.1737.

[26] Akram, U.; Khalid, M.; Shafiq, S. An Improved Optimal Sizing Methodology for Future Autonomous Residential Smart Power Systems. IEEE Access 2018, 6, 5986–6000. https://doi.org/10.1109/ACCESS.2018.2792451.

[27] Jiang, H.; Ning, S.; Ge, Q. Multi-Objective Optimal Dispatching of Microgrid With Large-Scale Electric Vehicles. IEEE Access 2019, 7, 145880–145888. https://doi.org/10.1109/ACCESS.2019.2945597.

[28] Dai, Q.; Liu, J.; Wei, Q. Optimal Photovoltaic/Battery Energy Storage/Electric Vehicle Charging Station Design Based on Multi-Agent Particle Swarm Optimization Algorithm. Sustainability 2019, 11, 1973. https://doi.org/10.3390/su11071973.

[29] Lan, T.; Jermsittiparsert, K.; Alrashood, S.T.; Rezaei, M.; Al-Ghussain, L.; Mohamed, M.A. An Advanced Machine Learning Based Energy Management of Renewable Microgrids Considering Hybrid Electric Vehicles' Charging Demand. Energies 2021, 14, 569. https://doi.org/10.3390/en14030569.

[30] Minh, P.V.; Le Quang, S.; Pham, M.-H. Technical Economic Analysis of Photovoltaic-Powered Electric Vehicle Charging Stations under Different Solar Irradiation Conditions in Vietnam. Sustainability 2021, 13, 3528. https://doi.org/10.3390/su13063528.

[31] Rafique, M.K.; Khan, S.U.; Saeed Uz Zaman, M.; Mehmood, K.K.; Haider, Z.M.; Bukhari, S.B.A.; Kim, C.-H. An Intelligent Hybrid Energy Management System for a Smart House Considering Bidirectional Power Flow and Various EV Charging Techniques. Appl. Sci. 2019, 9, 1658. https://doi.org/10.3390/app9081658.

[32] Zeng, B.; Dong, H.; Sioshansi, R.; Xu, F.; Zeng, M. Bilevel Robust Optimization of Electric Vehicle Charging Stations With Distributed Energy Resources. IEEE Trans. Ind. Appl. 2020, 56, 5836–5847. https://doi.org/10.1109/TIA.2020.2984741.

[33] Wu, H.; Pang, G.K.H.; Choy, K.L.; Lam, H.Y. An Optimization Model for Electric Vehicle Battery Charging at a Battery Swapping Station. IEEE Trans. Veh. Technol. 2018, 67, 881–895. https://doi.org/10.1109/TVT.2017.2758404.

[34] Chung, C.-H.; Jangra, S.; Lai, Q.; Lin, X. Optimization of Electric Vehicle Charging for Battery Maintenance and Degradation Management. IEEE Trans. Transp. Electrif. 2020, 6, 958–969. https://doi.org/10.1109/TTE.2020.3000181.

[35] Hosseinzadeh, M.; Salmasi, F.R. Robust Optimal Power Management System for a Hybrid AC/DC Micro-Grid. IEEE Trans. Sustain. Energy 2015, 6, 675–687. https://doi.org/10.1109/TSTE.2015.2405935.

[36] Sigalo, M.B.; Pillai, A.C.; Das, S.; Abusara, M. An Energy Management System for the Control of Battery Storage in a Grid-Connected Microgrid Using Mixed Integer Linear Programming. Energies 2021, 14, 6212. https://doi.org/10.3390/en14196212.

[37] Moser, A.; Muschick, D.; Gölles, M.; Nageler, P.; Schranzhofer, H.; Mach, T.; Ribas Tugores, C.; Leusbrock, I.; Stark, S.; Lackner, F.; et al. A MILP-Based Modular Energy Management System for Urban Multi-Energy Systems: Performance and Sensitivity Analysis. Appl. Energy 2020, 261, 114342. https://doi.org/10.1016/j.apenergy.2019.114342.

[38] Abou El-Ela, A.A.; El-Sehiemy, R.A.; Allam, S.M.; Shaheen, A.M.; Nagem, N.A.; Sharaf, A.M. Renewable Energy Micro-Grid Interfacing: Economic and Environmental Issues. Electronics 2022, 11, 815. https://doi.org/10.3390/electronics11050815.

[39] El-Ela, A.A.A.; El-Seheimy, R.A.; Shaheen, A.M.; Wahbi, W.A.; Mouwafi, M.T. PV and Battery Energy Storage Integration in Distribution Networks Using Equilibrium Algorithm. J. Energy Storage 2021, 42, 103041. https://doi.org/10.1016/j.est.2021.103041.

[40] Shaheen, A.M.; Hamida, M.A.; El-Sehiemy, R.A.; Elattar, E.E. Optimal Parameter Identification of Linear and Non-Linear Models for Li-Ion Battery Cells. Energy Rep. 2021, 7, 7170–7185. https://doi.org/10.1016/j.egyr.2021.10.086.

[41] Hamida, M.A.; El-Sehiemy, R.A.; Ginidi, A.R.; Elattar, E.; Shaheen, A.M. Parameter Identification and State of Charge Estimation of Li-Ion Batteries Used in Electric Vehicles Using Artificial Hummingbird Optimizer. J. Energy Storage 2022, 51, 104535. https://doi.org/10.1016/j.est.2022.104535.

[42] Sechilariu, M.; Locment, F. Photovoltaic Source Modeling and Control. In Urban DC Microgrid; Elsevier: Amsterdam, The Netherlands, 2016; pp. 35–91. ISBN 978-0-12-803736-2.

[43] Sechilariu, M.; Locment, F. Backup Power Resources for Microgrid. In Urban DC Microgrid; Elsevier: Amsterdam, The Netherlands, 2016; pp. 93–132. ISBN 978-0-12-803736-2.

[44] Cheikh-Mohamad, S.; Sechilariu, M.; Locment, F. PV-Powered Charging Station: Energy Management and Cost Optimization. In Proceedings of the 2021 IEEE 30th International Symposium on Industrial Electronics (ISIE), Kyoto, Japan, 20–23 June 2021; pp. 1–6.

[45] Sechilariu, M.; Locment, F. Direct Current Microgrid Power Modeling and Control. In Urban DC Microgrid; Elsevier: Amsterdam, The Netherlands, 2016; pp. 133–170. ISBN 978-0-12-803736-2.

[46] Sechilariu, M.; Locment, F. Experimental Evaluation of Urban Direct Current Microgrid. In Urban DC Microgrid; Elsevier: Amsterdam, The Netherlands, 2016; pp. 209–250. ISBN 978-0-12-803736-2.

[47] Montaño-Salcedo, C.E.; Sechilariu, M.; Locment, F. Human-System Interfaces for PV-Powered Electric Vehicles Charging Station. In Proceedings of the 2021 IEEE 30th International Symposium on Industrial Electronics (ISIE), Kyoto, Japan, 20–23 June 2021; pp. 1–6.

[48] Marra, F.; Yang, G.Y.; Træholt, C.; Larsen, E.; Rasmussen, C.N.; You, S. Demand Profile Study of Battery Electric Vehicle under Different Charging Options. In Proceedings of the 2012 IEEE Power and Energy Society General Meeting, San Diego, CA, USA, 22–26 July 2012; pp. 1–7.

[49] ILOG CPLEX Optimization Studio—Overview. Available online: https://www.ibm.com/products/ilog-cplex-optimization-studio (accessed on 16 March 2022).

[50] Cheikh-Mohamad, S.; Sechilariu, M.; Locment, F.; Krim, Y. PV-Powered Electric Vehicle Charging Stations: Preliminary Requirements and Feasibility Conditions. Appl. Sci. 2021, 11, 1770. https://doi.org/10.3390/app11041770

1.4 Case study: experimental results of solar charging of electric vehicles at CEA Cadarache

Sales of electric vehicles (EVs) are increasing, necessitating the development of systems to manage their charging and mitigate impacts on the power grid. This paper presents a supervision system for charging EVs used by employees at the CEA Cadarache research centre, which features over 80 charging points established in 2016. The system aims to fully charge EV batteries while synchronizing power consumption of 24 charging points with solar energy production. Experimental results indicate that it is feasible to increase the self-production ratio by up to 60 percentage points while meeting user needs[4].

1.4.1 Introduction

The European Commission plans to ban the sale of new non-zero-emission commercial and passenger light vehicles starting in 2035 [1]. This decision will accelerate the development of full Battery Electric Vehicles (BEVs), which represented 9% (880 000 units) of sales of light vehicles in Europe over 2021 [2]. This growth needs to be supported by the rapid development of the Electric Vehicle Charging Infrastructure (EVCI). By the end of 2021, there were 225 000 charging points available in the European Union [3], but by 2030, a total of four million charging points are expected [4], for approximately 34 million BEVs and 14 million Plug-in Hybrid Electric Vehicles (PHEVs). The impacts of this growth on the power grid must to be carefully anticipated: greater electricity production will be needed, and electricity transmission and distribution networks will have to be improved [5][6]. For example, the French transmission system operator, RTE, estimated in a recent study [7] that, in France, the electricity production will have to be increased by 100 TWh in 2050 in a 'reference scenario', considering that 95% of light vehicles and 21% of heavy-duty vehicles are electrified. This energy will represent approximately 15% of the projected electricity consumption in this scenario. Nonetheless, in the same study, RTE concludes that the control of the charge of electric vehicles (EVs) is a 'no regret' solution from a technical and economic standpoint, i.e., it is profitable in all situations.

Many control algorithms and associated systems have been proposed in the literature [8][9]. For example, some authors propose providing primary reserve [10][11], which involves changing the charging power of the EV according to the frequency deviation of the network, or limiting EV load to the available capacity of the power network [12] - [14]. Other authors suggest providing reactive power [15] or minimizing the effects on the grid from rapid fluctuations in photovoltaics (PV) production output due to cloud transients [16] or even balancing wind energy [17]. Additionally, some control algorithms aim to minimize charging costs for users [18], fleet managers [19], or parking operators [20]. Some studies also analyze the EV charging when integrated in to a microgrid with the consumption of residential or/and commercial buildings, solar carport and/or solar plant, and potentially an energy storage system [21] - [27]. All these articles are either based on synthetic data (i.e., generated from mathematical models only) or use real data (i.e., obtained from physical measurements) as inputs for simulations. Such real data are obtained from laboratories or from field scale demonstrators. Marinelli et al.

[4] This section is based on the following publication: B. Robisson, S. Guillemin, L. Marchadier, G. Vignal, and A. Mignonac, "Solar Charging of Electric Vehicles: Experimental Results," Applied Sciences, vol. 12, no. 9, p. 4523, Apr. 2022, http://dx.doi.org/10.3390/app12094523

propose a review of projects that address such demonstrators in Europe [28]. Descriptions of other demonstrators can also be found in [29] - [34].

Nonetheless, the literature lacks papers or public reports that describe in detail experiments controlling the charge of EVs in a field-scale demonstrator, except in the following four studies. In [30], the authors described tests conducted from January 2017 to December 2018 in the United Kingdom, involving more than 600 EV drivers. During one of these tests, called 'Trial 3', the users were financially incentivized to allow the system charge their EVs outside of peak hours. The results show that the incentive, combined with smart charging, significantly impacted drivers' behaviour. In [35], the authors describe an experimental setup involving commercial EVs and two commercial unidirectional charging stations in the test-site of University Campus Lyngby. The authors demonstrate that it is technically feasible to control the unidirectional charging of EVs to provide primary frequency regulation. The ChargeForward project [31] - [36] has managed a set of more than 400 EV-driving households (approximately 250–300 at any given time during the project) that participated in real-world experiments in the San Francisco Bay area. Several use cases of EV grid integration were studied. One of them, called 'Earth Week Renewable Energy Use Case', involved encouraging participants to charge during the middle of the day to utilize excess solar energy. This use case lasted one week in 2018. The project showed that 55% of the charging power came from renewable energy, compared to the national average of 23%. In [37], the authors describe the results of an experiment conducted over a year at a test site consisting of six 22 kW AC charging stations. They show that their algorithm ensures a fair distribution of the charging power between the six charging stations, even when the grid connection only allows two EVs to charge concurrently. In [32], a similar test was conducted but on a larger scale, involving an EVCI consisting of more than 1 000 public charging points in the Netherlands. The researchers demonstrated that it was possible to limit the charging speed of EVs to avoid exceeding the available power network capacity.

This paper describes the setup and results of smart charging tests conducted at the CEA Cadarache site. During these tests, the charging of EVs was controlled to recharge their batteries and maximize the self-production rate of the system, which consists of 24, 22 kW AC charging stations and a 160 kWp PV plant. More than 300 users, who own over 40 different EV models, participated in these tests.

The remainder of the paper is organized as follows: the experimental setup is detailed in Section 1.4.2, with a section focusing specifically on the control algorithm. The main results obtained over a four-month period and the lessons learned are presented in Section 1.4.3. Section 1.4.4 presents the conclusion of these experiments and discusses future perspectives.

1.4.2 Context of the experiments

This section describes the research centre where the experiments take place. The charging infrastructure is detailed, as well as the supervision system. A subsection will focus on the control algorithm developed by CEA, which consists of synchronizing PV production and EV charging.

1.4.2.1 R&D Centre of Cadarache

The experiments take place at the Cadarache research centre of the French Alternative Energies and Atomic Energy Commission, or CEA. It is a 60-year-old research centre located near Aix-en-Provence. This 60-year-old research centre is located near Aix-en-Provence and spans 1 600 hectares, of which 900 hectares are fenced (by a 22 km fence). The Cadarache centre consists of 480 buildings, including office spaces as well as research laboratories. The centre is directly connected to the electricity network. It is directly connected to the electricity network, and the CEA manages its own water network, heat network, and medium-voltage electricity distribution network (made up of 18, 15 kV loops). The research centre acts as a Distribution System Operator (DSO). A public lighting network and an Electric Vehicle Charging Infrastructure (EVCI) are connected to this power network. Two thousand five hundred CEA employees work at the Cadarache site, along with employees from partner companies. In total, around 5 000 people are employed at Cadarache. The CEA offers a private bus service for commuting. Thus, the Cadarache centre can be seen as a small town privately owned and managed by the CEA.

The CEA conducts research on solar thermal energy and solar photovoltaics. Therefore, PV solar plants are installed at the Cadarache site in two different locations: the internal solar platform and the Mégasol platform. On the internal platform, the CEA tests and evaluates innovative PV solutions ranging in size from modules to systems of a few tens of kilowatts. On the Mégasol platform, the CEA tests these innovative solutions on four PV plants totalling 12 MWp, owned by industrial partners.

1.4.2.2 EVCI

The CEA’s EVCI was set up during the summer of 2016. It involves 40 Diva-type terminals produced and installed by G²Mobility, which was bought out by TotalEnergies in 2018. Each Diva terminal has two 22 kW AC charging points. Each of these charging points has a Type 2 socket for mode 3 connections and a Type E socket for mode 1 and 2 connections. These charging stations have been installed individually or in groups of up to four Diva terminals, creating 30 charging stations spread throughout the entire centre. Each charging station has an embedded IoT gateway that enables communication through 3G networks using Open Charge Point Protocol (OCPP) commands.

The CEA maintains and operates this EVCI and, therefore plays the role of Charging Point Operator (CPO). The user must use a badge to authorize charging of the EV. To obtain a badge, the user must be registered and specify their contact details, such as mobile phone number, as well as their car’s model. Thus, the CEA assumes the role of e-Mobility Service Provider (e-MSP).

1.4.2.3 EVCI charging history

Before the experiments were performed, data were collected from an OCPP supervisor over a period of four years (from June 2016 to June 2020). During this period, a total of 17 045 charging sessions were recorded, resulting in an energy consumption of 253 MWh. The mean duration and mean energy consumption of each charging session were recorded as 12 h and 14,8 kWh. The histograms of the start and end times of the charging sessions were also computed (Figure 1.4-1). The X-axis was designated to represent local time. The start times of the charging sessions were shown in blue, while the end times were displayed in orange. It was observed that three main periods could be identified for the start of the charging sessions: primarily at the beginning of the working day (around eight in the morning), then at lunchtime when cars were charged at the business restaurant, and finally at the end of the afternoon when service cars returned from business trips. Three main periods were also observed for the end of charging sessions. The first occurred at 09:00 AM when service cars that had been connected the day before were disconnected for business trips, the second took place at lunchtime, and the last period was at the end of the working day (around 05:00 PM – 06:00 PM) when employees left the centre.

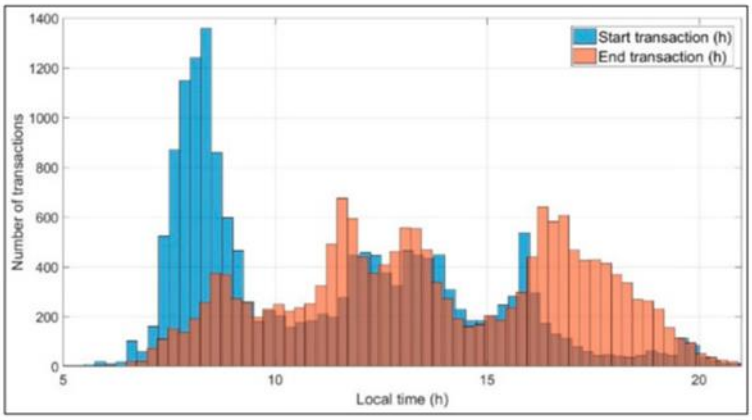

Figure 1.4-1 Histograms of start and end times of charging sessions

1.4.2.4 EVCI users

As of February 1st, 2022, 376 RFID badges were issued for EV (including PHEV) owners. The number of badges is steadily increasing by around 100 badges per year. Two hundred sixty cars are used by employees for personal use, and there are also 84 service cars. The Cadarache site has setup a taxi service provided by three Renault ZOE cars. Additionally, the CEA authorizes external companies to charge their 29 EVs.

There are three levels of user involvement in the experimentations:

- Seventy-five EV owners (about 78% of the volunteer experimenters) agreed to give control over the charging power of their charging sessions. They also consented to provide information about the State of Charge (SOC) of their batteries and their forecast departure times. Additionally, they supplied details about their cars' features (battery capacity and maximum power of the onboard charger). The set of these cars is further referred to as 'PControlled'.
- Twenty-one employees have not given control over the charging of their cars but have agreed to send information about their SOC and forecast departure times. They also provide details about their cars. The set of these cars is further referred to as 'PUncontrolled'.
- The remaining users do not participate to the experiments and are referred to as 'Others'.

The union of the first two categories of people is referred to as 'Participants', while the union of the last two categories is called 'Uncontrolled'.

In terms of car models, there is a clear predominance of the Renault ZOE, which represents 38% of all the EVs. Among others, there are 10% of Peugeot e-208, 7% of Renault Twingo, 8% of Tesla (Model 3 and Model S), and 5% of Nissan Leaf vehicles.

1.4.2.5 OCPP supervisor

From June 2021, the CEA has set up an IT architecture to control part of its EVCI. Twenty-four (out of 80) charging points have been connected to an information system developed by the CEA, called SIGE, which stands for 'Système d'Information pour la Gestion optimisée de l'Energie' in French (or EMIS for 'Energy Management Information System' in English). This information system stores all the data necessary to control the charging of the EVs (including data on EVs, the electrical network, characteristics of PV plants, and charging stations, etc.). SIGE can also automatically download external data. For example, SIGE is connected to servers to retrieve PV production forecasts and to PV plants to obtain the values of PV production. SIGE and the Diva stations communicate through a 3G connection using the OCPP 1,6 protocol. The interactions of SIGE with the managers of the EVCI and the EV users are described below.

1.4.2.6 SIGE for the Managers of the EVCI and for the EV Users

SIGE offers a web user interface for the managers of the EVCI. It allows operators not only to monitor the status of all the charging stations but also to act on them. For example, the operator can stop the current charging session or restart it. Additionally, the operator can unlock a plug or set the maximum charging power. The web interface also provides statistics categorized by user, area, charging station, and charging point.

The EV user must authenticate using the RFID badge issued by the CEA to connect their vehicle to one of the charging points. This badge is first presented to the RFID reader of the Diva. The reader then scans the ID number stored in the badge, and the Diva station queries SIGE. If the badge ID is in the database and the user participates in the experiments, SIGE sends a text message inviting them to fill in their forecast departure time (t_{dep}) and the SOC of their car at the start of the charging process (SOC_{init}). Without a response from the user, SIGE considers default values (t_{dep} = 05:00 PM and $SOC_{init} = 25\%$). At the same time, SIGE sends the authorization to charge to the charging station while the user plugs their EV into the Diva terminal connector. The charging station then communicates with the vehicle via the cable using carrier current, in accordance with the IEC 61851 standard, which is an international standard for electric vehicle conductive charging systems. SIGE then sends a charging test profile to the Diva consisting of two phases. The first phase, called the 'discovering phase', involves charging the EV battery at its maximum power for a short period. This phase enables SIGE to estimate the maximum charging power of the EV, P_{Max}, and also confirms to the user that their vehicle is electrically connected. In the second phase, SIGE controls the charge of the EV according to specified objectives (see Section 1.4.2.7). When the charge is finished, SIGE sends a text message to the user, inviting him to disconnect their vehicle and clear the parking place.

1.4.2.7 Control Algorithm

1.4.2.7.1 Objectives

The CEA has developed a software module in SIGE that controls the charging of the EVs connected to a set of charging stations. This module manages processes according to given objectives based on all the data stored and retrieved by SIGE. The primary objective is to satisfy the EV user, ensuring that their EV battery is fully charged by the forecasted departure time. The secondary objective is to maximize the self-production rate of the system, which consists of 24 charging points and 1,3% of the electricity produced by the Mégasol platform (160 kWp). The self-production rate is commonly defined as the value of the PV energy consumed when it is produced, divided by the total consumption. However, to isolate the effects of the EV charging control algorithm and the PV forecast algorithm, it was decided not to consider PV production in this definition; instead, the best forecast of this production will be considered, referred to as the 'available power' and detailed in the subsection 1.4.2.7.4. Thus, the self-production rate, SP , is defined as the value of the energy consumed when it is forecasted to be produced (E_{av}) divided by the total consumption (E_{cons}). It is defined by the following equation:

$$SP = \frac{E_{av}}{E_{cons}} \qquad (1.4\text{-}1)$$

1.4.2.7.2 Charging Power Models

In the considered set-up, controlling the charge of an EV involves managing its SOC by modifying over time the power that the station can deliver. The set of maximum power values over time is called 'SetPoints'. The function that links the SetPoints and the SOC is very complex. It depends on the maximum power accepted by the car when it is charging with an AC connection. This parameter is influenced by the car model, the size of its onboard charger, the type of connection with the charging station, and the cable used to connect the car to the station. It also depends on the external temperature and the traction battery temperature. Additionally, the user may utilize software (generally an application on a smartphone) that may also limit the value of P_{Max}. In the experiments, participants are encouraged to deactivate such external control. It is assumed that P_{Max} is constant and equal to the value measured during the 'discovering phase'. The energy that can be stored in the traction battery, further referred to as 'Capacity' (E_{Max}), is also a key parameter that depends on the vehicle model and options. For example, a Tesla Model 3 may have four sizes of battery: 55, 62, 75, and 82 kWh. In this case, Capacity is assumed to be constant and equal to the value declared by the participants. For the cars of individuals not participating in the experiments, Capacity is considered the maximum size of the battery for the EV model. Other parameters exist, such as the number of phases used to charge the car. Public information is utilized to obtain these data. Generally, if the onboard charger is less than 11 kW, it is a single-phase charger; otherwise, it is a three-phase charger. However, there are exceptions; for example, the Seat Mii charges at 7,4 kW with a two-phase charger.

1.4.2.7.3 Control Principle

The planning algorithm is executed at the start of each new charging session and periodically every 10 minutes. Let t_0 be the current time, with the 24 hours after the current time discretized by a time step of $\Delta t = 10\ min$, noted as t_n. In this setup, as it is not possible to directly measure SOC of the cars, the planning algorithm first estimates the SOC of all the EVs at the current time t_0 . These estimations are based on the initial values of the SOC and the measurements from the energy meters of the charging stations (see details in the subsection 1.4.2.7.5). Then, for all t_n, the control algorithm follows two steps:

The available power values are calculated, as detailed in the subsection 1.4.2.7.4. These values are allocated among the cars that are connected and waiting to be charged (i.e., their SOC estimate is lower than 100%). The allocation process is based on a basic scheduling mechanism, i.e., 'earliest deadline first' [20], which was adapted to achieve the objectives. In this context, the 'deadline' of a car, also called 'lead-time', is the difference between the time before departure (t_{dep}) and the time needed to recharge the battery without a charging control (t_{end}). The computation of this lead-time is detailed in the subsection 1.4.2.7.6. The planning algorithm estimates the lead-time of all the EVs. The available power is first allocated to the EVs that are not under control (i.e., EVs in the set 'Uncontrolled') and to the cars that have a negative lead-time. The maximum charging power is allocated to each of these cars. The remaining power is then distributed in the inverse order of the lead-time, with the maximum charging power allocated to the cars that have the smallest lead-time. If there is not enough available power for the cars with the highest lead-time, they do not recharge during this time step, but they will be charged during the subsequent time steps. The powers allocated to each EV for each time step are the SetPoints sent over the 3G network to the charging points.

The following simple example illustrates the principle of the control algorithm. Consider an EV owner not participating in the experimentation, who connects a car (a ZOE with a battery capacity of 50 kWh) to the EVCI. Since SIGE has no information about the initial SOC of the car battery, it takes $SOC_{init} = 25\%$ as a default value. Thus, SIGE considers that around 40 kWh are needed to fully charge the battery. In this example, it is assumed that there is enough available power to supply the car battery at P_{Max} (22 kW) during the time needed to fully charge the battery, which is about 1 hour and 50 minutes. In such a case, the planning algorithm sends the associated set points (i.e., 22 kW for 1 hour and 50 minutes) to the station. Then, SIGE estimates the charging power as explained in the subsection 1.4.2.7.5. Two cases arise during the charging process:

- The car may either stop charging prematurely because it is full (i.e., before 1 hour and 50 minutes of charge). SIGE may underestimate the real SOC. This situation may occur when the real initial SOC is greater than 25%. In that case, the set points are null power values, and the charging power is allocated to another car.
- Alternatively, the car may continue to charge even after 1 hour and 50 minutes. SIGE may overestimate the real SOC. This situation may occur when the real initial SOC is less than 25%. In that case, the set points do not change until the charging stops.

The effect of this control algorithm on the historical charging session data presented in Section 1.4.2.3 was simulated. This simulation step allowed for the confirmation of the choice of different parameters and proved the effectiveness of the control algorithm.

1.4.2.7.4 Available Power

Figure 1.4-2 illustrates how the power considered available in the future for the charging of EVs is computed. It shows the solar production data from November 1st, 2021. First, the PV production forecasts, based on weather forecasts, are retrieved every two hours from the web server of the National Oceanic and Atmospheric Administration in the United States of

America. These data are referred to as 'rawPowerForecast' and are represented as orange dots Figure 1.4-2. Second, the power production of the PV plant, assuming clear skies, is computed using homemade software based on the public software library PV_LIB [38]. These data are called 'clearskyPower' and are represented as a dark blue line. This curve is bell-shaped because solar production increases during the morning until it reaches solar noon (the time when solar production is at its peak) and then decreases at the same rate as it increased a few hours earlier. Third, a bell-shaped interpolation of the 'rawPowerForecast' is computed. These values are called 'powerForecast' and are represented as a black line. The power measured at the PV plant is collected with a System Control and Data Acquisition (SCADA) system and transmitted over the 3G network. These data are referred to as 'Power' and are represented as a blue line. From all these data, SIGE computes the 'correctedPowerForecast', which is represented by a green line. Roughly speaking, these last data are equal to the 'powerForecast', unless the previous values (i.e., in the near past) of 'powerForecast' are too far from the previous values of 'Power'. In that case, 'correctedPowerForecast' is computed using 'Power' and the persistence method (i.e., the weather in the near future is considered the same as the weather in the near past). Finally, the power considered available in the near future for charging EVs is the 'correctedPowerForecast'.

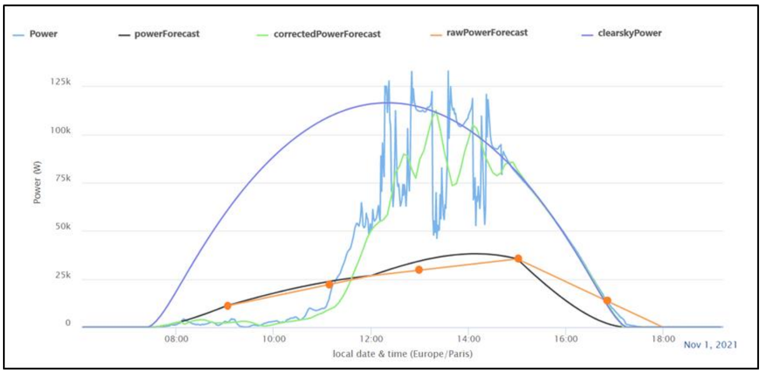

Figure 1.4-2 Illustration of the computation of the available power

1.4.2.7.5 SOC Estimation

The value of the SOC estimated at a given time t_0 is denoted as $SOC_{estimate}\ (t_0)$. This estimation is computed using the initial value of SOC_{init} and the values from the energy meter, which are read every $dt\ = 2\,min$. For many charging stations, this is the minimum time to retrieve data without encountering any synchronization or timestamp issues. The power withdrawn by the car $P_w(t_0)$ is first estimated from the values measured by the energy meters at the considered time t_0, denoted as $E_w\ (t_0)$, and from Q minutes before t_0, denoted as $E_w\ (t_{-Q})$. The power $P_w\ (t_0)$ is computed according to the following formula:

$$P_w(t_0) = \frac{E_w\ (t_0) - E_w\ (t_{-Q})}{Q\ \times \Delta t} \tag{1.4-2}$$

Q is a parameter chosen equal to 3 to obtain an accurate value of the power as quickly as possible (i.e., every 6 min). It is considered that if the car does not withdraw energy during the six minutes before t_0, the measured $P_w\ (t_0)$ withdrawn power is equal to zero. This phenomenon occurs because the car battery is fully charged, resulting in the $SOC_{estimate}$ being equal to 100%.

If $P_w\ (t_0)$ is not equal to zero, $SOC_{temporary}\ (t_0\ )$ is computed according to equation (1.4-3). In this equation, t_{init} represents the time at the start of the charging process, and Y is the yield of the charging process, which is assumed to be equal to 95%.

$$SOC_{temporary}\ (t_0\ ) = SOC_{init} + Y\ \times \frac{E_W\ (t_0) - E_W\ (t_{init})}{E_{max}} \times 100 \qquad (1.4\text{-}3)$$

If the car keeps charging (i.e., $P_w\ (t_0\ ) > 0$) while $SOC_{temporary}\ (t_0)$ equals a threshold value (typically 99%), the value of $SOC_{temporary}$ is considered overestimated compared to the real SOC. In that case, without any other information about the real SOC, $SOC_{estimate}$ is assumed to remain equal to the threshold value. In other cases, $SOC_{estimate}$ is considered equal to $SOC_{temporary}$.

1.4.2.7.6 Lead-time

As explained, the lead-time is the difference between the time before departure and the time needed to fully charge the battery without a charging control. This lead-time has to be estimated at each time step t_n. The set points from t_0 and t_{n-1} have been computed by the previous iteration of the planning algorithm. Let Setpoint (t_p) denote the power set point computed for the period $[t_p;\ t_p +\ \Delta t]$. During this period, it is considered that the car charges at the constant value Setpoint (t_p). Thus, at t_0, the value of the SOC_{future}, in a future point in time t_n, is calculated according to the following formula:

$$SOC_{future}\ (t_n) = max(100, SOC_{estimate}(t_0) + \frac{100\ \times Y}{E_{max}} \times \sum_0^{p=n-1} SetPoint(t_p) \times \Delta t) \qquad (1.4\text{-}4)$$

Then, from time t_n, it is considered that the EV charges at P_{Max} until its battery is fully charged. Given this SOC_{future} value, the point in time t_{end} can be computed such that the battery is full when charged with the following formula:

$$t_{end} = t_{init}\ + \left(100 - SOC_{future}(t_n) \times \frac{E_{max}}{100 \times E_{max}}\right) \qquad (1.4\text{-}5)$$

The lead-time is the difference between the time before departure t_{dep} and the time t_{end} taken to charge the battery at P_{Max} .

$$LeadTime(t_n) = t_{dep}(t_n) - t_{end} \qquad (1.4\text{-}6)$$

1.4.3 Results

1.4.3.1 Preliminary 1: Data Selection

The following experimental data were recovered between October 1st, 2021 and February 1st, 2022 inclusive (124 days in total). It is considered that 73 days provided exploitable results. The other days are either without any EV charging session (34 days) or with measurement errors or chad measurement errors, communication issues, or hardware breakdowns (17 days). During these field tests, a total of 887 charging sessions were recorded, and 12,4 MWh were transferred to the EVs. The batteries of the EVs were all charged before the departure time forecasted by the users, except in very few cases (mainly short sessions of 1 or 2 hours). In these cases, the users were informed by email or phone that there were issues with their charging sessions.

In order to estimate the efficiency of the control algorithm, two self-production rates were compared. The first rate, SP, is computed from the available power and the energy consumption measured by the charging stations, as explained in the subsection 1.4.2.7.1. The second rate is computed in the same way, except that the energy consumption is considered as the simulated consumption of all the EVs, under the assumption that none of them are controlled. In other words, the total energy is quantified in the case where the EVs charge at their P_{Max} from the start of the charging sessions until their batteries are fully charged. The associated self-production ratio is denoted as 'Uncontrolled Self-production ratio' or SP_u.

Figure 1.4-3 displays a scatter plot with the self-production ratio SP on the Y-axis and the uncontrolled self-production ratio SP_u on the X-axis, computed for the same days. As the points are clearly above the line $Y = X$, this scatter plot clearly shows that the control algorithm globally increases the self-production ratio. A small (resp. great) difference between SP and SP_u corresponds to a minor (resp. large) increase in the self-production ratio thanks to the control algorithm.

The days associated with the red dots in Figure 1.4-3 were chosen according to their different locations on the plot (in the middle, in the upper right corner, and at the top left). Indeed, these red dots represent cases that will be outlined in the following paragraphs:

- In the middle: low values for both SP and SP_u
- In the upper right corner: high values for both SP and SP_u
- At top left: high value for SP and low value for SP_u

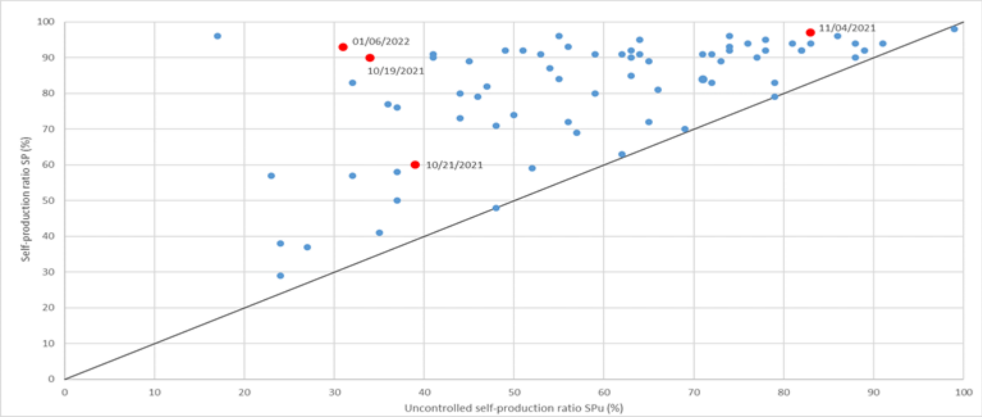

Figure 1.4-3 Distribution of the self-production ratio in both controlling scenarios on a scatter plot (red dots correspond to days that will be described in the next paragraphs)

1.4.3.2 Preliminary 2: Description of Figures 4-7

Figure 1.4-4 to Figure 1.4-7 are partly made up of three curves related to PV production, as described in the subsection 1.4.2.7.4:

- The blue curve corresponds to 'ClearskyPower'.
- The red curve represents the 'CorrectedPowerForecast', which is considered the available power.
- The green curve represents the measured PV production, noted as 'Power'. The measurement system of these data breaks down sometimes, as can be seen in Figure 1.4-4 and Figure 1.4-7 (when the green line is flat or missing).

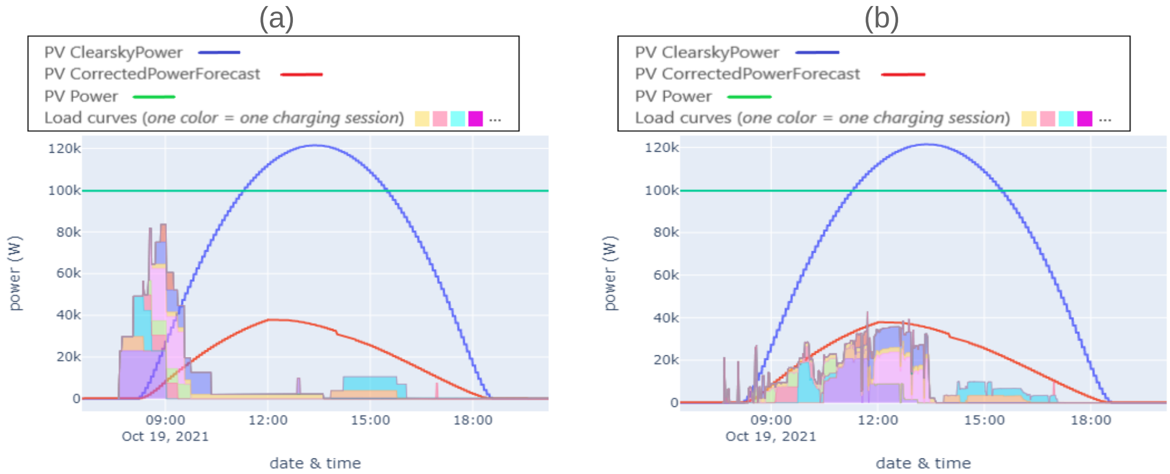

Figure 1.4-4 Results of October 19th, 2021:

(a) Stacked energies without control. The self-production rate SP_u is equal to 34%; (b) stacked energies with control. The self-production rate SP is equal to 90%

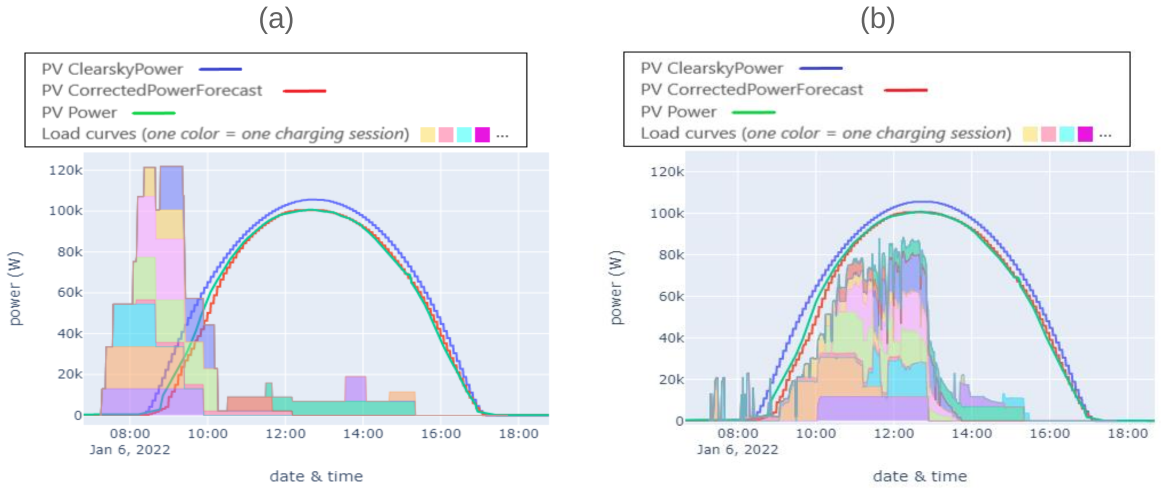

Figure 1.4-5 Results of January 6th, 2022:

(a) Stacked energies without control. The self-production rate SP_u is equal to 34%; (b) stacked energies with control. The self-production rate SP is equal to 90%

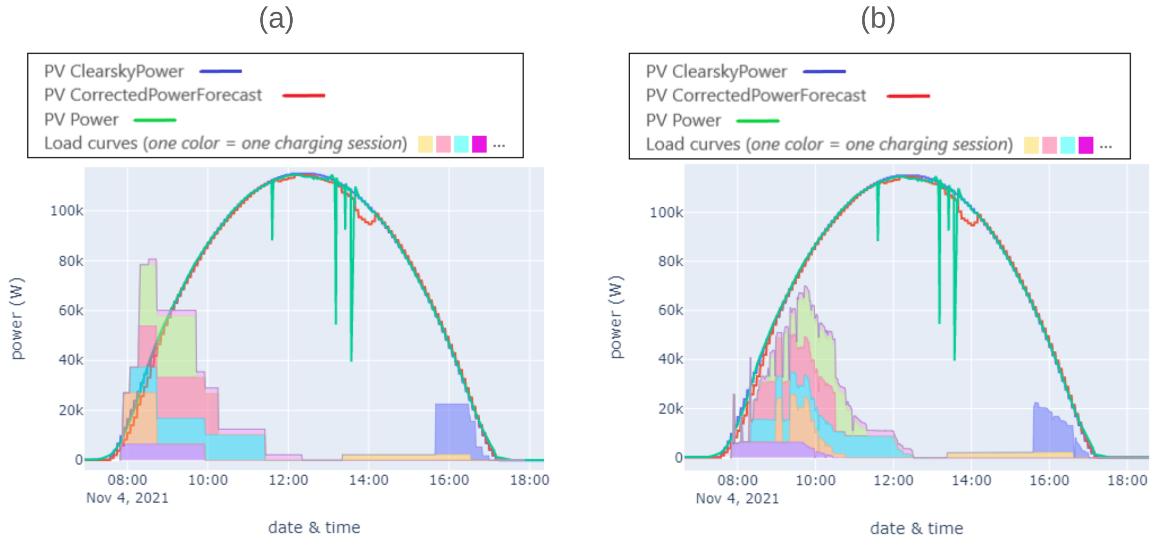

Figure 1.4-6 Results of November 4th,2021:

Stacked energies without control. The self-production rate SP_u is 83%; (b) stacked energies with control. The self-production rate SP is 97%

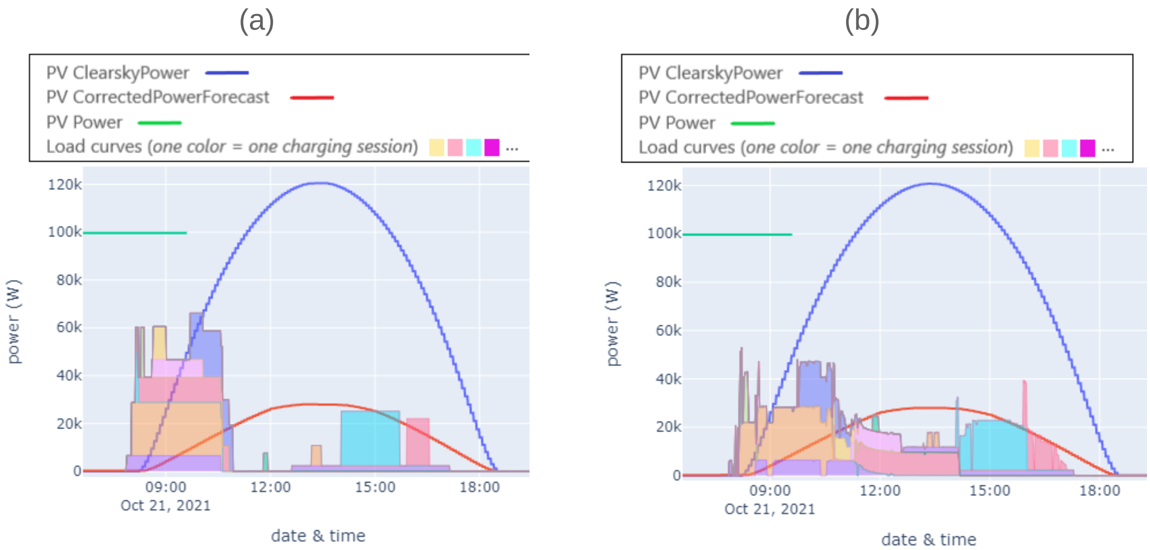

Figure 1.4-7 Results of October 21st, 2021:

(a) Stacked energies without control. The self-production rate SP_u is equal to 39%; (b) stacked energies with control. The self-production rate SP is equal to 60%

1.4.3.3 The Control of Charge Increases Drastically the Self-Production Ratio

Figure 1.4-4 represents the results obtained on October 19th, 2021. During this cloudy day, 17 charges occurred, resulting in a total energy consumption of 141 kWh and a total PV production of 221 kWh.

Figure 1.4-4 (a) shows that the charges, without any control, would have primarily taken place between 07:30 AM and 10:30 AM. he cumulative load curve is located above the red curve, indicating that the self-production rate is low (in this case, it is equal to 34%). In contrast, Figure

1.4-4 shows that the loads occurred mainly below the red curve, suggesting that the self-production rate is high (here 90%).

Figure 1.4-5 represents the results obtained on January 6th, 2022. On this particular sunny day, 15 charges occurred, resulting in a total energy consumption of 227 kWh and a forecast PV production of 551 kWh. On this day, the self-production rate increased from 31% to 93% thanks to the control algorithm.

These results emphasize that charging control can significantly increase the self-production rate during both sunny and cloudy days.

1.4.3.4 The Self-Production Rate Can Be High, Even without Control

Figure 1.4-6 illustrates the results obtained on November 4th, 2021. During this sunny day, nine charges occurred, resulting in a total energy consumption of 165 kWh and total PV production of 715 kWh. On this particular day, both self-production rates, with and without control, were high (97% and 83%, respectively). This is because the charging sessions primarily start at the beginning of the working day, as explained in Section 1.4.2.3. Thus, most of the charging sessions take place in the morning, when PV production is increasing. This example emphasizes that the self-production rate may be high, regardless of control.

1.4.3.5 The Self-Production Ratio May Be Relatively Low, Even with Control

Figure 1.4-7 illustrates the results obtained on October 21st, 2021. During this sunny day, 19 charges occurred, resulting in a total energy consumption of 214 kWh and a total PV production of 174 kWh. On this particular day, the self-production rates, with or without control, were relatively low (60% and 39%, respectively). This was due to two EV users (one Tesla Model S user and one ZOE user) who did not provide control over the charging of their EVs, charging their vehicles at high power, specifically 22 kW for both cars, early in the morning. Such results emphasize that user behaviour strongly influences the outcomes.

1.4.4 Conclusions and Perspectives

The experiments conducted at the CEA Cadarache site benefit from the city size of the research centre and from its roles as a CPO, eMSP, and DSO. They involve nearly 100 out of the 376 EV users and more than 40 different car models. The objectives of these experiments were to fully recharge the batteries of the users before their forecast departure times and to maximize the self-production rate of the system, which is composed of 24 charging points and part of the production from a PV plant.

The first goal was reached, except in very few cases. The second goal was considered partially reached. Indeed, the self-production rates obtained with or without control were compared. The analysis showed that the charging control always increases this ratio. On some days, especially during grey days, the ratio drastically increased (sometimes gaining more than 60 percentage points). However, there were several days, especially sunny ones, when the increase was rather low. It was also shown that, at times, the ratio remained low even with control. This is mostly due to users who do not give control over the charge of their EVs. One way to improve the ratio is to convince these users to change their minds. This could be accomplished, for example, by organizing ‘solar charging’ contests, by communicating intensively in the Cadarache centre about the obtained experimental results, or by offering a financial incentive. Another approach would be to enforce smart charging for all EVs, but the risk is that it may reduce user satisfaction and involvement in the experiments. Such an option could be counterproductive because user involvement is mandatory to access key data such as the initial SOC and the forecast time of departure.

As perspectives, the planning algorithm is intended to be improved in three main ways. First, the models that relate the value of the set points to the power withdrawn by the car will be enhanced, as suggested in [39]. These models are used during the allocation of the available power. In the current implementation of the algorithm, any error in the model translates into a loss of power. In other words, this loss of power is not allocated to other cars. To improve such models, it is expected that the number of charging points, users, and thus car models will increase. Additionally, there is a plan to monitor other physical variables useful for modeling, such as the state of charge (SOC) and battery temperature. Second, consideration will be given to turning the planning algorithm into an optimization problem and applying methods such as Mixed-Integer Linear Programming (MILP).

Finally, the retrieved data could serve as a basis for defining other Key Performance Indicators, such as the state of health of car batteries, the occupancy rate of each charging station, or the amount of power not extracted from the grid due to charging control. This latter measure could be used to quantify the economic benefit of EV solar charging. The satisfaction of users is also a key issue that could be estimated, especially when users are fully involved and accustomed to providing their charging preferences at the beginning of the charging sessions. In the long term, an assessment of the EV's capability to provide flexibility services to the electricity network and an estimation of the benefits for the grid are also planned.

REFERENCE

[1] European Commission: Proposal for a REGULATION OF THE EUROPEAN PARLIAMENT AND OF THE COUNCIL amending Regulation (EU) 2019/631 as regards strengthening the CO_2 emission performance standards for new passenger cars and new light commercial vehicles in line with the Union's increased climate ambition;

[2] New car registrations by fuel type, European Union. Available online: https://www.acea.auto/files/20220202_PRPC-fuel_Q4-2021_FINAL.pdf (accessed on 11 March 2022).

[3] Interactive map – Correlation between electric car sales and charging point availability (2021 update). ACEA - European Automobile Manufacturers' Association (accessed on 11 March 2022).

[4] ACEA: Proposal for the Alternative Fuels Infrastructure Regulation (AFIR); ACEA Position Paper (accessed on 11 March 2022).

[5] Richardson, D. B.: Electric vehicles and the electric grid: A review of modeling approaches, Impacts, and renewable energy integration. Renewable and Sustainable Energy Reviews, 19, 247–254 (2013). http://doi:10.1016/j.rser.2012.11.042.

[6] Muratori, M.: Impact of uncoordinated plug-in electric vehicle charging on residential power demand. Nature Energy, 3, 193–201 (2018). http://doi:10.1038/s41560-017-0074-z.

[7] RTE: Energy Pathways to 2050 Key Results, RTE 2021. Available online: https://assets.rte-france.com/prod/public/2022-01/Energy%20pathways%202050_Key%20results.pdf (accessed on 11 March 2022).

[8] Bañol Arias, N.; Hashemi, S.; Andersen, P. B.; Traeholt, C.; Romero, R.: Distribution System Services Provided by Electric Vehicles: Recent Status, Challenges, and Future Prospects. IEEE Transactions on Intelligent Transportation Systems, 20, 4277–4296 (2019). http://doi:10.1109/TITS.2018.2889439.

[9] Aghajan-Eshkevari, S.; Azad, S.; Nazari-Heris, M.; Ameli, M. T.; Asadi, S.: Charging and Discharging of Electric Vehicles in Power Systems: An Updated and Detailed Review of Methods, Control Structures, Objectives, and Optimization Methodologies. Sustainability, 14, 2137 (2022). http://doi:10.3390/su14042137.

[10] Hasanpor Divshali, P.; Evens, C.: Optimum day-ahead bidding profiles of electrical vehicle charging stations in FCR markets. Electric Power Systems Research, 190, 106667 (2021). http://doi:10.1016/j.epsr.2020.106667.

[11] Tsagkaroulis, P.; Thingvad, A.; Marinelli, M.; Suzuki, K.: Optimal Scheduling of Electric Vehicles for Ancillary Service Provision with Real Driving Data. In 2021 56th International Universities Power Engineering Conference (UPEC); IEEE: Middlesbrough, United Kingdom, (2021); pp. 1–6.

[12] de Hoog, J.; Alpcan, T.; Brazil, M.; Thomas, D. A.; Mareels, I.: Optimal charging of electric vehicles taking distribution network constraints into account. In 2017 IEEE Power & Energy Society General Meeting; IEEE: Chicago, IL, (2017); pp. 1–1.

[13] Frendo, O.; Gaertner, N.; Stuckenschmidt, H.: Real-Time Smart Charging Based on Precomputed Schedules. IEEE Transactions on Smart Grid, 10, 6921–6932 (2019). http://doi:10.1109/TSG.2019.2914274.

[14] Calearo, L.; Thingvad, A.; Ipsen, H. H.; Marinelli, M.: Economic Value and User Remuneration for EV Based Distribution Grid Services. In 2019 IEEE PES Innovative Smart Grid Technologies Europe (ISGT-Europe); IEEE: Bucharest, Romania, (2019); pp. 1–5.

[15] Sousa, T.; Hashemi, S.; Andersen, P. B.: Raising the potential of a local market for the reactive power provision by electric vehicles in distribution grids. IET Generation, Transmission & Distribution, 13, 2446–2454 (2019). http://doi:10.1049/iet-gtd.2018.5947.

[16] Brinkel, N. B. G.; Gerritsma, M. K.; AlSkaif, T. A.; Lampropoulos, I.; van Voorden, A. M.; Fidder, H. A.; van Sark, W. G. J. H. M.: Impact of rapid PV fluctuations on power quality in the low-voltage grid and mitigation strategies using electric vehicles. International Journal of Electrical Power & Energy Systems, 118, 105741 (2020). http://doi:10.1016/j.ijepes.2019.105741.

[17] Mets, K.; De Turck, F.; Develder, C.: Distributed smart charging of electric vehicles for balancing wind energy. In 2012 IEEE Third International Conference on Smart Grid Communications (SmartGridComm); IEEE: Tainan, Taiwan, (2012); pp. 133–138.

[18] Divshali, P. H.; Bong Jun Choi: Efficient indirect real-time EV charging method based on imperfect competition market. In 2016 IEEE International Conference on Smart Grid Communications (SmartGridComm); IEEE: Sydney, Australia, (2016); pp. 453–459.

[19] Sundström, O.; Binding, C. Optimization Methods to Plan the Charging of Electric Vehicle Fleets. Available online: https://www.zurich.ibm.com/pdf/csc/EDISON_ccpe_main.pdf (accessed on 11 March 2022).

[20] Kuran, M. S.; Carneiro Viana, A.; Iannone, L.; Kofman, D.; Mermoud, G.; Vasseur, J. P.: A Smart Parking Lot Management System for Scheduling the Recharging of Electric Vehicles. IEEE Transactions on Smart Grid, 6, 2942–2953 (2015). http://doi:10.1109/TSG.2015.2403287.

[21] van der Kam, M. J.; van Sark, W.: Smart charging of electric vehicles with photovoltaic power and vehicle-to-grid technology in a microgrid; a case study. Applied Energy, 152, 20–30 (2015). http://doi:10.1016/j.apenergy.2015.04.092.

[22] Zhang, Y.; Cai, L.: Dynamic Charging Scheduling for EV Parking Lots With Photovoltaic Power System. IEEE Access, 6, 56995–57005 (2018). http://doi:10.1109/ACCESS.2018.2873286.

[23] van der Meer, D.; Chandra Mouli, G. R.; Morales-Espana Mouli, G.; Elizondo, L. R.; Bauer, P.: Energy Management System With PV Power Forecast to Optimally Charge EVs at the Workplace. IEEE Transactions on Industrial Informatics, 14, 311–320 (2018). http://doi:10.1109/TII.2016.2634624.

[24] Ivanova, A.; Chassin, D.; Aguado, J.; Crawford, C.; Djilali, N.: Techno-economic feasibility of a photovoltaic-equipped plug-in electric vehicle public parking lot with coordinated charging. IET Energy Systems Integration, 2, 261–272 (2020). http://doi:10.1049/iet-esi.2019.0136.

[25] Cheikh-Mohamad, S.; Sechilariu, M.; Locment, F.; Krim, Y.: PV-Powered Electric Vehicle Charging Stations: Preliminary Requirements and Feasibility Conditions. Applied Sciences, 11, 1770 (2021). http://doi:10.3390/app11041770.

[26] Krim, Y.; Sechilariu, M.; Locment, F.: PV Benefits Assessment for PV-Powered Charging Stations for Electric Vehicles. Applied Sciences, 11, 4127 (2021). http://doi:10.3390/app11094127.

[27] Minh, P. V.; Le Quang, S.; Pham, M.-H.: Technical Economic Analysis of Photovoltaic-Powered Electric Vehicle Charging Stations under Different Solar Irradiation Conditions in Vietnam. Sustainability, 13, 3528 (2021). http://doi:10.3390/su13063528.

[28] Marinelli, M.; Calearo, L.; Ried, S.; Pfab, X.; Diaz Cabrera, J. C.; Spalthoff, C.; Braun, M.; Sale, H.; Torsater, B. N.; Divshali, P. H.; Hanninen, S.; Ceraolo, M.; Barsali, S.; Larsson, M.; Magdowski, A.; Gimenez, L.; Fernandez, G.: Electric Vehicles Demonstration Projects - An Overview Across Europe. In 2020 55th International Universities Power Engineering Conference (UPEC); IEEE: Turin, Italy, (2020); pp. 1–6.

[29] Nissan, Enel and Nuvve operate world's first fully commercial vehicle-to-grid hub in Denmark Available online: https://denmark.nissannews.com/da-DK/releases/nissan-enel-and-nuvve-operate-world-s-first-fully-commercial-vehicle-to-grid-hub-in-denmark (accessed on Mar 21, 2022).

[30] Charging EVs without stressing the electricity network. Powered Up Electric Nation Brochure Available online: https://electricnation.org.uk/resources/smart-charging-project /

[31] Lipman, T.; Callaway, D.; FierroMahdi Ghamkhari, G.; Liu, M.; von Meier, A.; Moura, S.; Peffer, T.; PhanivongElizabeth Ratnam, P.; Szinai, J. Open Source, Open Architecture Software Platform for Plug-In Electric Vehicle Smart Charging in California, California Energy Commission; March 2020. Available online: https://www.energy.ca.gov/sites/default/files/2021-05/CEC-500-2020-005.pdf (accessed on 11 March 2022)

[32] Invade: Algorithms successful in controlling the charging speed of electric cars; Available online: https://h2020invade.eu/news/algorithms-successful-in-controlling-the-charging-speed-of-electric-cars/ (accessed on 25 April 2022).

[33] Report: V2G Hub | V2G Around the world Available online: https://www.v2g-hub.com/reports/ (accessed on 16 March 2022).

[34] Sechilariu, M.; Reinders, A.;Krim, Y.; Cheikh-Mohamad, S.; Sierra, A.; Seiler, G.; Ben Slimane, K. PV-Powered Electric Vehicle Charging Stations: Preliminary Requirements and Feasibility Conditions. Report IEA-PVPS T17-02:2021, December 2021, ISBN 978-3-907281-26-0. Available online: https://iea-pvps.org/wp-content/uploads/2021/12/PVPS_Report_T17-02_2021-1.pdf (accessed on 25 April 2022)

[35] Askjær, R.J.; Andersen, P.B.; Thingvad, A.; Marinelli, M. Demonstration of a technology neutral control architecture for providing frequency control using unidirectional charging of electric vehicles. In Proceedings of the 55th International Universities Power Engineering Conference (UPEC), IEEE, Turin, Italy, 1–4 September 2020, pp. 1-6. https://doi.org/10.1109/UPEC49904.2020.9209821

[36] BMW ChargeForward Available online: https://bmwchargeforward.com/ (accessed on Mar 21, 2022).

[37] Frendo, O.; Gaertner, N.; Stuckenschmidt, H.: Open Source Algorithm for Smart Charging of Electric Vehicle Fleets. IEEE Transactions on Industrial Informatics, 17, 6014–6022 (2021). http://doi:10.1109/TII.2020.3038144.

[38] Holmgren, W. F.; Hansen, C. W.; Mikofski, M. A.: "Pvlib python: a python package for modeling solar energy systems," JOSS, vol. 3, no. 29, p. 884, Sep. 2018, https://doi.org/10.21105/joss.00884.

[39] Frendo, O.;Graf, J.; Gaertner, N.; Stuckenschmidt,H.: "Data-driven smart charging for heterogeneous electric vehicle fleets," Energy and AI, vol. 1, p. 100007, Aug. 2020, https://doi.org/10.1016/j.egyai.2020.100007

1.5 Solar park-ride parking for electric vehicles: case study in Lisbon

Solar parking lots combine the generation of clean solar energy with electric mobility. In particular, park-and-ride sites close to public transport connections, which allow commuters to head to the city Centre for the day, are particularly suited for solar charging since the vehicles are parked for most of the day—when solar power is available—and long enough to reduce the need for high-power fast charging.

This section presents updated modeling results for a PV-powered parking lot near a suburban train station on the outskirts of Lisbon, Portugal, using real parking occupancy data for a full year. Different charging strategies are explored, both with and without local energy storage.

Results highlight the relative mismatch between peak solar power and peak demand, as well as excess solar generation during weekends, which challenge the economic returns on the investment, but do not exceed a payback time of 9 years. Smart charging or battery storage increases self-consumption rates; however, at current prices, they lead to lower returns than simpler energy management. High electricity price scenarios could lead to payback times of about 5 years, primarily due to the contribution of the higher price of electricity sold to vehicle owners[5].

1.5.1 Introduction

The transition to electric mobility is accelerating, with electric vehicles (EVs) representing an increasing share of the vehicles sold in many geographies in 2021 [1] and predicted to reach 25% of all vehicles before 2030 [2]. The large-scale uptake of EVs brings new challenges, as drivers will not always be able to charge their vehicles at home or at work. One possible solution for urban contexts is solar-powered parking lots, which offer many benefits, including low CO_2 emissions, power generation, and a low impact on the grid, thus allowing for faster deployment and shading [3]. The combination of solar power and EV charging is particularly suitable for park-and-ride lots, where most cars are parked for long periods during the day, allowing for smart controlled charging.

Solar-powered parking lots are already being deployed commercially in many cities around the world [4], although mostly at small scales and in controlled environments. In this report, we explore the feasibility of a large-scale solar parking lot at a park-and-ride site on the grounds of a suburban train station near the city of Lisbon. This work is based on a prior preliminary study [5], with refined technical and economic analysis and updated cost inputs.

1.5.2 Description of the case study

For this study, the commuter parking lot at the train station located in Almada (38,66°N, 9,18°W), approximately 15 km from Lisbon, Portugal, is utilized. The hourly occupation data

---

[5] This section is based on the contribution of the Portuguese partners:

Guilherme Gaspar, Raquel Figueiredo, Pedro Nunes and Miguel C. Brito

Instituto Dom Luiz, Faculdade de Ciências, Universidade de Lisboa, 1749-016 Lisboa, Portugal.

for the car park was obtained for 2014. The parking site is open every day from 07:00 AM to 12:00 PM and has a capacity of 694 vehicles.

The overall system design includes: (i) PV system; (ii) EV chargers; (iii) stationary batteries; (iv) electric grid; (v) train station facilities; and (vi) central managing system. A schematic of the system is shown in Figure 1.5-1. The capital investment covers several components for the PV power plant, battery storage, and EV charging, as well as other costs, including labour, civil infrastructure, and management units.

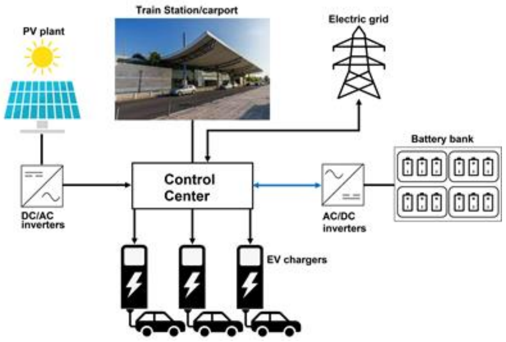

Figure 1.5-1 Schematic of the overall system, and how the different elements are interconnected.

The scenarios considered are Scenario 1 (Reference), Scenario 2 (Battery), which includes energy storage, and Scenario 3 (Smart), which considers smart charging. The different components are summarized in Table 1.5-1, according to the scenario.

Table 1.5-1 Main elements that are part of the proposed solar carport for EVs, which varies according to the scenario.

Scenario	Reference	Battery	Smart
PV			
Modules	×	×	×
Inverter	×	×	×
Infrastructures	×	×	×
Balance of plant (BOP)	×	×	×
Others (installation, transportation, etc.)	×	×	×
EV charging			
Charger	×	×	×
Pedestal	×	×	×
Remote management system			×
Infrastructures	×	×	×
Others (installation, transportation, etc.)	×	×	×
Storage			
Batteries		×	
Battery management system		×	
Bi-directional inverter		×	
Infrastructures		×	
Others (installation, transportation, etc.)		×	

The PV installation was designed to ensure minimal modules mutual shadowing, allowing for an installation of 991,8 kWp according to [5]. Power losses due to inverters, cables, and other electronics were assumed to be 14%. The hourly PV system energy output was simulated using PVGIS [6], corresponding to yearly and daily energy production of 1 474 MWh and 4 038 kWh, respectively. Considering a yearly degradation rate of 0,8% [7], this PV plant produces about 3 330 kWh/day in 25 years of operation.

EV chargers of different powers (3, 7 and 22 kW) were incorporated, assuming equal fractions. It is assumed that cars only charge enough energy to meet the daily needs corresponding to an average driving distance of 35 km [8]. Assuming an average EV energy consumption of 0,194 kWh/km [9], and an EV charger efficiency of 10,6% (AC/DC level 2 type) [10], the energy needs are about 7,6 kWh. Hence, charging always take less than 3 hours unless a controlled charging scenario is considered. The number of chargers to be installed corresponds to the maximum hourly occupation of the park, i.e. 694 chargers, which then results in carport daily energy needs of 2 916 kWh.

Figure 1.5-2 (a) and (b) show the occupancy and solar power generation, respectively. Generally, there is a good match between the two variables, except for weekends, holidays, and the summer vacation period, when occupancy rates decrease significantly, as the train station is mostly used by commuters and is therefore strongly correlated to working hours.

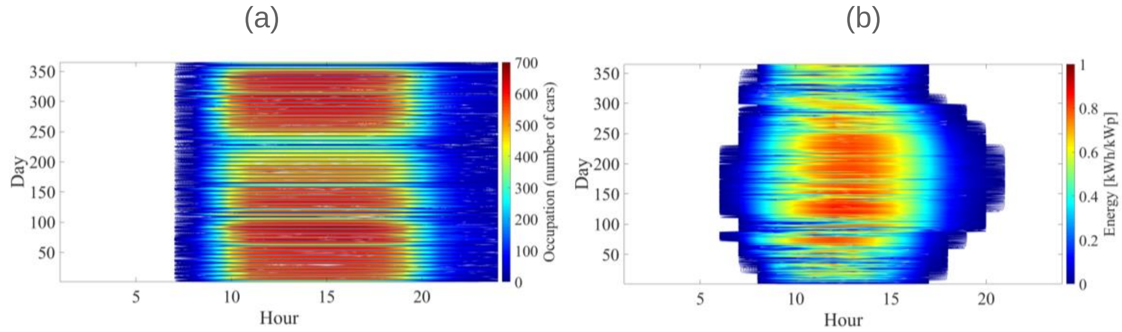

Figure 1.5-2 a) Occupancy rate and b) solar energy generation at the park-ride parking lot.

For the reference case scenario, without storage or smart charging, the charging of EVs occurs immediately upon arrival, leading to excess demand in the late morning (when, in general, most cars are charging and solar power has not yet reached peak power) and excess generation in the afternoon (when, in general, most vehicles are already fully charged), as shown in Figure 1.5-3(a). The distribution of the number of hours at a certain net energy (using bins of 50 kWh) is shown in Figure 1.5-3 (b). The hours corresponding to zero net energy (i.e., the white area in the energy demand map) are not considered in this distribution. It can be observed that although the larger number of hours corresponds to positive net energy, a considerable number of slots still require energy imports from the grid.

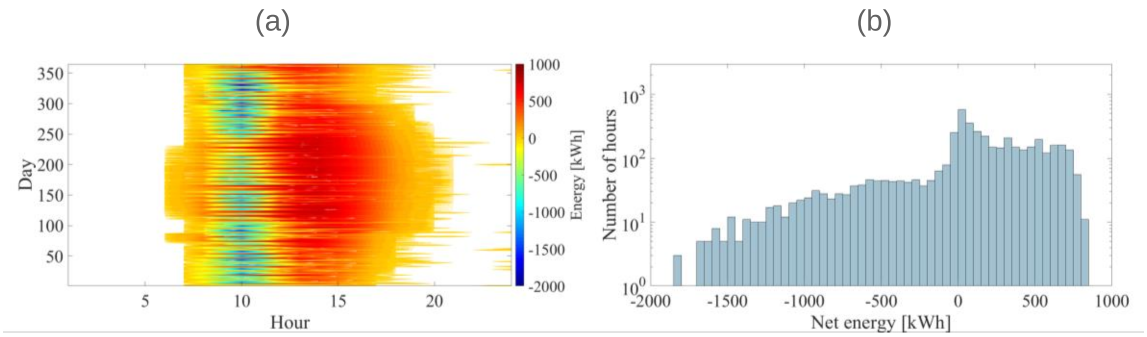

Figure 1.5-3 a) Energy demand, and b) histogram, for reference case, without batteries or smart charging. Vertical axis of b) is in logarithmic scale.

Some of the excess solar generation may be used to satisfy demand by introducing a level of battery storage, allowing for the shift of some of the solar-generated energy to hours of higher demand. This strategy is explored here as scenario 2 (Battery). To avoid oversizing the battery bank, which is the most expensive component of the system (per unit of energy), unlike the approach of Figueredo et al [5], the sizing of the battery capacity is designed to store only the extra PV energy generated each morning, if available. It stores just enough energy to suppress the net energy demand during the rest of the day, while its capacity calculations do not consider weekends and bank holidays to prevent battery oversizing.

The storage capacity was obtained based on the summer daily average (118 kWh), updated with an average 96% DOD (Depth of Discharge) resulting from a total of 1,750 yearly cycles needed for 12,5 years [11]. Additional capacity was considered to ensure that all energy in the morning could be shifted, resulting in a total capacity of 325 kWh. This result corresponds to an average DOD of 36% during the first year of operation, ensuring that the batteries experience shallow discharge throughout their lifetime. Since the assumed battery round-trip efficiency is 95%, the final battery bank size should be equivalent to 342 kWh. Therefore,

Figure 1.5-4(a) shows a slight update compared to the reference case scenario, indicating that no considerable reduction in energy imports is achieved. The histogram in Figure 1.5-4 (b) includes the additional zero net energy hours obtained with battery storage when compared to the reference scenario, highlighting the differences. The reduction is only significant during summertime, when the sun rises a couple of hours earlier than the opening of the park, allowing the battery to charge until carport consumption begins to increase considerably (generally after 09:00 AM). The amount of charged energy is clearly limited in reducing energy imports, particularly during winter, when battery charging is diminished.

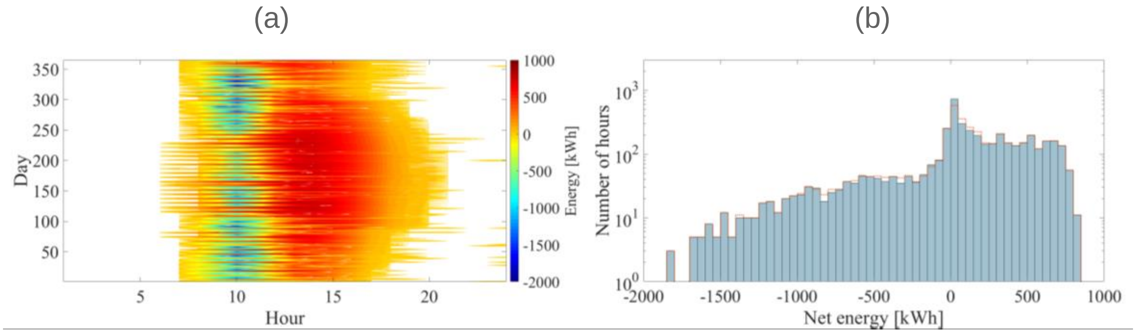

Figure 1.5-4 a) Energy demand, and b) corresponding histogram, for battery case. Vertical axis of b) is in logarithmic scale, and the red line represents the reference case.

An alternative strategy is the use of smart charging (scenario 3), set to maximize the use of PV energy by taking advantage of the long parking periods in these types of parking sites (the average parking period is 12 hours). The smart charging strategy follows the PV generation profile whenever possible, delaying excess charging needs to the afternoon period before sunset, when feasible. The energy demand is shown in Figure 1.5-5, where it can be observed that, with this strategy, excess demand is successfully shifted to peak generation hours, significantly reducing the need for imports from the grid to charge the parked vehicles. As shown in Figure 1.5-4(b), the histogram of Figure 1.5-5 (b) is also updated with the additional zero net energy hours achieved with this scenario, confirming that energy imports are clearly reduced.

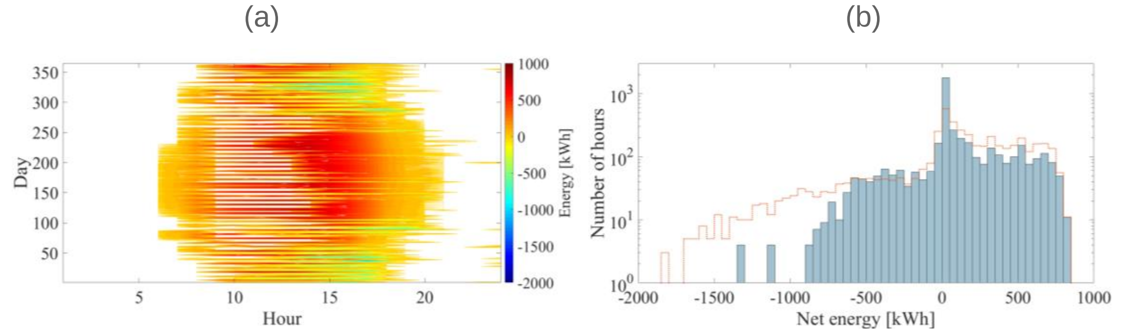

Figure 1.5-5 a) Energy demand, and b) corresponding histogram, for smart charging case. Vertical axis of b) is in logarithmic scale, and the red line represents the reference case.

1.5.3 Economic analysis

Table 1.5-2 summarizes the cost of the different components for the considered layouts. The prices of PV plant components were obtained from [12]. Current costs related to the EV chargers (Level 2) and associated components are mostly sourced from [13]. Prices associated with the storage system are inspired by [14] and [15], and the replacement predictions (taking place in 2033) are from [16]. Civil infrastructure prices are based on information collected locally, while other expenses related to installation, transportation, and more were assumed to be 1/6 of the total investment associated with technology and infrastructure.

Table 1.5-2 Price of the main elements that make the proposed solar carport for EVs.

PV (€/kWp)		EV chargers (€/charger)		Storage (€/kWh)	
Modules	200	Charger	619	Batteries	113
Inverter	30	Pedestal	206	Batteries replacement	19
Infrastructures	200	Infrastructures	170	Battery management system	14
Balance of plant (BOP)	170	Others (installation, transportation, etc..)	165	Bi-directional inverter	54
Others (installation, transportation, etc..)	100	Remote management system	50/year	Infrastructures	57
				Others (installation, transportation, etc..)	40

Modelling includes the cost of electricity purchased from the grid, which is assumed to be equal to the price of excess solar electricity fed to the grid or used in the train station (both assumed 0,072 €/kWh or, for a high electricity cost scenario, 0,144 €/kWh). These assumptions consider that the train station owns and operates the parking lot or, if the parking lot is managed by a third party, that a net metering scheme is in place. Additionally, modelling considers an end-of-life value of electronic equipment assumed to be 10% of the initial investment. Electricity charged to vehicle owners is set at 0,25 €/kWh, while for the high electricity cost scenario, it is set at 0,35 €/kWh.

All scenarios include operational and maintenance costs corresponding to 1% of the initial investment in the parking lot, as well as management costs, assumed to be 5% of the annual revenues.

The economic results are shown in Figure 1.5-6. It can be observed that for the reference case, the payback time is about 7 years, well below the lifetime of the system (i.e., 25 years).

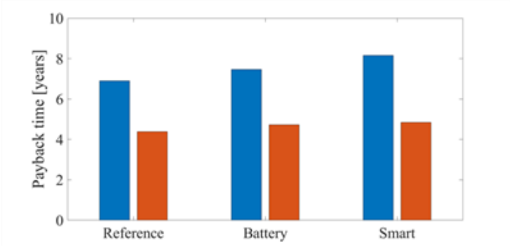

Figure 1.5-6 Payback time for baseline economic modelling (blue) and high electricity price conditions (red) for the studied strategies: reference, battery and smart charging.

The alternative strategies that optimize energy demand, whether using batteries or smart charging, lead to higher costs and payback times, primarily due to extra expenses associated with the battery bank and the energy management system.

In a high electricity price scenario, payback times decrease to 4-5 years, indicating minor differences among the scenarios and highlighting that the price of electricity charged to vehicle owners plays a major role in the economic viability of the park-and-ride parking lot. Among the strategies, smart charging remains the least favourable in terms of payback but shows the highest decrease when compared to the original scenarios. This is because smart charging makes the parking lot less susceptible to grid price fluctuations, as low electricity imports are expected.

1.5.4 Model limitations

The modeling exercise reported in this work implicitly assumes that occupancy patterns will not change throughout the operational lifetime of the project. Furthermore, the charging required per vehicle is set to the mean travel distance; however, in a commercial implementation, it could vary significantly between vehicles, with some potentially charging to full battery and others not charging at all, introducing wide uncertainty into daily energy needs.

It should also be noted that the Battery and Smart scenarios assume perfect knowledge of both occupancy and solar generation for the day ahead. Therefore, in a practical implementation, detailed forecasting and skilled optimization would be required.

1.5.5 Conclusions

This work presents a technical and economic analysis of a PV-powered parking lot near a suburban train station close to Lisbon, Portugal, using real occupancy data for a full year. Electricity peak demand and peak PV generation showed a significant mismatch, resulting in economic constraints for the project. Three scenarios were considered: Reference (without batteries), Storage (with batteries), and Smart (smart charging), with the latter contributing to a significant reduction in electricity imports from the grid. However, both the Battery and Smart scenarios require additional forecasting and optimization.

The payback time of the project exceeds 7 years, well below the project's lifetime (i.e., 25 years). A scenario with a high electricity price leads to faster payback times, highlighting the sensitivity of the project's economics to the price of electricity charged to EVs.

1.5.6 Supplementary information

PV module, inverter, balance of plant, and infrastructure prices were obtained from [12], while installation, transportation, and other related costs were assumed to be 1/6 of the total PV investment.

Lithium-ion battery price was assumed to be 113 €/kWh [14], with the battery management system costing 1/8 of the installed battery price and the bi-directional inverter accounting for 48% of the same price [15]. The cost of the battery infrastructure is 50% of the battery price, partially shared with the PV plant. Other costs amount to 1/6 of the total storage system investment.

The commercial battery used in the simulation is an NMC-type LG Chem stationary battery model RESU10, with relevant technical parameters such as total energy (i.e., 9,8 kWh) entered into the simulation. Given that the final battery bank size corresponds to 342 kWh, 35 of these batteries are needed for the current project. Battery replacements are considered after 12 years, before their capacity decreases to below 80% of the initial capacity, according to the life cycle vs. DOD model. Battery price predictions for 2033 are based on the multifactor learning curve model of Penisa et al. for NMC Lithium-Ion battery packs [16]. Thus, a battery price of €19/kWh is predicted for the mentioned year, assuming that this is the only element replaced and that no significant additional labour is needed.

Level 2 EV chargers are considered in the current model together with pedestal kits, each of them holding 2 chargers. Thus, each charger costs 619 € [13] and the pedestal 206 €/charger [13]. The electric and civil infrastructures for EV chargers correspond to 100 €/m. It is assumed that only 3/4 of such length is effectively used for parking sites interconnection. Considering that a European compact car width is 2,5 m, it results in an investment of 170 €/charger of additional infrastructures. In addition, 1/6 of the total investment in EV chargers is for other expenses. In case smart charging is considered, a remote management system yearly license price of 50 €/charger must be included.

REFERENCES

[1] IEA (2021), Global EV Outlook 2021, IEA, Paris https://www.iea.org/reports/global-ev-outlook-2021

[2] Deloite (2019), Electric vehicles - Setting a course for 2030, https://www2.deloitte.com/us/en/insights/focus/future-of-mobility/electric-vehicle-trends-2030.html

[3] Nunes P, Figueiredo R, Brito MC. The use of parking lots to solar-charge electric vehicles. Renewable and Sustainable Energy Reviews, Volume 66, 2016, pages 679-693, ISSN 1364-0321 https://doi.org/10.1016/j.rser.2016.08.015.

[4] GJ Osório, et al. Rooftop photovoltaic parking lots to support electric vehicles charging: A comprehensive survey. International Journal of Electrical Power & Energy Systems, 133:107274, https://doi.org/10.1016/j.ijepes.2021.107274.

[5] Figueiredo R, Nunes P, Brito MC. The feasibility of solar parking lots for electric vehicles. Energy , Volume 140, Part 1, 2017, pages 1182-1197, ISSN 0360-5442 https://doi.org/10.1016/j.energy.2017.09.024.

[6] Photovoltaic geographical information system (PVGIS) - European Commission, Joint Research Centre. https://ec.europa.eu/jrc/en/pvgis (accessed 07 June 2021).

[7] Skoczek, A., Sample, T. and Dunlop, E.D. (2009), The results of performance measurements of field-aged crystalline silicon photovoltaic modules. Prog. Photovolt: Res. Appl., 17: 227-240. https://doi.org/10.1002/pip.874

[8] INE. Estatísticas dos transportes 2009. p. 2010.

[9] Electric Vehicle Database. Energy consumption of full electric vehicles. https://ev-database.org/cheatsheet/energy-consumption-electric-car (accessed 26 May 2021).

[10] Sears J, Roberts D, Glitman K. A comparison of electric vehicle Level 1 and Level 2 charging efficiency. IEEE Conference on Technology for Sustainability (SusTech) 2014. 10.1109/SusTech.2014.7046253.

[11] Wang Y, Zhou Z, Botterud A, Zhang K. Stochastic coordinated operation of wind and battery energy storage system considering battery degradation. J Mod Power Syst Clean Energy 2016;4:581-592. https://doi.org/10.1007/s40565-016-0238-z.

[12] Joint Research Centre (JRC) Science for Policy Report. PV Status Report 2019. p. 56.

[13] Fixr. Home Electric Vehicle Charging Station Cost. https://www.fixr.com/costs/home-electric-vehicle-charging-station#benefits-of-ev-charging-stations (accessed 16 June 2021).

[14] BloombergNEF. Battery Price Survey 2020. https://about.bnef.com/blog/battery-pack-prices-cited-below-100-kwh-for-the-first-time-in-2020-while-market-average-sits-at-137-kwh / (accessed 16 June 2021).

[15] Greentech Media. How Much Does a Rooftop Solar System With Batteries Cost? - Article, 12 April 2017. https://www.greentechmedia.com/articles/read/how-much-does-a-rooftop-solar-system-with-batteries-cost (accessed 16 June 2021).

[16] Penisa XN, Castro MT, Pascasio JDA, Esparcia EA Jr., Schmidt O, Ocon JD. Projecting the Price of Lithium-Ion NMC Battery Packs Using a Multifactor Learning Curve Model. Energies 2020;13:5276. https://doi.org/10.3390/en13205276.

1.6 Global Cost and Carbon Impact Assessment Methodology for Electric Vehicles' PV-Powered Charging Station

This section[6] highlights a methodology to assess the global cost and the carbon impact of photovoltaic charging stations (PVCS) based on a life cycle analysis taken into consideration technical, economic and environmental constraints. The proposed methodology is detailed through two tasks. The first one is the calculation of the global cost of the PVCS under 30 years of lifespan. The second task is dedicated to the assessment of the global carbon impact of the PVCS, in addition to the different actions proposed to reduce the carbon impact compared to a charging station based only on the power grid.

1.6.1 Introduction

Electric vehicles (EVs) have been presented for several years as a promising solution to reduce the carbon impact of the transport sector. The latter is the main emitter of CO_2 in France with 42% of total greenhouse gases (GHG) emissions, and the second emitter in the world and in the European Union with 24% and 28% of total emissions in 2018, respectively [1]. As road transport represents more than 80% of these emissions, it is remarkable that it is a priority axis for reducing GHG emissions in order to reduce the negative impact of humans on the planet and its ecosystems. However, the environmental impact of EVs is still far from neutral. In addition to the manufacturing processes for its highly emitting components, the environmental impact of these vehicles depends largely on the source of the electricity that allows them to operate. In order to limit GHG emissions related to the usage of EVs, it therefore seems advantageous to provide them with the most environmentally friendly electricity, which leads to turning to renewable energy sources, as photovoltaic (PV) [2]. EVs charging stations based on PV installations seem able to respond optimally to this challenge. However, while EVs do not directly emit CO_2 when in motion, they do indirectly emit CO_2 during their conception, maintenance, and recycling. Likewise, PV-powered charging stations (PVCS) do not emit CO_2 when they produce electricity, but it is possible to estimate their GHG emissions considering their conception, maintenance, and recycling processes. The GHG emissions of the PVCS require an estimation methodology. There are environmental analysis methodologies such as the single-criteria "Bilan Carbone®" analysis developed by ADEME and then taken up by the Bilan Carbone association [3], the simplified carbon assessment developed by the energy regulatory commission [4], Ecoinvent database [5], ISO 14040/44 life cycle assessment (LCA) [6], as well as tools for their implementation. Despite the importance of this topic, most research works have focused on maximizing the portion of PV production in the recharge of the EVs to minimize GHG emission from energy production [7][8].

Hence, research work emphases on estimating the carbon impact related to EVs and PV installations. In [9], a feasibility study was conducted on EV charging based on PVCS, which reduces CO_2 emissions and the overload on the local power grid. The study was carried out in several countries and the results demonstrate that countries with high irradiation (Australia and Brazil) are more likely to exploit the PV infrastructures to charge EVs. However, this analysis of CO_2 emissions is limited to the operational phase of PVCS, where the manufacturing and

---

[6] This section is based on the following publication: Y. Krim, M. Sechilariu, F. Locment, A. Alchami, "Global Cost and Carbon Impact Assessment Methodology for Electric Vehicles' PV-Powered Charging Station", Applied Sciences, vol. 12, no. 9, p. 4115, Apr. 2022, http://dx.doi.org/10.3390/app12094115

end-of-life phases are excluded. Thus, total CO_2 emissions are determined by adding the carbon impact of power given by PV to EV, stationary storage to EV, and EV to grid. In [10], a model for designing and optimizing a charging station based on PV panels and stationary storage for EVs was established. The study demonstrates an environmental benefit through CO_2 savings estimates, but it also includes a cost analysis. However, this work involves only electric light mobility, and does not have a detailed CO_2 estimation model; the embodied emissions, due to the manufacturing of the PV system components, were not considered. In [11], the environmental impact evaluation was discussed in term of CO_2 emissions integrated into the green energy systems. It also emphasizes the environmental benefits estimation of their implementation in the power supply of EVs' charging stations compared to the power grid.

Carbon emission assessment methodologies based on LCA were developed in [12] to compare the carbon impact of an EV (Tesla Model 3) and a hydrogen fuel cell vehicle (Toyota MIRAI). According to the results presented, there is a great need for transparency regarding the relevant information on the product carbon impact methodology adopted by the car manufacturers to allow the comparison of the emissions of their vehicles. This work excludes the examination of reports on the carbon impact for vehicles powered by renewable energy sources. Through LCA, the carbon impact of a battery EV and an internal combustion engine vehicle are calculated and compared under a nationwide electricity mix in China [13]. For provinces with a high share of electricity based on coal, the development of battery EVs should be encouraged. In [14], a statistical model that relates charging station infrastructure and other potential factors such as the adoption rate of rechargeable EVs in 58 counties in California was developed, where the life-cycle petroleum use, costs, and emissions, of light vehicles is studied. A modeling and comparison of two case studies from Los Angeles, California, and Detroit, Michigan for the two cities' current energy mix in 2017 was carried out [15]. LCA evaluation was presented in this study to measure the impact of climatic temperatures and different regional energy mix on both electric and conventional vehicles. The results demonstrate that low temperatures increase GHG emissions and lead to inefficient battery charging.

This paper [16] focuses on the United Kingdom's EVs' charging strategy toward the goals of 2030 and 2040, i.e., vehicle-to-grid or smart charging. This study results are lower CO_2 emission, higher integration of renewable energy sources, and more positive impact on the power grid. Hybrid EVs are found to be the most energy-efficient option, while EVs are found to be the least carbon-intensive vehicle option. However, the scope of this study is limited to the carbon impact of the EVs' charging strategy.

In addition to the study of CO_2 emissions from PVCS, an estimation of the global cost was discussed in the literature over the lifetime of an installation. Optimal technical sizing of the PV system and stationary storage systems for recharging EVs is critical to ensure their economic feasibility, which corresponds to sizing system components with minimum cost. In [17], an analysis of the technical and economic performances of autonomous PVCS associated with stationary battery storage is discussed using the HOMER software. In [18], an optimal configuration of PVCS is discussed economically and technically with several solar irradiation in Vietnam. The results of the study demonstrate that the irradiation is a crucial factor in choosing to install and invest in a PVCS. A sizing optimization of a PVCS with stationary storage is proposed in [19] for fast EV charging. The optimization method allows the cost of the charging station to be minimized, including the maintenance and investment costs of the PV and the storage system. A problem of sizing the EVs' charging station, i.e., decisions on the number and types of chargers, was resolved in [20] due to an optimization framework that reduces the investment cost of the operators' charging stations, subject to reaching a certain quality of service for their customers (EV owners).

Through the aforementioned literature review, it can be noticed that some problems have not been addressed by the existing investigations:

- The previously cited references have not discussed the carbon impact of a PVCS, or the LCA is not included (estimation of the carbon emission from the manufacturing phase to the disposal of each element of the infrastructure).
- In most works, the cost of building, allowing the creation and the coverage of parking places, is not included in the total cost, as well as the replacement cost of the charging terminals.
- It is not moderate to estimate the global cost of the PVCS and its carbon impact separately.
- Lack of approaches to reduce the CO_2 emissions.

In this paper, a methodology for estimating the global cost and the carbon impact of a PVCS for EVs is detailed, with an improvement strategy in order to reduce the global carbon impact. The PVCS includes PV sources, charging terminals, stationary storage, and connection with the public grid. Therefore, this work brings the following improvements by providing:

- A calculation methodology of the global cost of the PVCS, including the costs of investment, maintenance, exploitation, and externalities, to offer to the decision-maker a choice of infrastructure compatible with his spatial and budgetary constraints.
- Concretely, a definition of a methodology for calculating the carbon impact of a PVCS by defining an equation, making it possible to calculate the carbon impact of each subsystem composing the PVCS, in order to assess their usefulness compared to the grid-powered charging station (PGCS), using the LCA method based on the ISO 14,067 standard. The carbon impact estimation offers to the decision-maker a choice of infrastructure compatible with his ecological constraint. In addition, it is committed to researching the most relevant carbon emission coefficient, making it possible to better assess the carbon impact of the components of each subsystem.
- An identification of the levers of action, i.e., components that strongly influence the global carbon impact of PVCS, and on which it would be possible to act to reduce the carbon impact of such infrastructures. This reduction solution of the carbon impact is based on new data and recycled materials for the most emitting elements of CO_2.

A numerical application of the proposed calculation methodology of the global cost and carbon impact for a case study of an installation of the PV parking shade, located in the Innovation Centre of the Université de Technologie de Compiègne, has been discussed in the end of this paper, to validate the methodology and the proposed carbon impact reduction solutions. A comparison of the result with an EV charging station, similar but powered exclusively by the power grid, is proposed.

The rest of the paper is structured as follows: Section 1.6.2 describes the methodology for calculating the global cost of the PVCS, Section 1.6.3 shows the methodology for calculating the carbon impact of the PVCS, Section 1.6.4 depicts a numerical application and assessment of the global cost and the carbon impact of PVCS versus PGCS, and finally, Section 1.6.5 concludes this work and opens new perspectives.

1.6.2 Calculation Methodology of the PVCS Global Cost

In this section, the cost aspect of the PVCS is deepened. The purpose is to be able to provide the global cost of the PVCS, including the costs of investment C_i, exploitation C_{exp} , maintenance C_{maint}, and externalities Ext . This calculation methodology is detailed over a 30-year analysis period, as the average lifespan of a PV panel is 30 years. Then, the global cost is expressed in (1.6-1):

$$C_g = C_i + C_{exp} + C_{maint} + Ext \quad (1.6\text{-}1)$$

1.6.2.1 Investment Cost

The total investment cost Ci for a PVCS is calculated as follows:

$$C_i = C_{PV_{invest}} + C_{bat_{invest}} + C_{ter_{invest}} + C_{infra_{invest}} \quad (1.6\text{-}2)$$

Where $C_{PV_{invest}}$, $C_{bat_{invest}}$, $C_{ter_{invest}}$, and $C_{infra_{invest}}$ are the investment costs (€) of PV system, stationary battery, terminals, and infrastructure, respectively.

Thus, the total investment cost of the PVCS is obtained by adding the investment costs related to the entire energy chain and those of the infrastructure.

1.6.2.1.1 Energy Chain

The energy chain corresponds to all the components of the PVCS, allowing the production and distribution of electrical energy. These components are:

- PV system (PV panels, inverter, connection wiring, installation, and construction costs);
- Stationary storage and lithium-ion technology;
- Charging terminals.

The investment cost of these different components is estimated following the values recovered from the technical sheets [21] and from the Batiprix costing French database [22] specific to building and public works.

a) *PV System*

The investment cost of the PV system $C_{PV_{invest}}$ includes the PV purchase cost $C_{purchase_{PV}}$ and the cost of workforce $C_{wf_{PV}}$. The workforce cost of the component corresponds to the expenses generated by its installation. This cost includes the PV panels, the inverter, and the connection wiring. $C_{PV_{invest}}$ is calculated as follows:

$$C_{PV_{invest}} = \left(C_{purchase_{PV}} + C_{wf_{PV}}\right) \times x \times y \quad (1.6\text{-}3)$$

where x is the cost coefficient and y is the sales price.

The purchase cost of the PV system is calculated as follows:

$$C_{purchase_{PV}} = N_{PV} \times C_{PV_{un}} \quad (1.6\text{-}4)$$

where $C_{PV_{un}}$ is the unit purchase cost for a PV system for one PV panel in €/unit and N_{PV} is the number of PV panels of the PVCS.

Finally, the workforce cost of the PV system is calculated as follows:

$$C_{wf_{PV}} = A_{PV} \times C_{imp_{pv_{un}}} \quad (1.6\text{-}5)$$

where $C_{imp_{pv_{un}}}$ is the unit cost of the implementation of the PV system in €/m^2 and A_{PV} is the area of the PV panels.

b) Stationary Storage

The investment cost of the stationary batteries' storage $C_{bat_{invest}}$ includes the batteries' purchase cost $C_{purchase_{bat}}$ as well as the cost of workforce to install the batteries $C_{wf_{bat}}$. Thus, the investment cost of storage batteries is calculated as follows:

$$C_{bat_{invest}} = \left(C_{purchase_{bat}} + C_{wf_{bat}}\right) \times x \times y \quad (1.6\text{-}6)$$

The costs $C_{purchase_{bat}}$ and $C_{wf_{bat}}$ are expressed as follows:

$$\begin{cases} C_{purchase_{bat}} = C \times C_{bat_{un}} \\ C_{wf_{PV}} = N_{bat} \times C_{bat_{wf_{un}}} \end{cases} \quad (1.6\text{-}7)$$

where $C_{bat_{un}}$ is the unit cost of the batteries in €/kWh excluding tax, $C_{bat_{wf_{un}}}$ is the unit cost of the installation of the battery in €/battery, C is the total capacity of the stationary batteries' storage installed in the PVCS in kWh, and N_{bat} is the number of batteries.

c) Charging Terminal

The investment cost of the charging terminals $C_{ter_{invest}}$ includes the cost of fast terminals $C_{ter,fast\ invest}$ and the cost of slow terminals $C_{ter,slow\ invest}$. Thus, the investment cost of charging terminals is calculated as follows:

$$C_{ter_{invest}} = C_{ter,fast\ invest} + C_{ter,slow\ invest} \quad (1.6\text{-}8)$$

with

$$\begin{cases} C_{ter,fast\ invest} = N_{ter,fast} \times C_{ter,fast\ un} \\ C_{ter,slow\ invest} = N_{ter,slow} \times C_{ter,slow\ un} \end{cases} \quad (1.6\text{-}9)$$

where $C_{ter,fast\ un}$ and $C_{ter,slow\ un}$ are the unit cost of the fast and slow charging terminal, respectively. $N_{ter,fast}$ and $N_{ter,slow}$ are the number of fast and slow charging terminals, respectively.

1.6.2.1.2 Infrastructure

The infrastructure corresponds to all the components of the PVCS, allowing the parking of vehicles as well as the installation of the energy chain. These components are:

- The reinforced concrete (RC);
- Steel, in the case of a shade PV installation typology.

RC allows the creation of parking places, and the steel is the material of the shade covering the parking places. Thus, the investment cost of the infrastructure $C_{infra_{invest}}$ is calculated as a function of the cost of the RC $C_{infra_{rc}}$ and the cost of the steel $C_{infra_{steel}}$, as follows:

$$C_{infra_{invest}} = C_{infra_{rc}} + C_{infra_{steel}} \quad (1.6\text{-}10)$$

The cost of steel $C_{infra_{steel}}$ is calculated according to the total mass of steel M_{tot} and the unit cost of steel $C_{steel_{un}}$ in €/kg as follows:

$$C_{infra_{steel}} = M_{tot} \times C_{steel_{un}} = \left(N_{pp} \times M_{steel}\right) \times C_{steel_{un}} \quad (1.6\text{-}11)$$

where M_{steel} is the mass of steel unit to make a parking place in kg/place, and N_{pp} is the number of parking spaces.

The cost of the RC $C_{infra_{rc}}$ is calculated as a function of the unit cost of RC $C_{rc_{un}}$ in €/m^3 and the total volume of RC V_{BA} as follows:

$$C_{infra_{rc}} = V_{tot} \times C_{rc_{un}} = \left(N_{pp} \times V_{BA}\right) \times C_{rc_{un}} \quad (1.6\text{-}12)$$

where V_{BA} is the volume of the RC for the parking space in m^3.

As observed previously, the ISO 15686 standard adds, to these investment costs, maintenance costs.

1.6.2.2 Maintenance Costs

Maintenance costs are the total costs of the workforce and material necessarily incurred and other associated costs incurred to maintain an infrastructure or its parts in a condition enabling it to perform its required functions.

For a PVCS, there are two maintenance costs:

- Replacement cost: end-of-life components of the PVCS must be renewed;
- Maintenance cost: cleaning and verification must be carried out on the components of the PVCS at a certain frequency.

1.6.2.2.1 Replacement Cost

The replacement cost corresponds to the expenses incurred for the renewal of components reaching the end of their life. Since the analysis period is 30 years, the aging of the concrete and steel infrastructure, or of the building on which the system is deposited, is not considered. The components to be replaced concern the PVCS energy chain, such as charging terminals, stationary batteries, and inverters. These elements must be replaced because their lifespan is shorter than the analysis period (30 years). At the end of this period, a new investment must be made by the owner of the PVCS.

The cost quantified below corresponds to the redemption prices of the various components and includes the purchase and the installation of the material, excluding taxes.

a) PV Panels

A lifespan of 30 years is considered for the PV panels. This lifespan is thus estimated because the manufacturer's warranty states that the efficiency of the panels will be greater than 80% of the initial efficiency after 25 years. The assumption was therefore made that the panels are generally still usable 5 years after the end of this warranty. Since the overall cost analysis period is 30 years, there will be no replacement cost for the PV panels.

b) Inverter

It is considered that one inverter is installed on the PVCS. An inverter has an average lifespan of 15 years [23]. As the analyzed period is 30 years, a replacement will be necessary for this component. The replacement number of the inverter r_{inv} can be calculated using equation (1.6-13) according to the analysis period in years ($q = 30\,years$) and the lifespan of the inverter q_{inv} :

$$r_{inv} = \frac{q}{q_{inv}} - 1 \tag{1.6-13}$$

Then, to obtain the replacement cost of the inverter $C_{repl_{inv}}$, the following equation will be used:

$$C_{repl_{inv}} = C_{repl_{inv_{un}}} \times P_p \times r_{inv} \tag{1.6-14}$$

where $C_{repl_{inv_{un}}}$ is the unit replacement cost of the inverter in €/kWp and P_p is the total installed power in kWp. $C_{repl_{inv_{un}}}$ includes the purchase of materials and the manpower of the installation of the inverter.

c) Stationary Storage

The replacement cost of the stationary storage installed on the PVCS is estimated in this section. With a lifespan q_{bat} of 10 years and during 30 years as the analysis period, two replacements will be necessary for the stationary batteries. The number of replacements r_{bat} of the batteries can be expressed using the equation below:

$$r_{bat} = \frac{q}{q_{bat}} - 1 \tag{1.6-15}$$

To obtain the replacement cost of the battery, the following equation will be used:

$$C_{repl_{bat}} = C_{repl_{bat_{un}}} \times C \times r_{bat} \tag{1.6-16}$$

where $C_{repl_{bat_{un}}}$ is the unit replacement cost of the lithium-ion battery in €/kWh, including the purchase of materials and the manpower of the installation.

d) Charging Terminals

In this section, the method used to calculate the cost of replacing the charging terminals installed on the PVCS is detailed. As a reminder, two types of charging terminals are considered: the fast terminals placed on the ground and delivering a maximum power of 22 kW, and the slow terminals, which are suspended on a wall or pole and deliver a maximum power of 2,3 kW.

Since there is no information about the lifespan of the charging terminals (this technology is very recent), a change every 10 years is considered for both types of charging terminals.

As the analysis period is 30 years, two replacements will be necessary for these components. This value can be calculated using equation (1.6-17), where the lifespan of the charging terminal q_{ter} is 10 years:

$$r_{ter} = \frac{q}{q_{ter}} - 1 \tag{1.6-17}$$

Then, to obtain the replacement cost of the charging terminals of 2,3 kW and 22 kW, the following equations will be used:

$$\begin{cases} C_{repl_{ter_{slow}}} = C_{ter,slow\ un} \times N_{ter,slow\ un} \times r_{ter} \\ C_{repl_{ter_{fast}}} = C_{ter,fast\ un} \times N_{ter,fast\ un} \times r_{ter} \end{cases} \tag{1.6-18}$$

Where $C_{repl_{ter_{slow}}}$ and $C_{repl_{ter_{fast}}}$ are the replacement costs of slow and fast charging terminals, respectively (€), including the purchase of materials and the manpower of the installation; $C_{ter,slow\,un}$ and $C_{ter,fast\,un}$ are the unit cost of the slow and fast charging terminal, respectively (€); and $N_{ter,slow\,un}$ and $N_{ter,fast\,un}$ are the number of slow and fast charging terminals, respectively. From the previous calculations, it is possible to obtain the total replacement cost of the structural components during the analysis period, as shown in the following equation:

$$C_{rep} = C_{repl_{inv}} + C_{repl_{bat}} + C_{repl_{ter_{slow}}} + C_{repl_{ter_{fast}}} \tag{1.6-19}$$

In addition to the replacement cost, there are maintenance costs.

1.6.2.2.2 Maintenance Cost

The maintenance cost is the expense of services, such as cleaning and checking PVCS components.

a) *PV System Maintenance*

The PV system consists of the PV panels as well as the inverter. The maintenance services are diverse, varied, and consist mainly of the visual inspection of PV panels, checking and dusting of inverters, inspection of DC boxes and cables, cleaning of panels or recording of production data. According to [24], for large power installations, the maintenance cost of the PV system is estimated between 3 and 5 €/kWp. For medium PV power installations, between 36 and 500 kWp, it is estimated between 5 and 8 €/kWp. For small power installations (< 36kWp), the PV system maintenance cost is estimated between 250 and 500 €/year.

b) *Maintenance of Charging Terminals*

The total maintenance cost of terminals is defined by the following equation:

$$C_{maint_{ter}} = C_{maint_{ter_{slow}}} + C_{maint_{ter_{fast}}} \tag{1.6-20}$$

Finally, the maintenance cost formula, during the analysis period q, is therefore obtained:

$$C_{maint} = (C_{maint_{ter}} + C_{maint_{pv,inv}}) \times q \tag{1.6-21}$$

In addition to these maintenance costs, there are exploitation costs.

1.6.2.3 Exploitation Costs

Exploitation costs include bills for consumed energy to operate an infrastructure as well as money spent on insurance. The cost of the consumed energy is considered zero in the case of a PVCS because this energy comes from the PV panels. However, it is recommended to have insurance that covers civil liability and damage caused by this type of infrastructure. These types of insurance costs, per year, are between 0,5 and 0,8% of the cost of the implementation work of the PVCS [25]. By taking the maximum estimation, the following equation is obtained:

$$C_{ass} = 0{,}0065 \times C_{imp} \times q \tag{1.6-22}$$

where C_{ass} is the cost of insurance in €, C_{imp} is the cost of the implementation work of a PVCS in €, q is the lifespan of PV panels in years, and the 0,0065 factor is calculated by the average between 0,5% and 0,8%.

The following section presents a method of calculating externalities, completing the approach of the global cost.

1.6.2.4 Externalities

According to ISO 15686-5, externalities are the quantifiable costs or benefits that arise when actions taken by organizations or individuals affect stakeholders other than themselves. Regarding PVCS, the externalities are the benefits provided by selling electricity and green certificates.

a) *Gain by Selling Electricity*

A PVCS produces electricity that will then be sold. It can be partly resold directly during its production, if the PV panels produce at the same time a user charges its vehicle. Electricity from PV panels may be also sold indirectly, when stationary storage ensure the charge of a vehicle. Finally, in the case of surplus production, the energy produced by the PV panels can be sold when it is injected into the power grid. In this study, the selling price of electricity for PV panels is the same whether it is sold for the EV charge or for the power grid injection. The gain of the electricity sale over a 30-year lifespan is defined as follows:

$$G_r = T \times E_a \times q \qquad (1.6\text{-}23)$$

where T is the electricity purchase price in €/kWh, E_a is the energy produced annually, and $q$is the lifespan of PV panels in years.

b) *Gain by Sale of Green Certificates*

$$G_{cv} = E_a \times 10^{-3} \times C_{keco} \times C_v \times q \qquad (1.6\text{-}24)$$

where G_{cv} is the gain from the sale of green certificates in €, C_{keco} is the keco coefficient, C_v is the selling price of the green certificate, and q is the lifespan of the PV panels in years.

1.6.3 Calculation Methodology of the PVCS Carbon Impact

It seems important, before launching into the massive use of PVCS-type infrastructures, to evaluate their global carbon impact to assess their utility relative to an EV charging station supplied only by the power grid. A methodology to quantify this impact was therefore detailed using the LCA method based on the ISO 14067 standard [25][26].

1.6.3.1 GHG Assessment Methodology

In order to assess the carbon impact of the PVCS, a method for calculating the GHG emission has been implemented. Based on the Bilan Carbone Association and a Massive Open Online Course (MOOC) organized by Avenir Climatique [27], a calculation method for assessing the carbon impact of PVCS has been established. These databases are used to collect the carbon emission coefficients associated with each emission element of the initially considered PVCS.

The first step of this method is to define a study perimeter that sets the carbon emission limits that will be considered. Once this perimeter has been defined, the second step is to fill a data collection matrix, which contains the carbon emission coefficients associated with each emission element. These carbon emission coefficients are based on several references, including the “Ecoinvent” database [5], the study of national renewable energy laboratory in the LCA harmonization project [28], and the study presented in [29], in order to reduce the total carbon impact of the PVCS. The quantification of these carbon emission coefficients is studied in the carbon impact of a product defined in ISO 14067, and studied as part of this project.

Based on these carbon emission coefficients, it is then possible to assess the carbon impacts of the different sub-systems that made up the PVCS, such as, the PV system, the stationary storage, the charging terminals, the infrastructure related to the structure of the PVCS, and finally the electricity from the power grid, supplied in addition to that produced by the PV system. The sum of these carbon impacts constitutes the global carbon impact of the PVCS, based on the LCA approach over 30 years.

1.6.3.2 Presentation of the Study Perimeter

To carry out the GHG balance, it is first necessary to define the global perimeter of the study, in order to set a limit for the emissions to be considered. In accordance with ISO 14067, the definition of the boundaries of the system shall include all carbon emissions that may contribute significantly to the PVCS carbon impact.

Next, the global overview of the study methodology is defined by all of the GHG emitting steps involved in the manufacturing, transportation, maintenance, and even recycling of the various components required for PVCS to function properly. Thus, the chosen global overview is shown in the diagram depicted in Figure 1.6-1.

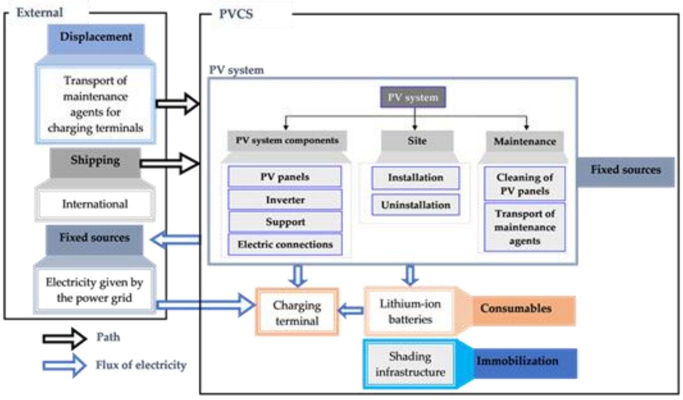

Figure 1.6-1 Perimeter of study

Therefore, this perimeter considers the manufacturing and the end-of-life treatment of the components that made up the PV infrastructure, such as the charging terminals and the batteries. For the shaded-type PVCS, the materials needed to construct the immobilization related to the infrastructure are also considered. The carbon impact of work related to the installation, maintenance, and repair of the PV system and charging terminals is also considered. Finally, the carbon impact of electricity provided by the power grid is also included in the study perimeter.

1.6.3.2.1 Carbon Impact of the PV System

To calculate the carbon impacts of the PV system components, a methodology using the LCA method is detailed. As depicted in Figure 1.6-1, the total carbon impact of the PV system includes the carbon impact of the manufacturing of the PV system components, the installation and uninstallation of the PV system, and the use and maintenance.

In this study, the environmental assessment is applied according to the PV system category. The product category is the group of products with equivalent functionality. These are PV systems connected to a public low voltage, medium voltage, or high voltage power grid. These categories differ according to the maximum power of the PV system, the voltage range, and the installation of the system. They vary between product category 1 and product category 3b.

The type of PV panels selected for the global overview of this study is the monocrystalline silicon panel, the most prevalent technology in France. The carbon emissions coefficient of the PV system $CO_{2\,PV_{syst}}$ ($kgCO_{2,eq}$/kWh) is calculated using the following general equation:

$$CO_{2\,PV_{syst}} = \frac{Imp_{PV_{syst}}}{E_{PV_{syst}}} \qquad (1.6\text{-}25)$$

where $E_{PV_{syst}}$ is the energy produced by PV installation (kWh) during the analysis period.

The carbon impact of the PV system $Imp_{PV_{syst}}$ is the sum of the carbon impacts of the PV system components $Imp_{PV_{infra}}$, construction site Imp_{site}, and maintenance Imp_{maint} in $kgCO_{2,eq}$,as shown in equation (1.6-26):

$$Imp_{PV_{syst}} = Imp_{PV_{infra}} + Imp_{site} + Imp_{maint} \qquad (1.6\text{-}26)$$

Each of these three carbon impacts is calculated in the same way. The equations evaluating these carbon impacts are shown below.

The $Imp_{PV_{infra}}$ is calculated as follows:

$$Imp_{PV_{infra}} = Imp_{PV_{panels}} + Imp_{inv} + Imp_{support} + Imp_{elec_{cnx}} \qquad (1.6\text{-}27)$$

$$= CO_{2\,PV_{panels}} \times P_p + \left(CO_{2\,inv_a} \times P_{inv} + CO_{2\,inv_b}\right) + CO_{2\,support} \times A_{PV} + CO_{2\,elec_{cnx}} \times P_p$$

Where $Imp_{PV_{panels}}$,Imp_{inv} ,$Imp_{support}$,and $Imp_{elec_{cnx}}$ are the carbon impacts of the PV panels, the inverter, the support, and the electric connections, respectively ($kgCO_{2,eq}$), $CO_{2\,PV_{panels}}$ is the carbon emission coefficient of PV panels ($kgCO_{2,eq}$/kWp), $CO_{2\,inv_a}$ is the carbon emission coefficients of inverter a ($kgCO_{2,eq}$/kVA), $CO_{2\,inv_b}$is the carbon emission coefficients of inverter b ($kgCO_{2,eq}$), $CO_{2\,support}$ is the carbon emission coefficient of the support ($kgCO_{2,eq}/m^2$), $CO_{2\,elec_{cnx}}$ is the carbon emission coefficient of the electric connections ($kgCO_{2,eq}$/kWp), P_p is the peak power of the PV installation in kWp, P_{inv} is the power of inverters in kVA, and A_{PV} is the area of PV panels in m^2.

The assessment of the carbon impact of the site (installation and uninstallation) of the PV system is provided by equation (1.6-28) :

$$Imp_{site} = Imp_{installation} + Imp_{uninstallation} = (CO_{2\,installation} + CO_{2\,uninstallation}) \times P_p \qquad (1.6\text{-}28)$$

where $Imp_{installation}$ and $Imp_{uninstallation}$ are the carbon impacts of installation and uninstallation of the PV system in $kgCO_{2,eq}$ respectively, $CO_{2\,installation}$ and $CO_{2\,uninstallation}$ are the carbon emission coefficients of installation and uninstallation of the PV system ($kgCO_{2,eq}$ /kWp).

The maintenance carbon impact of the PV system Imp_{maint} is calculated according to the following equation:

$$Imp_{maint} = Imp_{clean} + Imp_{agt_{transport}} = CO_{2_{clean}} \times A_{PV} + CO_{2_{agt_{transport}}} \times d \times q \qquad (1.6\text{-}29)$$

Where Imp_{clean} and $Imp_{agt_{transport}}$ are the carbon impacts of PV cleaning and transporting maintenance agents to the PV system in $kgCO_{2,eq}$, respectively, $CO_{2_{clean}}$ is the carbon emission coefficient for cleaning PV panels in $kgCO_{2,eq}/m^2$, $CO_{2_{agt_{transport}}}$ is the carbon emission coefficient of transporting maintenance agents to the PV system in $kgCO_{2,eq}$/km, A_{PV} is the area of PV panels in m^2, d is the annual distance traveled by maintenance agents in km/year, and q is the lifespan of PV panels in years.

1.6.3.2.2 Carbon Impact of Stationary Lithium-Ion Batteries Storage

To obtain the carbon emission coefficient for Lithium-Ion batteries $CO_{2_{Li_{batt}}}$ ($kgCO_{2,eq}$/kWh), it only remains to sum the manufacturing carbon emission coefficient $CO_{2_{Li_{batt_{manfu}}}}$ with the recycling one $CO_{2_{Li_{batt_{recy}}}}$. There are two recycling approaches, by hydrometallurgy and by pyrometallurgy. Therefore, this carbon emission coefficient was defined in the following equation:

$$CO_{2_{Li_{batt}}} = CO_{2_{Li_{batt_{manfu}}}} + CO_{2_{Li_{batt_{recy}}}} \qquad (1.6\text{-}30)$$

Since the carbon assessment is carried out over a period of 30 years and the life of the stationary batteries is equal to 10 years, it will be necessary to multiply this carbon emission coefficient by three to obtain the carbon impact of stationary batteries over 30 years. In fact, there will be three battery generations over the analysis period, the initial generation, and two replacement generations.

Thus, the carbon impact $Imp_{Li_{batt}}$ of the stationary batteries installed in the PVCS is defined in (1.6-31) :

$$Imp_{Li_{batt}} = CO_{2_{Li_{batt}}} \times C \times (r_{bat} + 1) \qquad (1.6\text{-}31)$$

where r_{bat} is the number of replacements of the batteries.

1.6.3.2.3 Carbon Impact of Charging Terminals

The carbon impact of charging terminals depends on their installation type: grounded or suspended.

a) *Carbon Impact of Suspended Charging Terminal*

For the suspended charging terminals, the carbon impact will be based on the model of the EVLink Wallbox Plus [30]. The environmental profile of this product, provided by its manufacturer Schneider Electric, presents the LCA realized on the following lifecycle phases: Materials and Manufacturing (M), Distribution (D), Installation (I), Usage (U), and End of life (E). Therefore, the carbon emission coefficient associated with the suspended charging terminal $CO_{2_{suspended_{CT}}}$ is obtained by the equation below:

$$CO_{2_{suspended_{CT}}} = CO_{2_{suspended_{CT_M}}} + CO_{2_{suspended_{CT_D}}} + CO_{2_{suspended_{CT_I}}} + CO_{2_{suspended_{CT_U}}} \qquad (1.6\text{-}32)$$

where $CO_{2\,suspended_{CT_M}}$, $CO_{2\,suspended_{CT_D}}$, $CO_{2\,suspended_{CT_I}}$, and $CO_{2\,suspended_{CT_U}}$ are the carbon emission coefficients of Manufacturing (M), Distribution (D), Installation (I), and End of life (E), respectively ($kgCO_{2,eq}$/unit).

In addition, the carbon impact of the maintenance $Imp_{suspended_{CT_{maint}}}$ of these charging terminals must be taken into account, which can be calculated as indicated in equation (1.6-33), according to the carbon emission coefficient for transporting maintenance agents to the terminals in $kgCO_{2,eq}$/km , the annual average distance traveled by maintenance agents in km/year d, and the considered analysis period, q.

$$Imp_{suspended_{CT_{maint}}} = CO_{2\,suspended_{CT_{maint}}} \times d \times q \qquad (1.6\text{-}33)$$

Thus, the carbon impact $Imp_{suspended_{CT}}$ of the suspended charging terminals of the PVCS is obtained based on equation (1.6-34) :

$$Imp_{suspended_{CT}} = CO_{2\,suspended_{CT}} \times N_{suspended_{CT}} \times (r_{ter} + 1) + Imp_{suspended_{CT_{maint}}} \qquad (1.6\text{-}34)$$

where $N_{suspended_{CT}}$ is the number of suspended charging terminals, and r_{ter} is the number of replacements of the terminals.

b) Carbon Impact of Grounded Charging Terminal

Next comes the estimation of the carbon impact of the grounded charging terminals. The carbon coefficient will be detailed according to the EVLink City mode [31]. Unlike the suspended charging terminal, the environmental profile of this grounded charging terminal is not provided by its manufacturer. It is assumed, therefore, that the composition of the latter is proportionally identical to that of the suspended charging terminal. The mass of the terminals and the emission coefficient of a suspended charging terminal make it possible to estimate the emission coefficient of the grounded charging terminal $CO_{2\,grounded_{CT}}$ ($kgCO_{2,eq}$/charging terminal) as follows:

$$CO_{2\,grounded_{CT}} = \frac{CO_{2\,suspended_{CT}} \times m_{grounded_{CT}}}{m_{suspended_{CT}}} \qquad (1.6\text{-}35)$$

where $m_{grounded_{CT}}$ and $m_{suspended_{CT}}$ are the mass of the grounded and suspended terminals, respectively (kg).

In addition, to calculate the carbon impact of the grounded charging terminal, the carbon impact of the civil engineering $Imp_{civil_{engi}}$ must also be considered, as given in equation (1.6-36). This carbon impact will only be considered for the first generation of grounded terminals. The civil engineering necessary to install of the grounded terminals is considered as reusable during terminal replacements.

$$Imp_{civil_{engi}} = V_{RC} \times CO_{2\,RC} \times \rho_C \times N_{grounded_{CT}} \qquad (1.6\text{-}36)$$

where V_{RC} is the volume of RC required for the foundation of the grounded charging terminals in m^3, ρ_C is the density of concrete in kg/m^3, $CO_{2\,RC}$ is the RC carbon emission coefficient in $kgCO_{2,eq}$/ton, and $N_{grounded_{CT}}$ is the number of suspended charging terminals.

For maintenance, the same equation is intended as for the suspended terminal.

Finally, the carbon impact $Imp_{grounded_{CT}}$ ($kgCO_{2,eq}$) of the grounded charging terminals in the PVCS is defined by the following equation:

$$Imp_{grounded_{CT}} = CO_{2_{grounded_{CT}}} \times N_{grounded_{CT}} \times (r_{ter} + 1) + Imp_{grounded_{CT_{maint}}} + Imp_{civil_{engi}} \quad (1.6\text{-}37)$$

r_{ter} is the number of replacements of the terminals.

1.6.3.2.4 Carbon Impact of the PVCS Infrastructure

The carbon impact of the PVCS infrastructure Imp_{infra} is presented by the carbon impact of the car parking shades. In order to obtain the desired quantities of materials used for construction of the car parking shades, the volume V_{RC} of necessary RC for these foundations in m^3 is required. This volume is expressed in the equation below:

$$V_{RC} = L_{fondation} \times W_{fondation} \times H_{fondation} \times N_{poles} \quad (1.6\text{-}38)$$

where N_{poles} is the number of poles, and $L_{fondation}$, $W_{fondation}$, and $H_{fondation}$ are the length, width, and the height of the RC foundation in m.

The carbon impact $Imp_{RC_{fondation}}$ of the RC for the foundations of N_{pc} car parking shades is calculated according to the following equation:

$$Imp_{RC_{fondation}} = CO_{2_{RC}} \times \rho_C \times V_{RC} \times N_{pc} \quad (1.6\text{-}39)$$

where $CO_{2_{RC}}$ is the carbon emission coefficient of RC in $kgCO_{2,eq}/m^3$.

The calculation of the carbon impact Imp_steel of steel in the metal structure of a shade unit is expressed by equation (1.6-40):

$$Imp_{steel} = m_{steel} \times CO_{2_{steel}} \quad (1.6\text{-}40)$$

where m_{steel} is the mass of steel of a shade unit in tons and $CO_{2_{steel}}$ is the steel carbon emission coefficient in $kgCO_{2,eq}$/ton.

Thus, the carbon impact $Imp_{N_{pc_{shades}}}$ ($kgCO_{2,eq}$) for a shade with N_{pc} parking places is calculated by as a function of the carbon impact of the RC used for the foundation of the shades units $Imp_{RC_{fondation}}$ and the carbon impact of the steel contained in the shades units Imp_{steel} :

$$Imp_{N_{pc_{shades}}} = Imp_{RC_{fondation}} + Imp_{steel} \quad (1.6\text{-}41)$$

Finally, according to the obtained results, it is possible to calculate the carbon emissions coefficient for one parking place $CO_{2_{shade}}$ and Imp_{infra} :

$$\begin{cases} CO_{2_{shade}} = \dfrac{Imp_{N_{pc_{shades}}}}{m} \\ Imp_{infra} = CO_{2_{shade}} \times N_{pp} \end{cases} \quad (1.6\text{-}42)$$

1.6.3.2.5 Carbon Impact of Electricity Provided by the Power Grid

The carbon emission coefficient of the power grid depends on the electricity production method. It represents the average emissions emitted during a year depending on the composition of the energy mix of primary energy. The entire electricity production process is considered. The main primary energies used are nuclear, hydraulic, coal, gas, etc.[32].

Each production mode has an associated carbon emission coefficient. The carbon emission coefficient of the power grid is calculated in proportion to the amount of electricity used for each type multiplied by its own emission coefficient. In France, the carbon emission coefficient $CO_{2_{PG}}$ of the French energy mix is 59 $gCO_{2,eq}$/kWh. It should be noted that the carbon emission coefficient of the French power grid is particularly low, as most electricity is nuclear power with a carbon emission coefficient of only 0,006 $kgCO_{2,eq}$/kWh.

Therefore, the carbon impact Imp_{PG} ($kgCO_{2,eq}$) of the electrical energy provided by the power grid is expressed in the equation below:

$$Imp_{PG} = CO_{2_{PG}} \times E_{PG} \tag{1.6-43}$$

where E_{PG} is the energy provided by the power grid in kWh.

Now, it is possible to assess the global carbon impact of PVCS, given as the sum of the carbon impacts of the different sub-systems constituting them, as expressed in the following equation:

$$Imp_{PVCS} = Imp_{PV_{syst}} + Imp_{Li_{batt}} + Imp_{suspended_{CT}} + Imp_{grounded_{CT}} + Imp_{infra} + Imp_{PG} \tag{1.6-44}$$

1.6.4 Results and Analyses of the Numerical Application of Global Cost and Carbon Impact of the PVCS

The carbon impacts and costs of PVCS various components allow realizing environmental and financial reports over 30 years. Here is a calculation example and assessment of these reports for a PVCS, with the following characteristics: shade type PVCS covering five parking places for EVs, equipped with 22 kWh stationary battery storage capacity and recycled by pyrometallurgy, 28 kWp as peak power of 70 panels installed on a surface of 124 m^2. The infrastructure is located in Compiègne, the north of France, with an average annual irradiation of 1 309,11kWh/m^2. The installed inverter's power is assumed to be 90% of the PV's peak power. Based on the PVGIS website, the electricity produced and used by the PVCS during the 30 years is estimated at 1,257 GWh, where 307,476 MWh are provided by the public grid. The occupancy rate of the charging terminals is distributed by a time slot of 2 h, as follows:

- Between 08:00 AM and 10:00 AM: two EVs at 2,3 kW;
- Between 10:00 AM and 12:00 PM: one EV at 22 kW, four EVs at 2,3 kW;
- Between 12:00 PM and 02:00 PM: two EVs at 2,3 kW;
- Between 02:00 PM and 04:00 PM: one EV at 22 kW, four EVs at 2,3 kW;
- Between 04:00 PM and 06:00 PM: one EV at 22 kW, three EVs at 2,3 kW.

1.6.4.1 Results of the Numerical Application of the Global Cost of the PVCS

As depicted in Figure 1.6-2, the PVCS investment cost is calculated and displayed in the form of a pie chart. The total investment cost is calculated as a function of the capacity of the stationary storage, the number of PV panels, and the number of charging terminals.

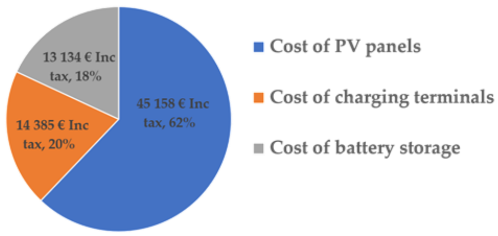

Figure 1.6-2 Distribution of the investment cost of the PVCS

As depicted in Figure 1.6-3 (a),(b), the exploitation and maintenance costs are then calculated and displayed in the form of pie charts, respectively.

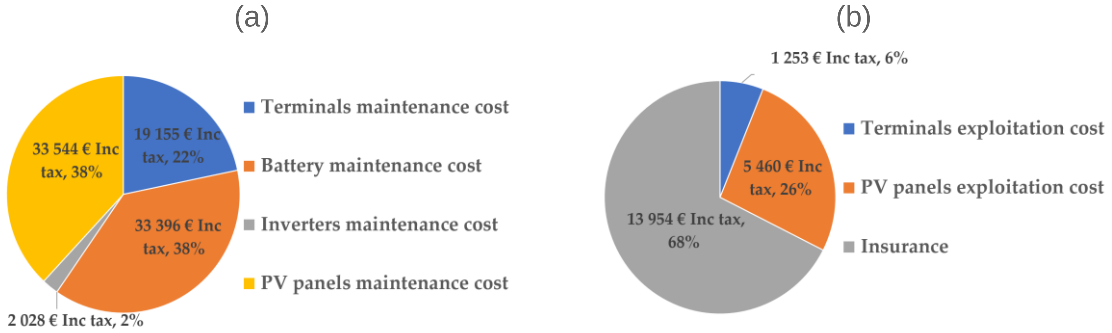

Figure 1.6-3 (a) Maintenance cost, (b) exploitation cost

The vision from an economic point of view is then global; the stockholders are aware of the excepted cost magnitude orders over the next 30 years.

It should be noted that each cost, maintenance, or exploitation is multiplied by 30 to obtain a balance over 30 years, except the costs related to the investment of the PVCS.

Then, to address the economic part of the PVCS over 30 years, a two-sided approach has been adopted. The first, in the form of a pie chart, provides a direct overview of the various costs (investment, maintenance, and exploitation) and their distribution (Figure 1.6-4 (a)). The second, in the form of a curve over time, provides an annual view of the cost to be invested (Figure 1.6-4 (b)). The maintenance cost presents the most important part in the global cost.

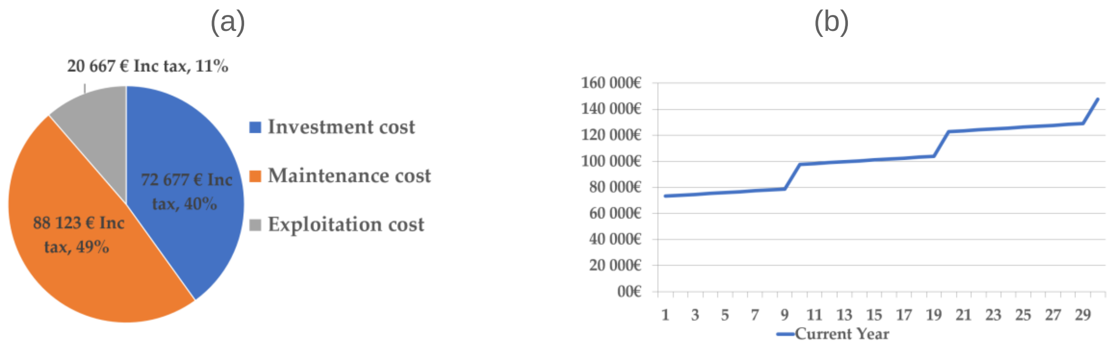

Figure 1.6-4 The 30-year financial report: (a) Distribution of the global cost; (b) evolution of the global cost

1.6.4.2 Results of the Numerical Application of the PVCS Carbon Impact

In this example, the assessment of the PVCS carbon impact is calculated using PV panels with a carbon emission coefficient of 40 $gCO_{2,eq}$/kWh, according to the NREL laboratory in the context of the LCA harmonization project [28]. Numerical applications of formulas give:

$$Imp_{PV_{infra}} = 48\,546\ kgCO_{2,eq} \qquad (1.6\text{-}45)$$

$$Imp_{site} = 2\ kgCO_{2,eq}$$

$$Imp_{maint} = 447\ kgCO_{2,eq}$$

The carbon impact of this PV system is therefore:

$$Imp_{PV_{syst}} = 48\,995\ kgCO_{2,eq} \qquad (1.6\text{-}46)$$

In addition to this carbon impact, there is also the impact of batteries, charging terminals, infrastructure related to the shade, and electricity provided by the power grid. As summarized in Table 1.6-1, the numerical application provides a value of $Imp_{PVCS} = 85\,961\ kgCO_{2,eq}$ as the total carbon impact of the PVCS. Compared to the amount of power that PVCS supplies from the PV system and the power grid in the analysis period, this carbon impact is equivalent to an global emission coefficient of the PVCS of 0,068 $kgCO_{2,eq}$/kWh.

Table 1.6-1 Summary table of the carbon impact of each component of the initially considered PVCS.

PVCS			$Imp\ (kgCO_{2,eq})$
PV system	PV system components	PV panels	37 996
		Inverter	1 501
		Support	7 087
		Wiring	1 962
	Site	Installation	1
		Uninstallation	1
	Maintenance	Cleaning	23
		Servicing	424
Charging terminals	Maintenance		1 023
	Fabrication		1 095
Lithium-Ion battery			5 869
Infrastructure			15 439
Public grid			13 540
Total			85 961

It is interesting to compare the carbon impact of the PVCS with the carbon impact of PGCS. This station therefore provides the same quantity of electricity over 30 years as the PVCS, and also includes the same number of charging terminals. Thus, its carbon impact Imp_{PGCS} can be calculated using this equation:

$$Imp_{PGCS} = Imp_{CT} + Imp_{PG} \qquad (1.6\text{-}47)$$

where Imp_{CT} and Imp_{PG} are the carbon impact of the charging terminals and the public grid, respectively. The numerical application gives that the carbon impact for this PGCS is equal to $Imp_{PGCS} = 77\,436\ kgCO_{2,eq}$. The comparison of these two carbon impacts is given by calculating the variation rate.

$$Variation\ rate = \frac{Imp_{PVCS} - Imp_{PGCS}}{Imp_{PGCS}} \qquad (1.6\text{-}48)$$

In this example, the numerical application indicates that the carbon impact of the PVCS is 11% higher than that of the PGCS. Once the carbon impact of the PVCS is established, it is necessary to estimate the action levers allowing one to reduce the carbon impact of the system.

1.6.4.3 Analyses of Action Levers to Reduce the Carbon Impact of the PVCS

To identify the action levers required to reduce the carbon impact, the most emitting positions within the PVCS have been identified. It is then necessary to determine these levers. Once these levers are determined, it is sufficient to reduce their carbon emission coefficient or their carbon impact. This reduction relies on recycled materials and newer data. Once the component's carbon impact is reduced, the new carbon impact of the PVCS is compared to that of the initially considered PVCS and PGCS, to show the gains obtained.

According to the chart pie shown in Figure 1.6-5, the most impactful element, in terms of carbon impact, is the PV system, which emits 57% of the total carbon impact of the PVCS. The second most impacting element is infrastructure, which emits 18%.

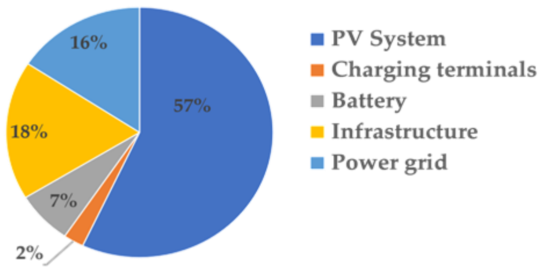

Figure 1.6-5 Distribution of the impact carbon of the PVCS

The power grid is not considered for estimating action levers that reduce carbon impacts. Therefore, the other components of the PVCS are considered to determine the levers of action. Figure 1.6-6 shows the distribution of the carbon impact of the PVCS without the power grid.

Without considering the carbon impact of the power grid, the most impactful element in terms of carbon impact is the PV system, which emits 68% of the PVCS carbon impact.

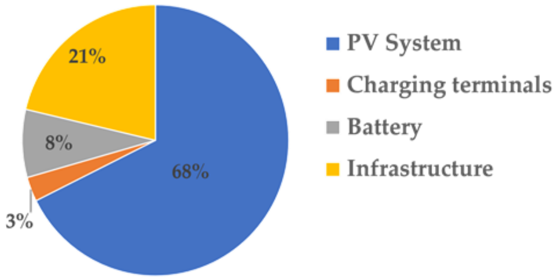

Figure 1.6-6 Distribution of carbon impact of the PVCS without considering the power grid

Since the PV system is made up of many other components, it is then necessary to determine which components emit the most which within the system. As shown in Figure 1.6-7 the PV panels are the most impactful elements in term of carbon impact. Their carbon impact is about 78%.

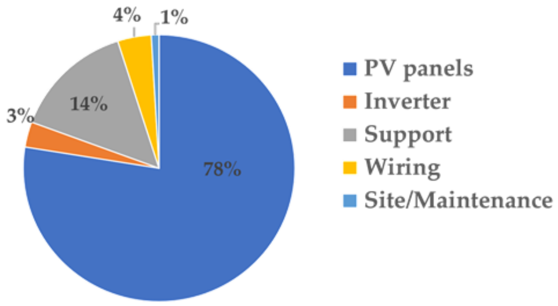

Figure 1.6-7 Distribution of carbon impact of the PV system

Indeed, the PV panels' manufacturing is the most energy-intensive step. For example, a large quantity of energy is used to convert silica sand into high purity silicon. The main action lever in order to reduce the carbon impact is then the PV panels, thereby reducing the impact of the PV system, and therefore of the PVCS. According to the aforementioned analysis, the PV panels and infrastructure will be considered.

The carbon impact of new PV panels decreased sharply over the years, due to the use of less carbon emitting processes and materials during manufacture, and their improved efficiency.

In this study, the values of emission coefficients used to calculate the carbon impact of the considered PVCS came from the Ecoinvent database and the study carried out by NREL in the LCA harmonization project [29], which explains an emission coefficient of 0,04 $kgCO_{2,eq}$/kWh for PV panels.

Thus, in order to calculate the reduction of the carbon impact, the emission coefficient of the PV panels will be changed. In this framework, the reduction of the carbon impact of PVCS is analyzed according to five scenarios.

1.6.4.3.1 Scenario 1: Reduction of the Emission Coefficient of the PV Panels from 40 gCO2,eq/kWh to 25 $gCO_{2,eq}$/kWh

By taking PV panels with a carbon emission coefficient of 25 $gCO_{2,eq}$/kWh, the carbon impact of the panels drops from 37 996 $kgCO_{2,eq}$ to 23 748 $kgCO_{2,eq}$. As depicted in Figure 1.6-8, the carbon impact of the PVCS drops from 85 961 $kgCO_{2,eq}$ approximately to 71 713 $kgCO_{2,eq}$, a decrease of 17,2% compared to the initially considered charging station.

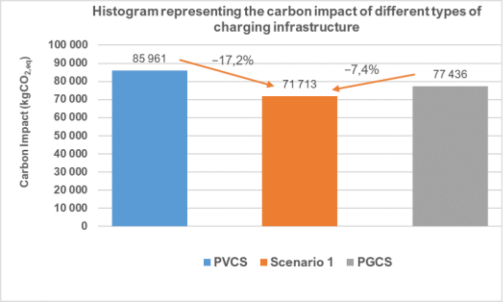

Figure 1.6-8 Result of scenario 1

In addition, knowing that the carbon impact of a PGCS is around 77 436 $kgCO_{2,eq}$, then over 30 years, the variation rate becomes −7,4%, which means that the carbon impact of the PVCS is lower than the PGCS' one.

1.6.4.3.2 Scenario 2: Reduction of the PV Panels' Emission Coefficient to 25 $gCO_{2,eq}$ and the Infrastructure Is Based on Recycled Materials

In addition to the PV panels, it is possible to reduce the carbon impact of the infrastructure by using recycled materials. The constituent materials of the infrastructure are steel and the concrete. For concrete, RC from wastes will be used, which will prevent some emissions from the use of new concrete. For steel, the metal structure will be made of recycled steel. Thus, the carbon impact of the immobilization drops from 15 439 $kgCO_{2,eq}$ to 8 616 $kgCO_{2,eq}$. For the emission coefficient of the PV panels, scenario 1 is considered.

Thus, for these values, the carbon impact of the PVCS decreases from 85 961 $kgCO_{2,eq}$ to 64 890 $kgCO_{2,eq}$, approximately 24,5% reduction compared to the initially considered infrastructure (Figure 1.6-9).Thus, over 30 years, the carbon impact of a PGCS is 16,2% higher than PVCS that contains PV panels with an emission coefficient of 25 $gCO_{2,eq}$/kWh and recycled infrastructure.

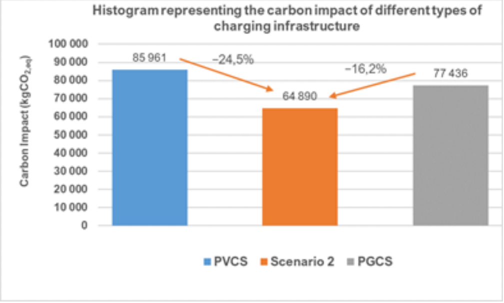

Figure 1.6-9 Result of scenario 2

1.6.4.3.3 Scenario 3: Reduction of the PV Panels Emission Coefficient to 12 $gCO_{2,eq}$/kWh

A study published in 2017 [29] demonstrates that the carbon emission factor of PV modules in 2050 will vary between 35 and 12 $gCO_{2,eq}$/kWh.

By taking PV panels with a carbon emission coefficient of 12 $gCO_{2,eq}$/kWh, the carbon impact of the panels drops from 37 996 $kgCO_{2,eq}$ to 11 399 $kgCO_{2,eq}$.

As depicted in Figure 1.6-10, the carbon impact of the PVCS decreases from 85 961 $kgCO_{2,eq}$ to 59 364 $kgCO_{2,eq}$, a 31% reduction compared to the initially considered charging station.

In comparison with the PGCS, the variation rate becomes −23,3%, which means that the carbon impact of the PVCS is lower than the PGCS' one.

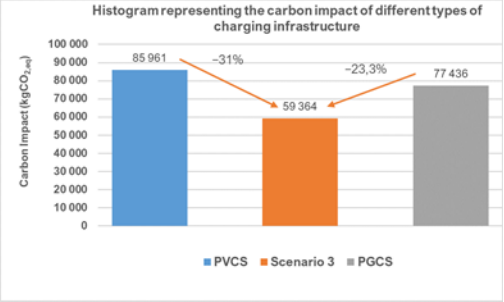

Figure 1.6-10 Result of scenario 3

1.6.4.3.4 Scenario 4: Combination of Scenario 3 and an Infrastructure Based on Recycled Materials

As presented in Figure 1.6-11, the carbon impact of the PVCS with a recycled infrastructure and PV panels with the emission coefficient of 12 $gCO_{2,eq}$/kWh is approximately 52 541 $kgCO_{2,eq}$, a decrease of 38,9% compared to the carbon impact of the initially considered PVCS. In comparison with the PGCS, the variation rate becomes −32,1%, which means that the carbon impact of the PVCS is lower than the carbon impact of the PGCS.

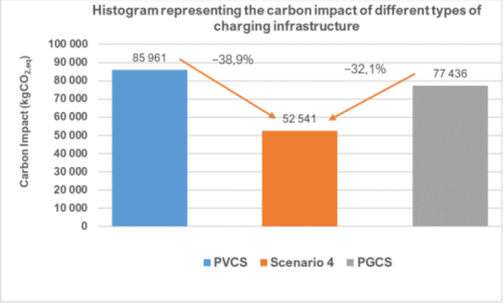

Figure 1.6-11 Result of scenario 4

1.6.4.3.5 Scenario 5: Reduction of the PV Panels Emission Coefficient to 10 $gCO_{2,eq}$/kWh and an Infrastructure Based on Recycled Materials

In this scenario, consideration is given to PV panels produced locally in France [33], with a low emission coefficient of 10 $gCO_{2,eq}$/kWh. The use of these panels, combined with recycled materials, will reduce the carbon impact of the PVCS by 40,4% compared to the initial PVCS. Additionally, there will be a significant decrease of 33,9% compared to the PGCS (Figure 1.6-12).

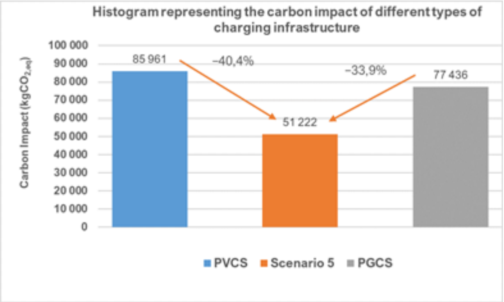

Figure 1.6-12 Result of scenario 5

1.6.4.4 Discussion

The environmental benefits of the PVCS are assessed as the function of the energy mix of each country. The carbon impact of each country depends mainly on the thermal power plants, nuclear energy distribution, and the capacity of the renewable energies. For example, in France, with the high nuclear energy use, the charging infrastructure based only on the power grid has a lower carbon impact than the PVCS initially considered in this study. Each country displays its coefficient without giving details concerning the life cycle of each category of power plant. Thus, in this study, the developed methodology offers, with more details, to the decision maker a choice of infrastructure compatible with his spatial, ecological, and budgetary constraints.

Similar works have been published by other researchers. In [18], an optimal configuration of PVCS for EVs has been analyzed technically and economically under different conditions of solar irradiation in Vietnam. However, the cost of building, allowing the creation and the coverage of parking places, is not included in the total cost, as well as the replacement cost of the charging terminals. In [34], a technical, environmental, and financial analysis of the feasibility of PVCS associated with a stationary battery storage for EVs (EV) located in China and the United States has been discussed, using the estimation of the energy balance, annual costs, and CO_2 emissions. However, the carbon impact from the manufacturing phase until the disposal of each element of the PVCS is not included in the CO_2 estimation, as well as there being a lack of actions to reduce this emission.

In this context, this work details the entire methodology followed for the calculation of the global cost and the carbon impact of the PVCS, as well as the different actions to reduce it.

According to the aforementioned analysis, the PV system is the most impacting element of CO_2, which emits 57% of the total carbon impact of the PVCS. On this basis, four scenarios have been suggested to reduce the PVCS carbon impact using recent data. Each scenario presented in the previous sections was able to reduce the carbon impact of PVCS compared to the initially considered charging station and PGCS.

Each scenario presented in the previous sections was able to reduce the carbon impact of PVCS compared to the initially considered charging station and PGCS.

Thus, scenario 5 presents the lowest carbon impact, combining a carbon emission coefficient of 10,61 $gCO_{2,eq}$/kWh for PV panels produced locally and an infrastructure based on recycled materials. The variation rate of each scenario compared to the charging station only grid-connected is summarized in Figure 1.6-13.

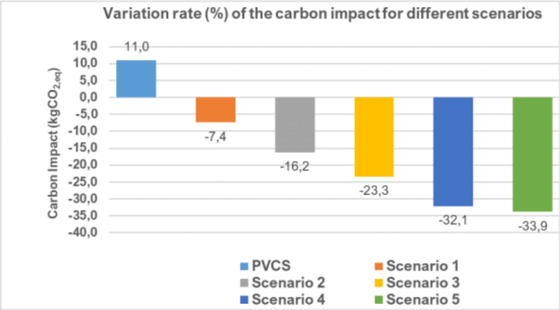

Figure 1.6-13 Variation rate for the different scenarios

Thus, the analysis of action levers demonstrates that despite a very carbon-free French energy mix, it is possible to have a lower carbon impact of PVCS than PGCS. PV technologies are evolving very quickly. Thus, for recent PV panels with a greatly reduced emission coefficient and produced in country with low energy mix, the carbon impact of the PVCS will be also greatly reduced.

Figure 1.6-14 depicts the carbon impact of the PVCS compared with the PGCS in different countries [35][36][37].The calculated carbon emission coefficient of the initially considered PVCS of 68 $gCO_{2,eq}$/kWh is lower than the PGCS based on the energy mix of different countries, with the exception of that of France, because the French energetic mix is very low.

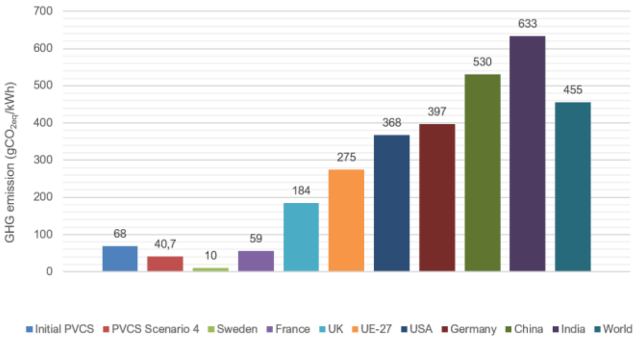

Figure 1.6-14 Comparison of the carbon emission coefficient of PVCS with the PGCS in different countries

Scenario 5 makes the carbon emission coefficient of PVCS becomes 40,7 $gCO_{2,eq}$/kWh lower than the energy mix of different countries, even that of France.

1.6.5 Conclusions

Electric mobility and PVCS installation are positioned as solutions to the dynamic issues linked to environmental challenges. The purpose of this work is to disseminate through the development of methodology based on LCA to calculate the global cost of this type of installation, and to quantify the savings of the carbon impact of the PVCS. Thus, estimating the global cost will provide a clearer view of the financial impact of this type of installation over the 30-year lifespan. Moreover, the PVCS carbon impact estimation provides an approach to quantify the environmental impact of this type of installation by quantifying the pollution of the installation in the CO_2 equivalent.

According to the results obtained, the carbon impact of the PV system is largely responsible for the global carbon impact of the PVCS. Thus, the impact of using more recent data of the

PV panels' carbon emission coefficient and recycled materials on the global carbon impact of the PVCS is analyzed in this paper. For recent PV panels with 10 $gCO_{2,eq}$/kWh and an infrastructure with recycled materials, the carbon impact of the PVCS is 34% lower than the carbon impact of the PGCS. In this scenario, the carbon emission coefficient of the PVCS becomes 40,7 $gCO_{2,eq}$/kWh lower than the energy mix of different countries.

The carbon emission coefficient of the studied PVCS is compared to than that of PGCS in several countries; where the carbon emission coefficient different from one country to another, it depends mainly on the thermal power plants, the distribution of the nuclear energy, and the capacity of the renewable energy's installations. However, each country displays its coefficient without giving details concerning the life cycle of each category of power plant. This represents a limit for constructing a precise comparison framework. In addition, difficulties are encountered in collecting recent data based on the evolution of technologies related to PVCS and defining a calculation methodology of the global cost and the carbon impact, which presents a concern with the proposed methodology.

As future works, it would be possible to resume and deepen the calculation of the carbon emissions of each subsystem of the PVCS based on any more recent data, by deepening the analysis method based on the life cycle using second-life batteries, and also, by completing the methodology of the global cost by providing updated prices and rectifying the evolution of technologies related to PVCS.

REFERENCES

[1] Manuel, B.; Aurore, C.; Jérôme, D.; Alexis, F.; Charlotte, V. Key Figures on Climate France, Europe and Worldwide; General Commission for Sustainable Development: New York, NY, USA, 2020; p. 88.

[2] Cheikh-Mohamad, S.; Sechilariu, M.; Locment, F.; Krim, Y. PV-Powered Electric Vehicle Charging Stations: Preliminary Requirements and Feasibility conditions. Appl. Sci. 2021, 11, 1770. https://doi.org/10.3390/app11041770

[3] Bilan Carbone® France. Available online: http://www.basecarbone.fr/ (accessed on 20 July 2021).

[4] Synapsun, Commission de Régulation de l'énergie, ECS (Simplified Carbon Evaluation). Available online: https://www.synapsun.com/en/introduction-to-simplified-carbon-footprint-calculation/ (accessed on 5 September 2017).

[5] EcoInvent—Switzerland. Available online: http://www.ecoinvent.ch/ (accessed on 20 July 2021).6

[6] ISO 14040; Environmental Management—Life Cycle Assessment—Principles and Framework. International Standards Organization: Geneva, Switzerland, 2006. Available online: https://www.iso.org/standard/37456.html (accessed on 23 December 2019).

[7] Jianli, Z.; Yunna, W.; Chenghao, W.; Feiyang, H.; Buyuan, Z.; Fangtong, L. A geographical information system based multi-criteria decision-making approach for location analysis and evaluation of urban photovoltaic charging station: A case study in Beijing. Energy Convers. Manag. 2020, 205, 112340.

[8] Fachrizal, R.; Shepero, M.; van der Meer, D.; Munkhammar, J.; Widén, J. Smart charging of electric vehicles considering photovoltaic power production and electricity consumption: A review. eTransportation 2020, 4, 100056. https://doi.org/10.1016/j.apenergy.2021.118139

[9] Rodriguez, A.S.; de Santana, T.; MacGill, I.; Ekins-Daukes, N.; Reinders, A. A feasibility study of solar PV-powered electric cars using an interdisciplinary modeling approach for the electricity balance, CO_2 emissions, and economic aspects: The cases of The Netherlands, Norway, Brazil, and Australia. Prog. Photovolt. Res. Appl. 2020, 28, 517–532. http://dx.doi.org/10.1002/pip.3202

[10] Esfandyari, A.; Norton, B.; Conlon, M.; McCormack, S.J. Performance of a campus photovoltaic electric vehicle charging station in a temperate climate. Sol. Energy 2019, 177, 762–771. https://doi.org/10.1016/j.solener.2018.12.005

[11] Filote, C.; Felseghi, R.A.; Raboaca, M.S.; A¸schilean, I. Environmental impact assessment of green energy systems for power supply of electric vehicle charging station. Int. J. Energy Res. 2020, 44, 10471–10794. https://doi.org/10.1002/er.5678

[12] Wong, E.; Ho, D.; So, S.; Tsang, C.-W.; Chan, E. Life Cycle Assessment of Electric Vehicles and Hydrogen Fuel Cell Vehicles Using the GREET Model—A Comparative Study. Sustainability 2021, 13, 4872. https://doi.org/10.3390/su13094872

[13] Wu, Z.; Wang, C.; Wolfram, P.; Zhang, Y.; Sun, X.; Hertwich, E. Assessing electric vehicle policy with region-specific carbon footprints. Appl. Energy 2019, 256, 113923. https://doi.org/10.1016/j.apenergy.2019.113923

[14] Javid, R.J.; Salari, M.; Javid, R.J. Environmental and economic impacts of expanding electric vehicle public charging infrastructure in California’s counties. Transp. Res. Part D Transp. Environ. 2019, 77, 320–334. https://doi.org/10.1016/j.trd.2019.10.017

[15] Aljohani, T.; Alzahrani, G. Life Cycle Assessment to Study the Impact of the Regional Grid Mix and Temperature Differences on the GHG Emissions of Battery Electric and Conventional Vehicles. In Proceedings of the 2019 SoutheastCon, Huntsville, AL, USA, 11–14 April 2019; pp. 1–9. https://doi.org/10.1109/SoutheastCon42311.2019.9020666

[16] Vadium, I.T.; Das, R.; Wang, Y.; Putrus, G.; Kotter, R. Electric vehicle Carbon footprint reduction via intelligent charging strategies. In Proceedings of the 2019 8th International Conference on Modern Power Systems (MPS), Cluj-Napoca, Romania, 21–23 May 2019; pp. 1–6. https://doi.org/10.1109/MPS.2019.8759783

[17] Grande, L.S.A.; Yahyaoui, I.; Gómez, S.A. Energetic, economic and environmental viability of off-grid PV-BESS for charging electric vehicles: Case study of Spain. Sustain. Cities Soc. 2018, 37, 519–529. https://doi.org/10.1016/j.scs.2017.12.009

[18] Minh, P.V.; Le Quang, S.; Pham, M.-H. Technical Economic Analysis of Photovoltaic-Powered Electric Vehicle Charging Stations under Different Solar Irradiation Conditions in Vietnam. Sustainability 2021, 13, 3528. Appl. Sci. 2022, 12, 4115 23 of 23 https://doi.org/10.3390/su13063528

[19] Liu, G.; Xue, Y.; Chinthavali, M.S.; Tomsovic, K. Optimal Sizing of PV and Energy Storage in an Electric Vehicle Extreme Fast Charging Station. In Proceedings of the IEEE Power & Energy Society Innovative Smart Grid Technologies Conference (ISGT), Washington, DC, USA, 17–20 February 2020; pp. 1–5. https://doi.org/10.1109/ISGT45199.2020.9087792

[20] Alireza, K.; Georgios, T.; Prodromos, M.; Konstantinos, S.; Nikolaos, E.; Emmanouel, V. Sizing of electric vehicle charging stations with smart charging capabilities and quality of service requirements. Sustain. Cities Soc. 2021, 70, 102872.

[21] ADEME, French Agency for Ecological Transition. Know The Costs and Evaluate The Profitability, Investment Costs. Available online: https://www.photovoltaique.info/fr/preparer-un-projet/quelles-demarches-realiser/choisir-son-modele-economique/ #couts_dinvestissement (accessed on 25 May 2021).

[22] Collectif. Le Moniteur Editions, Batiprix Bordereau; Groupe Moniteur: Paris, France, 2017; 3644p, ISBN 978-2-281-14172-6. EAN 9782281141726.

[23] ADEME, French Agency for Ecological Transition. Key Figures. Available online: https://www.ademe.fr/expertises/mobilite-transports/chiffres-cles-observations/chiffres-cles (accessed on 9 April 2018).

[24] Miquel, C.; Gaiddon, B. Systèmes Photovoltaïques: Fabrication et Impact Environnemental; HESPUL, Energies Renouvelalbes et Efficacité Energétique: Lyon, France, 2009; pp. 1–35. Available online: https://www.photovoltaique.info/media/filer_public/36/fe/36fe92bb-d625-4712-abb4-47470c864208/pv_fab_envt_final_26082009.pdf (accessed on 26 January 2020).

[25] ISO 14067; Greenhouse Gases—Carbon Footprint of Products—Requirements and Guidelines for Quantification. ICS: 13.020.40 Pollution, Pollution Control and Conservation, Sustainable Development Goal. International Standards Organization: Geneva, Switzerland, 2018; pp. 1–46.

[26] ISO 14064; International Standards Organization: Geneva, Switzerland, 2018. Available online: https://www.iso.org/standards. html (accessed on 20 July 2021).

[27] Avenir Climatique. MOOC Energie & Climate. 2017. Available online: https://avenirclimatique.org/mooc/ (accessed on 26 January 2020).

[28] NREL, National Renewable Energy Laboratory. Life Cycle Greenhouse Gas Emissions from Solar Photovoltaics; NREL/FS-6A20-56487; NREL: Golden, CO, USA, 2012; p. 2.

[29] Pehl, M.; Arvesen, A.; Humpenöder, F.; Popp, A.; Hertwich, E.G.; Luderer, G. Understanding future emissions from low-carbon power systems by integration of life-cycle assessment and integrated energy modelling. Nat. Energy 2017, 2, 939–945. https://doi.org/10.1038/s41560-017-0032-9

[30] Schneider Electric. EVlink Wallbox Plus-T2S Socket Outlet with Shutters-3 Phase-32A/22kW. Available online: https://www.se.com/fr/fr/product/EVC1S22P4E4ERF/evlink-city---borne---22kw---2xt2s-tri-32a-%2B-2x2p%2Bt---rfid / (accessed on 26 January 2020).

[31] Schneider-Electric. Product Environmental Profile EVLink Wallbox, 08/2015, ENVPEP1502002_V1/PEP Ecopassport SCHN-2015-019-V0-EN. Available online: https://download.schneider-electric.com/files?p_Doc_Ref=ENVPEP1502002EN (accessed on 26 January 2020).

[32] Lévy, J.-B. Producing a Climate-Friendly Energy. 2020. Available online: https://www.edf.fr/en/the-edf-group/producing-aclimate-friendly-energy (accessed on 26 January 2020).

[33] https://www.photowatt.com/en/photovoltaic-products/photovoltaic-panels/pw60max-c-monofacial/

[34] Sierra, A.; Gercek, C.; Geurs, K.; Reinders, A. Technical, Financial, and Environmental Feasibility Analysis of Photovoltaic EV Charging Stations With Energy Storage in China and the United States. IEEE J. Photovolt. 2020, 10, 1892–1899. https://doi.org/10.1109/JPHOTOV.2020.3019955

[35] RTE (2022), Bilan électrique 2022, RTE, France https://assets.rte-france.com/analyse-et-donnees/2023-02/Bilan%20e%CC%81lectrique%202022%20principaux%20resultats.pdf

[36] Ember, Global Electricity Review 2023 Available Online: https://ember-climate.org/insights/research/global-electricity-review-2023/#supporting-material

[37] Ember, European Electricity Review 2022 Available Online: https://ember-climate.org/insights/research/european-electricity-review-2022/#supporting-material

2 SOCIETAL IMPACT AND SOCIAL ACCEPTANCE OF PVCS AND NEW SERVICES

Electric vehicles (EVs) appear to be one of the possible solutions for limiting greenhouse gas emissions from the transportation sector. Hence, the transport sector must be redesigned to facilitate the installation of EV charging stations powered by renewable energy from photovoltaic (PV) panels. Described as a new innovation, the social acceptability of these PV-powered charging stations should be studied alongside the technical aspects, aiming to improve the project and increase public awareness.

The goal of the present chapter is to determine whether this innovative energy system is socially accepted and to analyze the concept's limitations from a public perspective through a study conducted in 2022 by one of the French contributors. Social acceptability revealed a very promising outlook for electromobility coupled with renewable energies. Regarding social acceptance, the study shows that the majority of those polled are eager to use PV-powered charging stations and the new associated services, such as vehicle-to-grid (V2G) and vehicle-to-home (V2H); however, this acceptance is conditional on a number of users' needs and constraints.

2.1 Case study in France: new survey on the social acceptance of PVCS and associated new services

The purpose of this study[7] is to assess the acceptability of IIREVs and their new associated services, such as smart charging and bidirectional energy transfer, through a study conducted in 2022 by the Université de Technologie de Compiègne. The study was carried out on a city scale and involved a large number of stakeholders. Hence, it aims to analyze the concept's limitations from a public point of view and highlights the evolution of people's mindsets over the years by comparing it with a similar survey conducted in 2018.

2.1.1 Introduction

The Paris Agreement, adopted by 196 parties at COP 21, is an international treaty on climate change. Its goal is to limit global warming to less than 2°C [1]. To reach this long-term goal, countries aim to reduce global greenhouse gas emissions as soon as possible to achieve carbon neutrality by the mid-21th century. Low-carbon solutions and new markets have emerged, particularly in the power and transportation sectors, which account for 41% and 24% of CO_2 emissions, respectively [2]. In this context, the shift to low-carbon mobility requires the deployment of electric vehicles (EVs), whose emissions depend on their manufacturing processes and the energy sources that operate them [3]. In fact, in the worst-case scenario, an EV with a battery produced in China and driven in Poland still emits 37% less CO_2 than a gasoline vehicle [4].

However, the growth in EVs implies an increase in power demand, and the public grid would not be able to meet this demand without involving fossil fuel-based power plants, leading to higher CO_2 emissions. To address this issue, integrating renewable energy sources, such as photovoltaic (PV) could reduce electricity consumption and grid power peaks while ensuring EVs charging [5] with a significant proportion of PV energy. The power generated by PV sources cannot directly feed the EVs due to their intermittent nature. Therefore, the most effective solution for recharging EVs is a microgrid, which combines renewable sources, stationary storage devices, loads, and connection to the public grid [6]. The microgrid also includes a user-machine interface [7] that enables data collection via a communication system and transfers it to an optimization algorithm to ensure real-time power management [8]. Additionally, the installation of such intelligent EV charging infrastructures (IIREVs) based on microgrids is expected to allow users to charge their vehicles during the day without limitation. Nonetheless, social acceptability and acceptance are central to many debates surrounding energy projects, particularly in urban areas.

---

[7] This section is based on the following publication: A. Alchami, N. Darene, M. Sechilariu, and F. Locment, "Social Acceptability and Acceptance of Photovoltaic Powered Charging Stations", in Colloque InterUT Systèmes sûrs et durables, Feb 2023. https://hal.science/hal-04011818

Social acceptability is the result of a collective or critical analysis of a new technological object, project, plan, or policy that considers the moral issues arising from its introduction. This collective critical analysis may be positive or negative, but it represents only an opinion at a given moment, which may evolve over time. Social acceptability can be described but not quantified, and can be achieved at all territorial levels (local, regional, or national) [9][10].

Social acceptance is defined as the respondents' attitudes, including their behavioural responses, and refers to whether a new technology is highly accepted, weakly accepted, simply tolerated, or clearly not accepted by a community. Since the opinions of stakeholders are not included in these surveys, the final studies lack relevant empirical data for an in-depth ethical evaluation. Consequently, social acceptance surveys cannot encompass all morally relevant characteristics of risky technologies [9][10].

Hence, social acceptability and social acceptance are examined together to ensure both types of analysis are relevant to the assessment of risks. Ultimately, social acceptability and social acceptance are largely complementary.

This paper first aims to present studies on the social acceptability and acceptance of IIREVs and the new associated services in urban areas. To facilitate and guide both the qualitative and quantitative surveys, a study on the societal impact of IIREVs was carried out at the outset. The study then highlights the evolution of public opinion over the years by comparing the results with those of a similar survey conducted in 2018 [11]. In summary, the social acceptability study, defined as a prospective judgment on future implementation, focuses on three main questions:

- What primary goals should be accomplished before IIREVs implantation?
- How will city dwellers react to the structures' presence in urban areas?
- How will stakeholders react to this innovation, and how will users change their habits to take advantage of these stations?

The rest of the paper is structured as follows. Section 2.1.2 describes IIREVs, primarily powered by PV sources, while Sections 2.1.3 and 2.1.5 discuss their societal acceptability and social acceptance, respectively. Improvement plans based on the survey results are presented in Section 2.1.5. Conclusions and perspectives are provided in Section 2.1.6.

2.1.2 Intelligent Evs Charging stations powered by PV

The IIREVs, based on PV energy and connected to a nearby building or home, and their interactions are represented in Figure 2.1-1. The microgrid integrates PV panels, stationary storage, and a public grid connection, all managed by a smart control system that ensures the power management and energy distribution between the IIREVs, the public grid, the EVs, and nearby buildings [12]. The IIREVs not only provide green energy to the EVs but may also supply power to the public grid and buildings according to demand. The priority is to charge EVs with PV energy, with any excess PV power being used to charge stationary storage, supply nearby buildings (I2H, infrastructure-to-home), or inject power into the utility grid. This is done based on an optimization algorithm that considers several factors, such as the state of charge of the stationary storage, grid conditions, weather forecasts, and energy market costs [8]. Additionally, assuming the EV battery is a flexible load and considering the user's needs, the energy management system can shift the charging period to provide the EV with a significant amount of PV power while avoiding grid power consumption during peak hours.

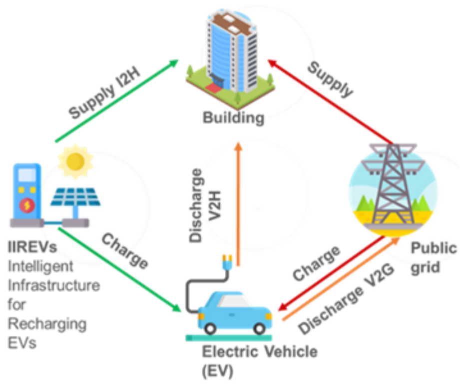

Figure 2.1-1 IIREVs and its interactions

On the other hand, the EV battery is seen as an energy reservoir and can be discharged, within a set limit, either into the grid through the V2G operation mode or into the building through the V2H operation mode [13].

Figure 2.1-2 illustrates the possibilities of energy management [14]. The goal is to maximize the use of energy from the PV system while minimizing the total energy cost.

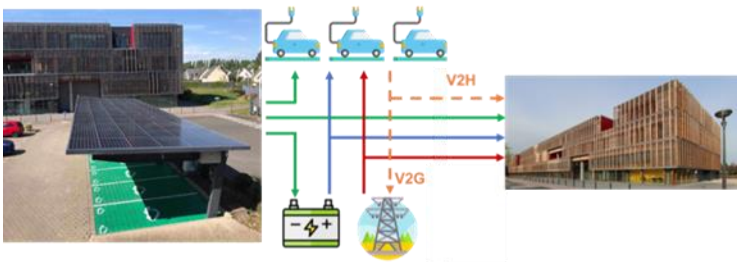

Figure 2.1-2 Energy management for IIREVs

The V2G services could help the power grid regulate frequency, smooth peaks of consumption, and maintain nominal voltage [13]. Meanwhile, V2H services could smooth consumption peaks at the building level and supply electricity during power cut-offs. Although various works discuss the potential of employing V2G for ancillary services, the V2G strategy has not yet been implemented in real life, except at some test sites.

The implementation of IIREVs is quite challenging since economic, social, and environmental factors must be considered. Thus, several studies are necessary before implementation. These studies should consider all factors, from irradiation, location, power limitations, and financial constraints to environmental issues like carbon emissions [15]. However, some questions arise: to what degree will users accept these services, and what challenges stand in the way of their development?

2.1.3 Social Acceptability of IIREVs

The realization of the social acceptability study follows two phases [9]: societal impact and qualitative survey. These are also the preliminary studies for the acceptance study, referred to as the quantitative survey. In the first step, the societal impact study defines the product IIREVs, the market, and the actors [16]. In the second step, the qualitative survey, conducted with a limited sample of respondents, reveals their reflections on the IIREVs. This section presents these two studies.

2.1.3.1 Societal Impact

The implementation of IIREVs and their V2G/V2H services will impact society and the mobility of its citizens. This marketing and societal impact study defines the IIREVs project, its market, and its stakeholders to reveal their reflections on this innovation and characterize their expectations and requirements. For IIREVs, two innovations can be distinguished: charging with PV energy and the V2G/V2H services. These are defined as 'technology push' (i.e., users will be encouraged to recharge their EVs) and 'market pull' (i.e., innovations developed in response to identified market needs). Indeed, IIREVs connect, directly or indirectly, multiple stakeholders in these innovations:

- Active stakeholders: suppliers, productors, constructors, assemblers, design firms, holders;
- Utility grid: energy suppliers, energy distributors, network managers;
- City and state services: local authorities, municipal services, private and public agencies devoted to energy transition;
- Users: EV users, future users, buildings owners, private companies with PV-powered charging stations;
- Others: maintenance agencies.

The societal impact study identified a list of expectations and obstacles at each stakeholder level related to the implementation of IIREVs:

- Socio-economic: The high cost of EVs discourages users from choosing this option. However, it's important to note that EVs are considered a long-term investment, and a full charge with electricity is cheaper than refuelling a combustion vehicle with fuel.
- Political: New policies encourage the development of cleaner transportation modes to minimize dependence on petroleum and limit its environmental impact. Polluting vehicles face fines, and new government incentives are available for the purchase of EVs.
- Technological: New technologies are being developed to overcome the main obstacles regarding PV efficiency and EV battery lifespan.
- Environmental: The low environmental impact of EVs and IIREVs encourages their sale and the use of PV energy.

2.1.3.2 Qualitative survey

The purpose of a qualitative survey, which consists of open-ended questions, is to allow respondents to fully and freely express themselves. This survey will generate new hypotheses that will aid in constructing the subsequent quantitative survey, specifically the acceptance study. In fact, the qualitative survey enables the examination of how these stakeholders will react to the innovation, including how existing users may change their habits and how future users will respond. Therefore, it is important to use familiar words and avoid technical language, adjusting the vocabulary to suit each person's background. The methodology used for collecting information is based on three criteria: age, socio-professional categories, and type of vehicle. A total of 55 stakeholders were interviewed: 3 from institutions, 7 from private companies, and 45 users, whose vehicle types are shown in Figure 2.1-3 compared to the 2018 study.

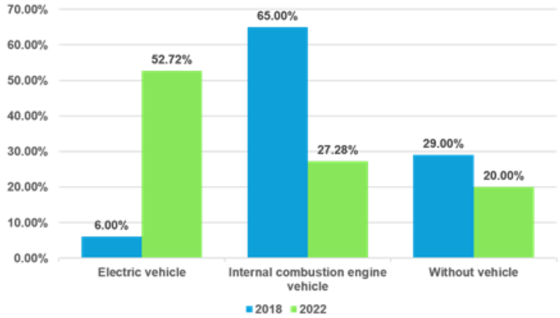

Figure 2.1-3 Type of vehicle of respondents

The questions were broken up into three separate sections: a general introduction to the project; a section on PV energy; and a section on the related V2G and V2H systems. Finally, a section with specific questions for professionals and institutions was introduced. This distinction was important insofar as the institutions could provide more details on the installation and management of infrastructure according to their activities.

Following the qualitative interviews, the participants seemed to easily understand the project and found it attractive after its presentation. It was noted that what appealed to them the most was the ecological aspect, especially when mentioning the use of green energy and the sharing and optimization of electricity. Despite the high number of positive opinions, some found this utopian project financially and socially unfeasible due to the significant and premature changes in habits required at this stage of electromobility development. This analysis of the feedback highlighted the needs and expectations of future users of IIREVs, which will be developed in the quantitative survey.

2.1.4 Social Acceptance of IIREVs: Quantitative survey

The quantitative survey aims to gather substantial feedback on IIREVs and associated services. The marketing and social approaches (societal impact) and the results of the qualitative survey were examined to identify the key considerations for formalizing the quantitative survey. These main points include travel habits, obstacles to electromobility development, the impact of ecology, expectations regarding IIREVs, IIREV locations, IIREV ownership, partial EV discharge, PV energy recharge, and the existence of parking shades in urban areas.

The quantitative survey was conducted by creating a multiple-choice questionnaire and distributing it to a large number of participants. Its objective is to confirm certain common beliefs and assess the acceptability of a potential change in habits. The survey closely resembles one carried out in 2018 [11], which evaluated changes in opinions regarding this subject over the previous four years. It includes an introduction to the topic to facilitate understanding of IIREVs, followed by 33 closed-ended questions divided into distinct thematic sections: information about the respondent and their travel habits; a section about IIREVs and the discharge/charge system; a section concerning the use of PV energy; and a final section on attractions and obstacles.

The distribution of the questionnaire is crucial as it characterizes the sample. It was necessary to vary the sources of diffusion to represent the diversity of the population's profile, rather than focusing solely on the entourage of students and teachers. This was achieved through the following means of communication: the survey team's personal network, the Université de Technologie de Compiègne's Facebook group, the Facebook group of the city of Compiègne, and the distribution of a QR code in common places. Within 30 days, 864 responses from different categories were collected.

2.1.4.1 Profiles of the respondents

Figure 2.1-4 shows that all age groups are represented. However, the proportion of individuals aged 15 to 25 differs from France's actual age distribution. This overrepresentation is due to the survey being distributed via social networks, where the online format was not suitable for people over 60. Note that this overrepresentation is not a significant issue, as young people will be directly affected by this innovation in the upcoming years.

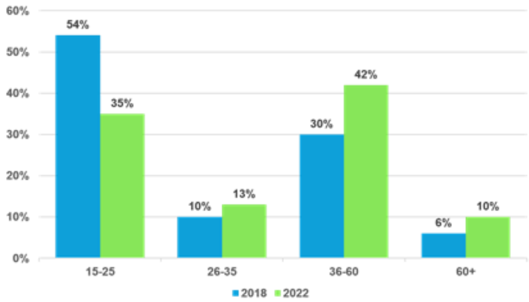

Figure 2.1-4 Age repartition of the respondents

Comparing this data with 2018 data published in [11], it can be seen that the percentage of adults has increased, which will influence the socio-professional distribution of the respondents (Figure 2.1-5), and, consequently, the mean mode of transport (Figure 2.1-6).

Figure 2.1-5 presents a strong representation of students and staff, likely due to the project’s network. The high representation of staff and the absence of workers and agriculturalists can be attributed to the fact that purchasing a vehicle is often constrained by each person's social status.

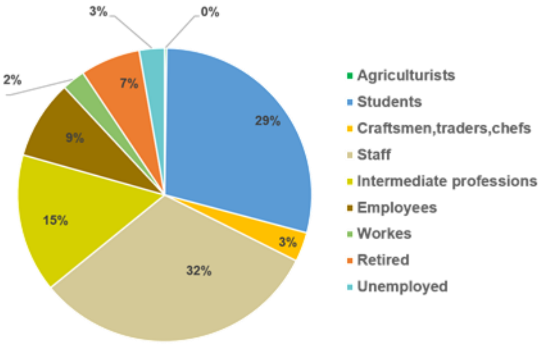

Figure 2.1-5 Socio - professional distribution of the respondents

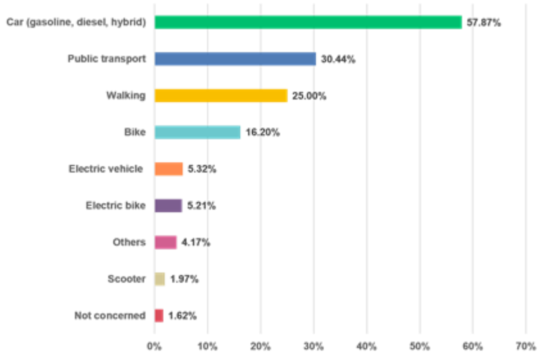

Figure 2.1-6 Mean of travel

Combustion and hybrid vehicles remain the most reliable and practical means of transportation for commuting to work or for leisure. In fact, 58% prefer them. When combining this criterion with the respondents' place of residence, it is noted that most of them reside in rural areas and small cities. However, the share of public transport has increased significantly since 2018 [11], from around 21% to 30,44%. Of this 30,44%, 75% of respondents live in medium-sized or large cities where car traffic is complicated. The percentage of people who cycle to work has nearly doubled since 2018 [11], from 9% to 16,2%. This can be explained not only by ecological awareness but also by the COVID-19 pandemic impact. Thus, this could be an indicator of how flexible the French people are to changing their mobility habits.

The answers to the last question in this section concerning the main obstacles that prevent each person from purchasing an EV are represented in Figure 2.1-7.

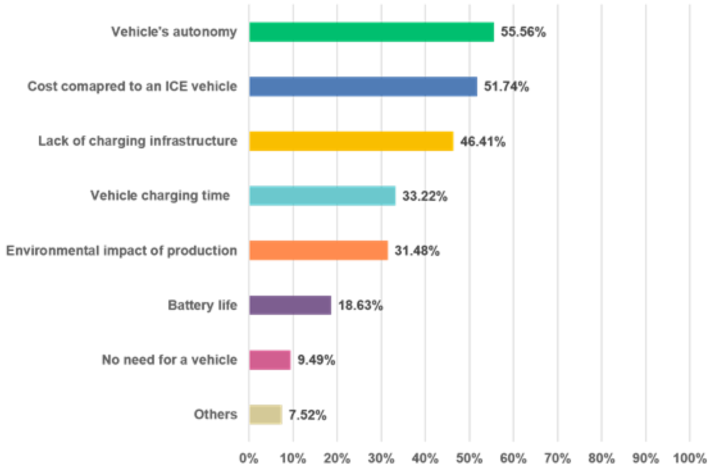

Figure 2.1-7 Mains obstacles to the acquisition of an EV

The results are not surprising because the autonomy of the vehicle, its cost compared to a conventional vehicle, and the lack of charging stations had already been identified a few years earlier. Users are still hesitant about the possibility of making long journeys with an EV without having to stop for a long time to recharge the battery. In fact, the environmental issue has increased from 20% in 2018 to 31,48% in 2022, and the questionees are now more aware regarding the ecology.

2.1.4.2 Generalities on IIREVs: discharge/charge

This section of the quantitative study examines public perceptions of IIREVs and related services for discharge and charging systems, such as V2G and V2H. It focuses on the conditions that would enable users to accept the idea of regularly discharging and recharging their vehicles. At the same time, it considers the profit they would like to gain from the discharge.

The locations, availability, and charging modes of the charging terminals are the main expectations regarding their characteristics. It is interesting to note that their percentages are comparable, at around 59%. However, for older individuals, ease of use is critical, whereas for younger individuals, fast charging is essential. Subsequently, the respondents mentioned their preferred locations for charging terminals (Figure 2.1-8), with the workplace being the most prevalent.

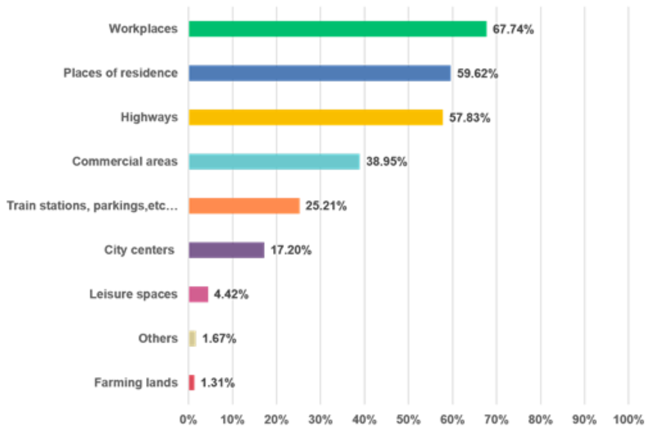

Figure 2.1-8 IIREVs location preference

Indeed, EVs are generally parked all day; this aligns with the use of IIREVs with slow charging to maximize the utilization of PV energy. The place of residence ranks second, followed by highway stops. It is worth noting that the results are very similar to those obtained in 2018 [11]. However, some users express concerns about the installation of IIREVs in city centres (26% in 2018) [11]; they do not want massive installations in large cities, as this could discourage the use of public transport, cycling, or walking.

The question of whether to approve the discharge was raised twice in the survey to assess acceptability with and without certain information. The first instance occurred at the beginning of this section, and the second occurred after a few questions regarding the discharge conditions, compensations, etc. Initially, 78% of the respondents answered ‘Yes’ or ‘Yes, but under certain conditions,’ with a significant majority (62% of the total respondents) selecting ‘Yes, but under certain conditions.’ In contrast, 22% showed complete refusal (Figure 2.1-9(a)). However, some respondents changed their minds after subsequent questions regarding compensation and profits; 83% answered ‘Yes,’ while 17% answered ‘No’ (Figure 2.1-9 (b)).

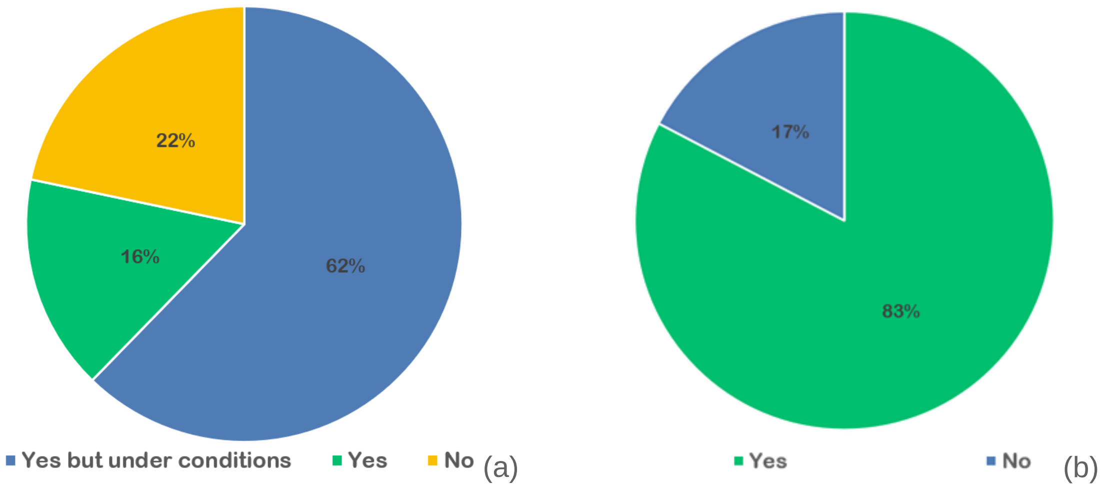

Figure 2.1-9 (a) Acceptability of the discharge initially (b) Acceptability of the discharge after several questions)

In fact, half of the drivers who accept V2G/V2H would be willing to discharge their vehicles as long as there are no additional costs, and only 31% would like to financially benefit from V2G/V2H. Therefore, the primary motivation is not necessarily financial. However, only 4% clearly accept the discharge without any conditions.

The next question concerned the desired compensation as a contribution to their energy shares. Not everyone wishes to benefit equally from the V2G/V2H services. With 60% of the votes, a deduction on the electricity bill ranked first. This is a very logical option since it involves electricity discharged from the EV's battery. Additionally, it would simplify automatic compensation via bank transfers. Free parking came in second with 52% of the votes; citizens always seek out services that are becoming increasingly rare and expensive in urban areas. Financial compensation and tax deductions ranked third and fourth, at 39% and 33%, respectively.

Another question addressed the desire to know the destination of the battery energy, with 65% indicating interest. This suggests that such information could encourage and motivate EV users to share their electricity.

In conclusion, respondents are generally tolerant of V2G/V2H services, but users must still be assured they can leave with the minimum amount of required energy. It is sufficient to keep them informed about important information via an interface and, above all, to obtain their consent in advance.

2.1.4.3 Integration of PV energy and shades structures

The last part of the questionnaire concerns PV energy and shading structures, which are essential to the operation of IIREVs. An image of the STELLA platform (Smart Transport and Energy Living Lab) at the Université de Technologie de Compiègne, shown in Figure 2.1-2, precedes the questions to help visualize this type of structure.

Three-quarters of the respondents believe that the use of renewable energy sources influences their opinion of the acceptability of IIREVs, and 95% of people support charging EVs with PV energy. This proportion is significantly higher than in the qualitative survey, where the results on this question were more varied. During the qualitative interviews, the barriers identified regarding PV panels included low efficiency and intermittent production.

However, the results in Figure 2.1-10 confirm the hypotheses, as efficiency ranks first with 48% of the votes. Although the yield of PV systems is relatively low (around 20%), this technology is recognized as a viable alternative to fossil fuels and remains more advantageous. Second, the recycling of photovoltaic modules poses an obstacle. Currently, 90% of panels are recyclable, but misinformation circulating among the public leads them to perceive PV recycling as a problem. Pollution during the production of PV systems ranks third, with 39% of the votes.

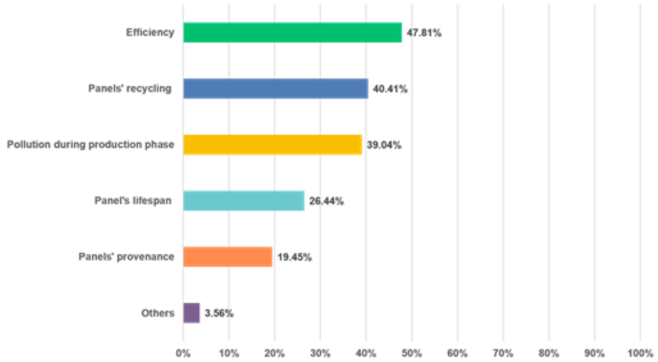

Figure 2.1-10 Main obstacles to the use of PV panels

Regarding the installation of car parking shade structures with photovoltaic (PV) sources, the first question gathered general opinions on the use of these structures. Ninety-five percent do not view their use as an obstacle to the project's success. The minority considers this infrastructure problematic for aesthetic reasons; among them, 81% would support the implementation of innovative integrated renewable energy vehicles (IIREVs) if asked about their preferences in advance.

To satisfy future users, it was important to ask respondents about the main locations that would concern them regarding the integration of a car parking shed. The results are presented in Figure 2.1-11, where half of the respondents do not identify any significant issues with the installation of shade structures. For the other half, tourist areas, agricultural zones, city centres, and residential neighbourhoods are the most disruptive locations for this type of infrastructure. Conversely, cinemas, stadiums, highway gas stations, supermarkets, shopping malls, and workplaces do not pose any issues for the installation of these IIREVs.

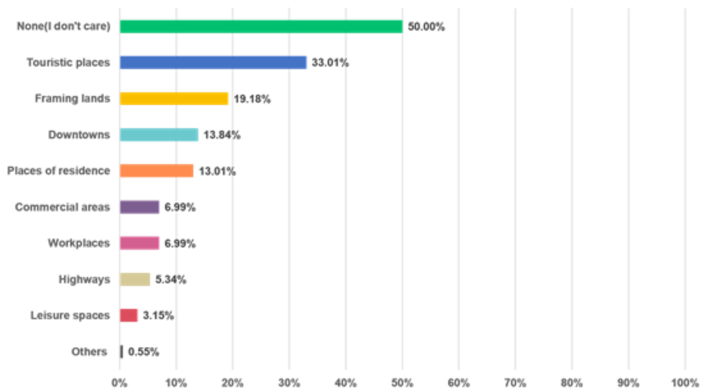

Figure 2.1-11 Disturbing places for the establishment of shade structures

Otherwise, older people are more reluctant to install these car shades at their residences. It should be noted that, when compared to the 2018 study, these locations were cited in nearly the same order and with approximately the same percentage (Figure 2.1-12).

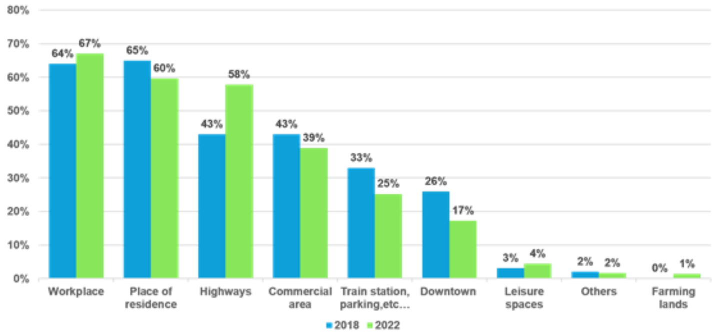

Figure 2.1-12 Places for the establishment of shade structures

2.1.4.4 General comprehension

The results of the quantitative survey show that the project has been evaluated since 2018, and the IIREVs are well accepted socially by the respondents. Notably, 78% of respondents are in favour of the V2G/V2H discharge process, and 95% have no objection to their EV being recharged by PV. Additionally, 95% support the installation of shading structures for placing PV panels. EV users appear to be interested in EV discharge and PV energy use: 75% accept discharging while parked and recharging later during low consumption periods in return for financial compensation.

Those interested in V2G/V2H services do not want to incur additional costs when using such infrastructure, while some view it as a way to earn money or profit by sharing their energy. Furthermore, nearly three-quarters of respondents believe that public authorities should own the IIREVs and be responsible for their implementation and maintenance.

Lastly, respondents expressed a preference for a user-friendly graphical interface, as they want to stay updated on two main pieces of information: the vehicle's autonomy and the state of charge of their battery. Other data, such as remaining charging time and operational history, are considered less important. They desire as much detail as possible from the interactive pages, provided they remain simple to use.

2.1.5 Project limitations and improvements

This final section focuses on understanding the subject and its limitations. As seen in Figure 2.1-13, only 9,73% of respondents still believe there are no boundaries to the development of IIREVs in France, while 35,62% find the investments and costs associated with developing, installing, and maintaining these facilities to be too high. Therefore, these factors constitute the most significant limitations of the project. It is difficult for the population to imagine the benefits of these structures, given the significant changes in habits that their implementation would necessitate. In fact, when compared to the 2018 study, the importance of these limitations appears to have decreased by 15%. The low efficiency of PV modules and the ecological concerns also seem to be limitations of the project, as indirect pollution occurs during the manufacturing process of PV cells and EV batteries. Approximately 30% also highlight the low impact of IIREVs if they are deployed on a small scale, and 25,34% fear that the charge/discharge process could affect the lifespan of their EV batteries.

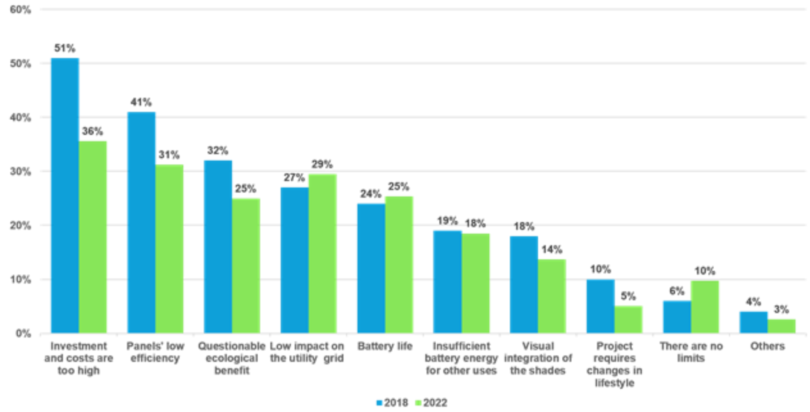

Figure 2.1-13 Project's Limitations

A general question about the project's complexity allows for evaluating whether participants have correctly understood the topic. The more they understand, the more valuable their answers will be for the study. In 2022, the project was easier to comprehend, with 80% of respondents answering 'yes,' and the data indicate greater confidence in the survey results.

For the development of IIREVs, it is noted that addressing certain weaknesses is necessary to enhance social acceptability. Establishing a sustainable business model that aligns the charging price and benefits of V2G/V2H services with users' needs is essential. Once this business model has been established among IIREV owners, network operators, and users, it is crucial to implement a communication plan to promote electromobility and inform individuals about related new technologies. Finally, users require an appropriate interface to simplify their operations and control their EV batteries. The suggested activities are intriguing and could become the focus of new research aimed at customizing IIREVs to meet actual demands.

2.1.6 Conclusions and perspectives

This paper directly questioned the population to assess their tendencies and formulate certain hypotheses regarding the current acceptability of electromobility, IIREVs, and associated services. It was shown that 80% of the population is in favour of using PV energy and would like to highlight its environmental impact. Regarding V2G/V2H services, respondents indicated they are willing to share their energy under certain conditions and in exchange for financial compensation. It can also be observed that there is a higher level of acceptability for IIREVs when the general public is surveyed before the installation of these infrastructures. The researchers' work and the analysis of this survey will inform new studies to test their relevance and feasibility.

REFERENCES

[1] United Nations Climate Change, The Paris Agreement https://unfccc.int/process-and-meetings/the-paris-agreement/the-paris-agreement (acceded in January 2023)

[2] International Energy Agency, CO_2 emissions by sector, World 1990 – 2019, Data & Statistics - IEA.

[3] Y. A. Alhazmi and M. M.A. Salama, “Economical staging plan for implementing electric vehicle charging stations”, Sustainable Energy, Grids and Networks, vol. 10, pp.12-25, 2017

[4] Transport & Environment, how clean are electric cars, https://www.transportenvironment.org/discover/how-clean-are-electric-cars/ (acceded in January 2023)

[5] S. Cheikh-Mohamad, M. Sechilariu, F. Locment, Y. Krim: “PV-Powered Electric Vehicle Charging Stations: Preliminary Requirements and Feasibility Conditions”, Applied Sciences, vol. 11, no.4, pp 1770, 2021, https://doi.org/10.3390/app11041770

[6] W. Bai, M. Sechilariu, F. Locment, “DC microgrid system modelling and simulation based on specific algorithm for grid-connected and islanded modes with real-time demand-side management optimization”, Applied Sciences, vol. 10, no.7, pp 2544, 2020, https://doi.org/10.3390/app10072544

[7] C. E. Montaño-Salcedo, M. Sechilariu, F. Locment: “Human-System Interface for PV-Powered Electric Vehicles Charging Station”, IEEE 30th International Symposium on Industrial Electronics (ISIE) ISIE21, Kyoto 20-23 June 2021, https://doi.org/10.1109/ISIE45552.2021.9576251

[8] S. Cheikh-Mohamad, M. Sechilariu, F. Locment: “Real-time power management including optimization problem for PV-powered charging station”, Applied Sciences, vol. 12, no.9, pp 4323, 2022, https://doi.org/10.3390/app12094323

[9] Y. Fournis and M.-J. Fortin, “From social ‘acceptance’ to social ‘acceptability’ of wind energy projects: towards a territorial perspective”, Journal of Environmental Planning and Management, 60:1, 2017, pp 1-21, https://doi.org/10.1080/09640568.2015.1133406

[10] B. Taebi, “Bridging the Gap between Social Acceptance and Ethical Acceptability” Risk Analysis, Vol. 37, No. 10, pp 1817 – 1827, 2017, https://doi.org/10.1111/risa.12734

[11] M. Sechilariu, F. Locment and N. Darene, “Social Acceptance of Microgrids Dedicated to Electric Vehicle Charging Stations “, IEEE 7th International Conference on Renewable Energy Research and Applications (ICRERA), Paris, France, 14 - 17 oct 2018

[12] M. Sechilariu, N. Molines, G. Richard et al: “Electromobility Framework Study: Infrastructure and Urban Planning for EV Charging Station Empowered by PV-based Microgrid”, IET Electrical Systems in Transportation, vol. 9, issue 4, pp 176–185, 2019. DOI: https://doi.org/10.1049/iet-est.2019.0032 , Print ISSN 2042-9738, Online ISSN 2042-9746

[13] D. Wang, M. Sechilariu, F. Locment: “PV-powered charging station for electric vehicles: power management with integrated V2G”, Applied Sciences, vol. 10, no.6, pp 6500, MDPI Ed., 2020, https://doi:10.3390/app10186500

[14] M. Sechilariu, J. Baert, F. Locment, H. Martell-Flores, N. Molines, G. Richard, C. Henriot, C. Pronello, “Smart Microgrid and Urban Planning for Better Electromobility”, IEEE Vehicle Power and Propulsion Conference (IEEE-VPPC 2017), pp. 1-6, Belfort, France, 11-14 Dec 2017

[15] Y. Krim, M. Sechilariu, F. Locment, A. Alchami, “Global Cost and Carbon Impact Assessment Methodology for Electric Vehicles PV-powered Charging Station”, Applied Sciences, vol. 12, no.9, pp 4115, 2022, https://doi.org/10.3390/app12094115

[16] Michael J.C. Martin, “Managing Innovation and Entrepreneurship in Technology-based Firms”, Wiley-IEEE. p. 44, 1994, ISBN 0471572195

3 CONCLUSIONS AND FUTURE WORKS

The integration of EVs with PV energy systems presents both significant challenges and remarkable opportunities for modern energy management. As global adoption of EVs accelerates, it becomes imperative to manage the rising demand for electricity, particularly during peak hours. The incorporation of PV energy systems emerges as a promising solution, enabling the generation of clean, renewable energy to charge EVs while reducing reliance on fossil fuels.

Analysis indicates that, while well-developed infrastructure can accommodate the energy consumption of EVs, peak power demand remains a critical concern. Under optimal conditions, EV charging could account for over 18.5% of total installed capacity, underscoring the urgent necessity for effective charging control measures and peak demand management strategies to alleviate stress on the grid.

The introduction of a HSi for PVCS marks a pivotal advancement in energy management. This interface facilitates real-time monitoring of EV load patterns and renewable energy consumption, yielding valuable insights into grid dynamics and enhancing the sustainability of EV charging operations. Future efforts will focus on validating data collection methods through experimental testing, which is expected to further refine the management of charging sessions.

Moreover, the comparison MILP optimization with the storage priority algorithm showcases the efficacy of the proposed supervisory control system in integrating EVs with the smart grid. These findings illustrate that real-time data-driven optimization of EV charging significantly enhances energy distribution, particularly when accommodating various charging speeds and grid interactions.

Experiments conducted at the CEA Cadarache site reveal the complexities involved in aligning user demands with system objectives. Although the goal of fully recharging EV batteries was largely achieved, maximizing self-production rates remains a challenge due to varying levels of user participation. Engaging users through initiatives such as 'solar charging' contests could foster acceptance of controlled charging, while further refining the planning algorithm to accommodate diverse user behaviours will be essential for optimizing energy distribution.

An economic analysis of a PV-powered parking facility near Lisbon highlights a notable mismatch between peak electricity demand and PV generation, raising questions about the project's viability. While smart charging reduces dependence on grid power, the payback period exceeds seven years. Future studies should examine how fluctuations in electricity prices influence the economic feasibility of similar projects and develop targeted strategies to enhance profitability.

Regarding the necessity of evaluating the environmental and financial impacts of PVCS, adopting a LCA approach reveals the substantial carbon footprint associated with PV systems, advocating for the use of recycled materials and innovative technologies to mitigate emissions. Future investigations should aim to refine LCA methodologies and update them with current data to enhance the accuracy of carbon impact estimations.

Finally, survey results indicate that 80% of the public supports the utilization of PV energy, reflecting a robust willingness to engage with sustainable energy practices, particularly in relation to V2G and V2H services. This favourable public sentiment presents substantial opportunities for promoting electromobility and related services. To capitalize on this support effectively, further studies should explore the feasibility of proposed infrastructures and investigate financial incentives that could bolster public acceptance.

The next technical report for the subtask 2 will focus on**:**

- Optimal sizing and optimal energy management;
- Empirical sizing: case study of an industrial site in France;
- Energy management for EV Solar Hub from Netherlands;
- PVCS with Energy Cost Optimization via V2G;
- Experimental validation and analyze of experimental results;
- Requirement for Fast Solar EV Charging in Australia;
- Case Studies on e-Bus Fleet Charged from PVCS in Australia;
- Modeling of e-Bus Charging Process;
- Business Models Derived from Energy and Economic Simulations on a Business Park.